REVIEW OF FILL SLOPE FAILURES IN HONG KONG

GEO REPORT No. 96

H.W. Sun

GEOTECHNICAL ENGINEERING OFFICE
CIVIL ENGINEERING DEPARTMENT
THE GOVERNMENT OF THE HONG KONG
SPECIAL ADMINISTRATIVE REGION

REVIEW OF FILL SLOPE FAILURES IN HONG KONG

GEO REPORT No. 96

H.W. Sun

This report was originally produced in May 1998 as GEO Special Project Report No. SPR 4/98

First published, December 1999
Reprinted, January 2002

Prepared by:

Geotechnical Engineering Office,
Civil Engineering Department,
Civil Engineering Building,
101 Princess Margaret Road,
Homantin, Kowloon,
Hong Kong.

PREFACE

In keeping with our policy of releasing information which may be of general interest to the geotechnical profession and the public, we make available selected internal reports in a series of publications termed the GEO Report series. A charge is made to cover the cost of printing.

The Geotechnical Engineering Office also publishes guidance documents as GEO Publications. These publications and the GEO Reports may be obtained from the Government's Information Services Department. Information on how to purchase these documents is given on the last page of this report.

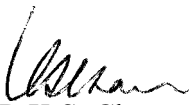

R.K.S. Chan
Head, Geotechnical Engineering Office
December 1999

FOREWORD

The majority of substandard loose fill slopes in Hong Kong are upgraded by means of excavation and recompaction of the top 3 m and provision of suitable drainage measures following the recommendation of the Independent Review Panel for Fill Slopes set up in 1977. With the adoption of such a prescriptive technique to tackle the potential problem of liquefaction of loose fill slopes, there appears to have been little systematic work carried out to examine the fundamental behaviour of loose fill materials. Since the mid-1980's, much research work has been done overseas on the behaviour of loose soils under different stress paths and significant advances have been made in the conceptual understanding of the generalised behaviour of collapse of materials in a loose state with a metastable structure.

Apart from initiating a research programme on systematic testing of typical local fill materials using conventional and advanced laboratory equipment, a review of the state-of-the-art research on the behaviour of loose soils has been carried out by the Special Projects Division. An effective stress soil model which incorporates the newly advanced concepts of collapse surface to allow for the phenomenon of liquefaction caused by water ingress has also been developed.

This Report was prepared by Dr H.W. Sun under the supervision of Mr K.K.S. Ho. It documents the findings of the literature review on the behaviour of loose fill. It presents the results of the preliminary analyses of the 1976 Sau Mau Ping failure using the soil liquefaction model developed and implemented in the finite difference computer program FLAC. Also, some issues related to investigation of fill slopes are highlighted

Professor K.T. Law of the Carleton University of Canada, formerly visiting professor of the University of Hong Kong, reviewed the report and provided valuable comments. His assistance in this project is gratefully acknowledge.

P.L.R. Pang
Chief Geotechnical Engineer/Special Projects

ABSTRACT

It is projected that about 6000 fill slopes constructed before 1977 will be registered in the New Slope Catalogue that is currently being compiled by the GEO. Many of these are potentially substandard and require upgrading to current geotechnical safety standards. To facilitate a proper assessment of the range of feasible upgrading solutions, there is a need for a better understanding of the fundamental behaviour of loose fill and the likely failure mechanisms.

Failure initiation of a fill slope may involve shearing failure along a sliding surface, washout of the soil mass caused by concentrated flow of surface water and liquefaction of the loose soils with a metastable structure. Possible failure triggering mechanisms and contributory factors are reviewed in this Report, along with the statistics on fill slope failures in Hong Kong. As liquefaction generally involves sudden collapse of the loose soil structure with little prior warning, resulting in relatively mobile debris which may lead to significant damage, the characteristic behaviour of loose soils that may be prone to liquefaction is examined in detail in this Report.

Since the mid-1980's, much research work has been done overseas and significant advances have been made in the conceptual understanding of the generalised behaviour of collapse of soils in a loose state with a metastable structure. A review of the state-of-the-art international research on the behaviour of loose soils has been carried out. In addition, an effective stress soil model which incorporates the concepts of collapse surface and critical state to allow for the phenomenon of liquefaction caused by water ingress has been developed.

The soil model developed has been implemented in the finite difference computer program FLAC and used in a back analysis of the 1976 Sau Mau Ping failure. Field stress paths corresponding to surface infiltration of rainfall were imposed. Although further work may be carried out to refine the model, the results from the preliminary analyses were able to illustrate the nature of progressive failure involving stress redistributions in a strain-softening material. In addition, the model used to assess the mobility of the failure debris was able to replicate the observed profile of the landslide debris.

Numerical modelling shows that the collapse of a saturated (or near-saturated) loose zone in a slope can cause significant yielding of non-liquefiable materials leading to progressive failure. It is important to note that given unfavourable boundary conditions, only a portion of soil in the slope needs to be metastable and become saturated (or near-saturated) for a flowslide to develop. This suggests that if a loose fill layer is present at some depth that is liable to become wetted up via subsurface seepage from the upslope area or rising groundwater table, a global failure may take place even if the slope has a surface cover to prevent direct infiltration.

Conventional limit equilibrium calculations based on 'generalised' shear strength parameters for fill in Hong Kong (e.g. 33° to 35°) are not necessarily conservative if the material is prone to collapse with markedly strain-softening behaviour. Some pertinent issues related to investigation of fill slopes are highlighted in the Report.

CONTENTS

1. INTRODUCTION

Prior to the establishment of the Geotechnical Control Office (now Geotechnical Engineering Office, GEO) in 1977, earthwork construction in Hong Kong was not subjected to regulatory control to accepted engineering standards. Fill slopes for development platforms and roads were often constructed by end-tipping without proper compaction, partly due to pressures to provide housing and infrastructure associated with the development boom in the post-war years. The possibility of liquefaction upon saturation of the loose fill slopes and development of flowslides was not fully appreciated. The hazard from liquefaction of loose fill slopes arises principally from the extreme mobility of the debris (i.e. with a large runout distance), which can result in serious consequences in an urban environment.

Following the 1976 Sau Mau Ping landslide, the Independent Review Panel for Fill Slopes (Hong Kong Government, 1977) recommended that the "minimum treatment" of existing loose fill slopes should consist of "removing the loose surface soil by excavating ..... to a vertical depth of not less than 3 metres, and re-compacting to an adequate standard", and provision of "drainage of the fill behind the recompacted surface layer at the toe of the slope". This has become the standard practice for the upgrading of loose fill slopes in Hong Kong.

Although the surface recompaction approach has been used widely, it has practical limitations. Problems of plant access render it unsuitable for congested sites. Temporary cuttings into the loose fill reduce stability of the slope and pose a risk to life during construction. Construction time required for the recompaction work is often long and it is difficult to complete the work within one dry season. In certain situations, the presence of existing services or mature trees also hampers the recompaction.

It is projected that about 6000 fill slopes constructed before the setting up of the GCO will be registered in the New Slope Catalogue being compiled (Malone & Pun, 1997) and that less than 10% of these could be upgraded by the year 2000 when the current accelerated LPM Programme is completed. Thus, a great number of potentially substandard fill slopes is likely to remain, and there is a need to explore other alternatives to upgrade loose fill slopes.

In order to facilitate a proper assessment of the feasibility of other alternative solutions, there is a need to review the properties and failure mechanisms of loose fill slopes in Hong Kong. Special attention has been given to reviewing the advances made in the conceptual understanding of liquefaction of loose soils. To examine the validity of improved soil models, a preliminary study has been made to simulate the 1976 Sau Mau Ping landslide using state-of-the-art numerical modelling techniques. Through this study, the development of the failure mechanism has been examined and useful insight gained. The findings of the study are documented in this Report.

2. LOOSE FILL SLOPES IN HONG KONG

2.1 General

Many of the pre-1977 fill slopes in Hong Kong were formed by end-tipping without compaction. As such, the fill is generally in layers parallel to the slope surface and in a loose state. For fill deposited in layers and not compacted, voids may exist and preferential drainage paths may form between each layer of the fill. This effect may reduce at a deeper

level if self-weight compaction of the fill could cause the voids to collapse. The layered structure of the fill will give the fill body a highly anisotropic permeability. The anisotropic permeability may promote downslope seepage with a horizontal flow component and hence build up of seepage pressure. Under this circumstance, surface infiltration could trigger slope failure even if the gradient of the fill slope is fairly gentle.

2.2 Data on Fill Slopes in Hong Kong

The distribution of slope height against slope angle for about 2000 fill slopes in the New Slope Catalogue is shown in Figure 1. It can be seen that the majority of the fill slopes were inclined at an angle of between 30° and 45° to the horizontal.

Index properties of fill materials in 68 pre-GCO fill slopes (i.e. those constructed before the establishment of the GCO) have been collated. The distribution of void ratio (based on the results of 370 sand replacement tests) with depth is shown in Figure 2. It is noted that the insitu dry density can vary considerably but typically the void ratio ranges from about 0.6 to 1.3. Results of very high void ratio should be treated with caution as the reliability of the sand replacement tests could be questionable, particularly for sites where there are coarse fractions or other large foreign materials present in the soil matrix.

The variation of relative compaction (i.e. the ratio of insitu dry density to maximum dry density) with depth based on over 100 samples from the 68 fill slopes is shown in Figure 3. The values show a large scatter (ranging typically from 65% to 85%) and indicate that most of these fill slopes are in a loose state.

In terms of particle size distribution, 74% of the specimens tested in the laboratory had over 20% fines (viz. clay and silt content) whereas more than 50% of the specimens had over 40% fines. The particle size distribution tests were carried out with dispersants. Without dispersants, it is expected that the tests would give lower percentages of fines.

The profile of the degree of saturation with depth of the selected fill slopes is shown in Figure 4. The degree of saturation at shallow depths is subject to a high scatter and is likely to vary seasonally. It should be noted that drying was generally carried out at 105° C. If the soil contains hydrated minerals, then the actual water content and hence the degree of saturation should be lower than those determined previously.

There is insufficient data on the origin of the fill material to assess if there are significant differences in the properties of fills derived from granitic and volcanic rocks.

2.3 The 1976 Sau Mau Ping Investigation

A comprehensive investigation was carried out after the 1976 Sau Mau Ping failure. The main findings of the investigation are summarised by Morgenstern (1978) as follows:

> " (a) The soil type on the fill was decomposed granite soil, a coarse-grained sand with appreciable silt and clay content, of a texture well known in Hong Kong and having no special peculiarities.

(b) The soil on the slope was in an extremely loose state to a depth of at least 2 m below the slope surface, the dry densities being an average of 13.5 kN/m^3, corresponding to about 75% of standard compaction.

(c) The soil on the slope was layered parallel to the slope surface, with layers between about 100 mm and 300 mm thick, which was the result of end-tipping with no compaction.

(d) Beyond the crest of the slope, the dry densities were low but variable to a depth of 7 m, dropping from about 16.5 kN/m^3 to about 12 kN/m^3 (i.e. 90% to 70% standard compaction). At greater depths, the dry densities were around 15 kN/m^3 to a depth of 20 m below the surface.

(e) The fill contracts at a dry density lower than 15 kN/m^3 (about 85% standard compaction) but will dilate at higher densities."

The data obtained from the 1976 Sau Mau Ping landslide investigation have been further examined in the present study with reference to the current understanding of behaviour of loose materials.

Figure 5 presents the results of particle size distribution. The fines contents (silt size particles or finer) of over 50% of the fill samples tested were found to be in excess of 30%.

Figure 6 shows the distributions of dry density and relative compaction. For fill within the top 5 m, the majority of the data show a relative compaction well below 80%. If a relative compaction of 85% is taken as an indicator of the likelihood of collapse, this would correspond to a dry density of 1.48 Mg/m^3 (void ratio of about 0.8) for the Sau Mau Ping landslide site. However, it should be noted that this is a simplified, or pragmatic, approach as it does not take into account the stress level of the ground nor the failure triggering mechanism.

The degree of saturation, shown in Figure 7, is highly scattered within the top 5 m. Below this depth, the degree of saturation values are more consistent at 70% to 90%, but as these were obtained from drillhole samples taken with water flush they could be higher than the actual values insitu.

From an analysis of the triaxial, shear box and oedometer test data, appropriate critical state parameters for the fill may be interpreted. The definitions of critical state parameters in (1+e) - ln p' space and q – p' space are given in Figure 8. The deduced parameters from the Sau Mau Ping investigation are compared with test results for remoulded granitic soil from King's Park which has over 30% fines (Gray, 1980) and reconstituted completely decomposed granite from Shouson Hill which has 20% fines (Chung, 1997) in Table 1.

Figure 9 shows the distribution of critical state void ratios and measured insitu void ratios at the Sau Mau Ping landslide site.

For a soil with a void ratio higher than the critical state value, it will contract if it is subjected to drained shearing and positive excess pore water pressure will develop if it is subjected to undrained shearing. Most of the specimens tested were contractive. Due to the relatively low stress levels near the ground surface, a significant number of specimens within 2 m depth may however be dilatant. As a result, contractive behaviour is less likely for the overall fill mass at such shallow depths.

2.4 Laboratory Tests on Loose Fill

Gray (1980) reported the results of undrained triaxial compression tests on a decomposed granite at different densities. He observed collapse behaviour on specimens with a fines content of over 30%. Bulk samples of decomposed granite were mixed with water and test specimens were prepared from static compaction of the remoulded material in a mould. Gray suggested that the sensitivity (viz. brittleness behaviour) is caused by the aggregations/fabric structure generated in the material during mixing which was retained during remoulding. Such aggregations/fabric structure may remain intact if the soil remains unsaturated. However, upon saturation and/or shearing, the aggregations/fabric structure may break down. The behaviour may be similar to that of natural soils which exhibit a quasi-yield surface, a concept put forward by Leroueil & Vaughan (1990).

Shen (1985) reported on a series of dead load tests on partially saturated remoulded loose decomposed granite from King's Park. The results were reviewed by Law et al (1997) and it was found that the unsaturated soils had a higher state boundary surface than that for saturated soils and that within the stress range of fill slope failure, the fill in a loose unsaturated condition might dilate and yet behave in a brittle manner. This is attributed by Law et al (op cit) to the increase in shear strength due to dilation being smaller in magnitude than the strength reduction due to soil reaching a higher void ratio.

Results of shear box tests on loose fills in Hong Kong are discussed by Yim & Siu (1997) who noted that the critical dry density is "about 88% for decomposed granite (sandy) fill and 93% to 97% of MDD for decomposed volcanic (silty/clayey) fill", where MDD is the maximum dry density as determined in a standard Proctor compaction test.

It should be noted that in the shear box test the specimen is soaked and there is no control of drainage nor measurement of pore pressure. As such, the soil may not be fully saturated and it is not possible to interpret the test results in terms of effective stress. The shear box test can give at best the drained shear strength but not collapse strength of the soil.

3. FAILURE OF LOOSE FILL SLOPES

3.1 Possible Failure Triggering Mechanisms and Contributory Factors

It is instructive to consider the range of common landslide triggering mechanisms and contributory factors. Systematic landslide studies have permitted classification of the modes and mechanisms of failure and identification of generic factors that can give rise to failure. The failure mechanisms observed in loose fill slopes may be classified into liquefaction, sliding and washout (Wong et al, 1997b).

The possible triggers and contributory factors for failure of loose fill slopes are shown in Figure 10 and the major mechanisms of failure are summarised below:

Global Failure

(a) Global liquefaction of the fill mass or localized liquefaction within a zone in the slope. The failed mass may not necessarily flow like a liquid (i.e. with zero or near-zero effective stress and shear strength). For liquefaction that is confined to a zone, the mode of movement may involve a block (or a plug) of relatively intact material sliding along a liquefied underlayer.

(b) Shearing failure of the fill slope along a sliding surface. This may take place for an oversteep slope with sufficient compaction of the fill to prevent liquefaction failure. Retrogressive failure can occur as a result of stress redistribution and load transfer.

(c) Major washout of the fill mass caused by concentrated flow of surface water.

Localized Failure

(a) Local shearing failure of the fill slope caused by localized infiltration, leading to destruction of suction or build up of positive pore water pressure and sliding of a local area of fill.

(b) Minor washout of the fill mass caused by localized running surface water.

Water ingress into the slope can occur via surface infiltration through unprotected slope surface or slope crest, open trenches or excavations, subsurface seepage along preferential flow paths (e.g. erosion pipes) and leakage from water-bearing services. Apart from causing a rise in the main groundwater table and/or development of perched water tables, seepage pressure may also develop due to flow with a horizontal component where there is layering in the loose fill. The type and scale of failure is closely related to the amount of water ingress and its pathway.

As water is one of the primary contributory factors in triggering a failure, it is important to pay special attention in design to minimise surface infiltration and rectify conditions liable to give rise to uncontrolled discharge of surface water, such as overspill of surface water from roads, building platforms or blocked drainage channels. In addition, the potential for significant subsurface seepage and rapid rise in the main groundwater table (large catchment in the upslope area, presence of subsurface flow paths or streamcourse, adverse topography that promotes ponding in the slope crest, etc) should also be considered.

3.2 Review of Fill Slope Failures in Hong Kong

A detailed review of the available global failure statistics of fill slopes in Hong Kong for the years 1984 to 1995 has been carried out (Wong et al, 1997a). The average rate over this period of fill slope failure is estimated to be about 1 in 525 per year. Annual frequencies of occurrence of the different failure mechanisms for fill slopes of different heights and involving different failure volumes are also given by the review. Out of a total of over 250 failures reviewed in detail, 70% of the incidents involved a failure volume of less than 20 m^3, 15% involved a failure volume of between 20 m^3 and 50 m^3, and the remaining 15% were "major" incidents, i.e. with a failure volume of greater than 50 m^3.

Of the "major" fill slope failures, 33% involved a "sliding" type failure with little or no influence of surface water, 7% involved liquefaction of loose fill, 38% involved "washout" and 22% involved rupture of water-carrying services.

The available data indicate that the lower bound slope gradient involved in fill slope failures was about 25°. However, it should be noted that the possibility of failures involving more gentle slopes that have not been included in the landslide database cannot be ruled out.

3.3 Runout of Landslide Debris from Fill Slope Failures in Hong Kong

Wong & Ho (1996) noted that the mobility of landslide debris will be greatly affected by, inter alia, the mechanism and scale of failure. The available information on debris mobility for fill slope failures expressed in terms of travel angles (i.e. angle of reach) is shown in Figure 11. It can be seen that the travel angles generally vary between 30° and 40° for sliding failures. For liquefaction failures, the travel angles are typically between 15° and 28° while for major washout failures, the travel angle is between 18° and 34°.

3.4 Review of Notable Fill Slope Failures Reported in the Literature

Bishop (1973) provided detailed accounts of several flowslides, including the failure of colliery waste dump in Aberfan and emphasized the importance of brittleness of the loose material. Siddle et al (1996) also gave details of a number of liquefaction failures of colliery spoil slopes.

Flowslides of loose colliery waste exhibit highly mobile behaviour. Dawson et al (1992) reported the failure of a coal waste dump at Greenhills mine in Canada. A 100 m high stockpile of colliery waste failed and about 150000 m^3 of waste flowed downslope for some 700 m. Prior to the failure, there were no signs of instability. A 1 m thick layer of finer, wet material found adjacent to the failure zone was suspected to have played an active role in this failure.

Similar failures of stockpiles of coking coal in Australia were noted by Eckersley (1990). These failures involved "up to 10000 tonnes of coal slipping and flowing up to 60 m out from the toe of the initially 10-14 m high stockpile in 10 to 20 s".

Thus, it may be seen that major mobile failures of fill slopes, most of which occurred

as rapid events, have been observed in materials other than soils.

3.5 Model Tests on Loose Fill Slopes

The potential failure mechanism associated with static liquefaction has been investigated using model tests in the laboratory.

Mobile failures of Canadian quick clay slopes were studied in a centrifuge by Schofield (1980). It was noted that the behaviour of the material was affected by the presence of bonding in that the bonded soil collapsed rapidly only when tensile cracking formed with rapid and drastic changes in permeability.

Eckersley (1990) reported the results of laboratory tank tests of coal stockpiles. Flowslide was found to initiate under essentially drained conditions by a slowly rising water table. Measurements indicated that excess pore water pressure was generated during failure prior to significant movement of the stockpile. The displacements induced by the rise in water table were accompanied by a rapid generation of excess pore pressure in the shear zones and loss in undrained shear strength, resulting in a sudden acceleration of the sliding mass. Retrogressive failure mechanisms were developed in a rapid manner. The time between the initiation of building up of excess pore pressure and termination of movement was less than five seconds. Eckersley (op cit) concluded that static liquefaction was a result, rather than the cause, of shear failure, and that this can be initiated in drained slow loading events. Shear failure was followed almost immediately by rapidly sliding of the soil mass because of the brittle nature of the metastable soil structure and the processes are practically spontaneous.

As part of the Canadian Liquefaction Experiment (CANLEX), Phillips & Byrne (1994) investigated the phenomenon of static liquefaction of a submerged 16° loose sand slope in a centrifuge. There was a time-lag of about three seconds between the application of a dead weight on the slope crest and the development of a shear plane. The maximum pore water pressure response as observed from the pore pressure transducer occurred five seconds after load application. Liquefaction of the loose sand caused the debris to flow giving rise to a travel angle of 7° which reflects the mobile nature of the debris.

4. CONCEPTUAL FRAMEWORK FOR BEHAVIOUR OF LOOSE GRANULAR SOILS

4.1 Critical State Concept

For a granular soil, there is a set of combination of critical void ratio and confining stress under which shearing produces no change in volumetric strain. This state is referred to as the ‘critical state’ and may be defined as the state in which the soil element is continuously deforming at constant volume, constant mean effective stress and constant shear stress. The term ‘steady state’ is also used. According to Castro and Poulos (1977), “the steady state deformation is achieved only after all the particle orientation has reached a statistically steady state condition and after all particle breakage, if any, is complete so that the shear stress needed to continue deformation and the velocity of deformation remain constant”. In practice, the two definitions lead to the same set of soil parameters. For consistency, the term critical state is used throughout this Report.

The critical state strength is related to the void ratio of the material and is independent of initial stress conditions or stress path.

4.2 Collapse Surface Concept

Loose metastable granular soils that are on the 'wet' side of critical state are liable to abrupt strain weakening when sheared under conditions of negligible volume change. The sudden loss of strength is due to the collapse of the metastable soil structure. When the soil structure collapses under shear, excess pore water pressure is generated rapidly. Where this occurs over a sufficiently large mass of soil in a slope, a highly mobile failure, sometimes referred to as 'liquefaction flowslide', may take place.

A liquefaction flowslide is described by Hutchinson (1988) as an event "characterised by the sudden collapse and extensive, very to extremely rapid runout of a mass of granular material or debris, following some disturbance. An essential feature is that the material involved has a metastable, loose or high porosity structure. As a result of the disturbance this collapses, transferring the overburden load wholly or partly onto the pore fluid, in which excess pressures are generated. The consequent sudden loss of strength gives the failing material, briefly, a semi-fluid character and allows a flowslide to develop".

The brittle characteristics of the material is described by the undrained brittleness index (I_b) which is defined as follows:

$$I_b = \Delta q / q_{max} \quad \text{..... (1)}$$

where Δq = difference between peak and critical state deviator stress
q_{max} = peak deviator stress

Sladen el al (1985) observed that for a given void ratio, the peak strengths of soil samples tested at different confining stresses lie on a straight line that joins the point of initiation of collapse to the critical state in q-p' space, where p' is the mean effective stress. This is referred to as the collapse surface (Figure 12). It is noteworthy that the apparent angle of shearing resistance mobilised at collapse (ϕ_{app}') is less than the critical state strength (ϕ_{cv}'). Similar observations were made by Lade (1992) who denoted the collapse surface as the instability line.

Triaxial tests using different stress paths, such as reducing p' at constant q (i.e. dead load test), on a saturated loose sand by Sasitharan et al (1993) confirmed the validity of the collapse surface concept. Sasitharan et al (1994) also showed that the post-peak portion of the stress paths from undrained triaxial compression tests forms a boundary surface corresponding to a specific void ratio.

Strain softening occurs when a stress path tries to cross the collapse surface. In the event the rate of collapse is rapid compared with the rate of drainage, the resulting stress path will travel downwards along the collapse surface towards the critical state under undrained, no volume-change, condition and the loose sand loses strength with further straining (i.e. it exhibits strain-softening behaviour).

Sasitharan et al (1994) found from tests with a stress path corresponding to that in a conventional dead load test which simulates the condition of rising pore water pressure in a slope that the axial strains were only of the order of 0.5% prior to collapse. Large shear strains (of the order of 5% to 10%) were observed when the soil sample reduced rapidly from its peak strength at collapse to critical state strength.

It is important to note that although the framework of critical state and collapse surface defines the necessary boundary conditions for collapse, they are not sufficient conditions. Two conditions must be satisfied for collapse and subsequent strain-softening behaviour to occur (Dawson, 1994):

(a) the triggering stress path must approach the collapse surface in such a fashion as to force a rapid, rather than gradual, structural rearrangement, and

(b) pore pressures must be sufficiently impeded during structural collapse so that excess pore pressures develop and a significant loss of strength occurs.

In other words, collapse must be triggered and pore pressures sufficiently impeded to produce a mobile flow.

Dawson et al (1994) suggested that loading paths that result in decreases in mean effective stresses accompanied by small volume changes are particularly prone to collapse. They also noted that collapse might be triggered by high shear strains, weathering, creep and other processes, such as foundation strains.

If the material is saturated or near-saturated during collapse of the soil structure, then excess pore water pressures could develop leading to a liquefaction flowslide, provided the drainage is impeded due to geometry (i.e. distance to drainage boundary) or low permeability of the material. Sassa (1985) demonstrated that a degree of saturation of about 85% may initiate sufficient excess pore water pressures to cause liquefaction of "torrent deposits" with an initial void ratio of 0.8.

Although critical drainage lengths and permeability values have not been measured for the collapse process, most sands may exhibit sufficiently low permeability values to sustain excess pore water pressures if structural collapse is initiated (Dawson, 1994).

It is important to note that triggering of localised yield zones in a strain-softening material in a slope will cause stress redistributions that could lead to progressive failure. The release of unbalanced driving shear stress from the peak to critical state must induce redistribution of stresses in a slope. If these stress redistributions are not contained, overall collapse can result from progressive failure. Apart from the low strength of the collapsed material, significant unspent collapse energy at failure may also contribute to the high mobility of the debris runout.

Skopek et al (1994) showed that dry sand could also exhibit collapse behaviour at a strength less than that given by ϕ_{cv}'. In a collapsing dry sand, the sudden volume change may not be sufficiently impeded (because air is compressible whereas water is relatively incompressible) and thus a drop in shear strength commensurate with excess pore pressure

development does not take place. Therefore, the collapse of a dry material results in a less mobile flow than the collapse of the same material in a wet state. In this regard, a loose crushed rock fill is expected to behave like a dry sand on collapse due to its lower water retention potential.

De Matos (1988) suggested that liquefaction of unsaturated soils can be accomplished through the state boundaries associated with different void ratios as volumetric strain caused by the collapse of soil structure may lead to saturation of the soil. However, the presence of occluded bubbles is likely to give rise to a strength that is higher than the saturated strength. Also, the infiltration potential of a partially saturated soil will be less than that of a saturated soil because of lower permeability.

4.3 Practical Implications of Collapse of Loose Granular Soils

The collapse behaviour of loose granular soils has the following important practical implications on loose fill slopes:

(a) Mobile failure may potentially be triggered on a relatively gentle slope comprising loose granular soils through wetting due to infiltration because of collapse of the soil structure at a mobilized strength that is much smaller than that given by ϕ_{cv}'. The wetting reduces any suction present in the soil, leading to a lowering of p' of the soil elements essentially under the same shear stresses. Potential for failure initiation will further increase (i.e. failure initiation at a lower slope angle still) if significant seepage pressure builds up in the soil mass due to non-vertical descent of surface infiltration as a result of layering of the soil.

(b) There may be little prior warning (in the form of signs of distress) before a sudden failure takes place.

(c) The sudden collapse of the metastable structure (i.e. the starting point of the subsequent liquefaction process) dictates the initiation of failure. Although liquefaction may in principle be interpreted as a consequence of shearing failure on wetting and that the wetting that triggers slope failure is effectively a drained process, it will be unsafe even if ϕ_{cv}' is taken as the operational strength in stability assessment in the case where the soil is susceptible to "collapse". This is because liquefaction failure may be initiated at a much lower shear strength.

(d) Conventional limit equilibrium calculations based on 'generalised' shear strength parameters for fill in Hong Kong (e.g. 33° to 36°) are not necessarily conservative if the fill material is prone to collapse with markedly strain-softening behaviour.

4.4 Factors Affecting the Potential for Collapse

The static collapse potential of a soil element is defined by the collapse surface and the critical state strength.

Sladen et al (1985) reported that the gradients of the collapse surface of a sand in q-p' space were identical under different void ratios and different critical state strengths. Hird & Hassona (1990) suggested that the gradient of the collapse surface increases with increasing angularity of the sand grains.

Poulos el at (1985) showed that the intercept of the critical state line in e-ln p' space is related to particle size gradation but that its slope is mainly affected by grain shape.

De Matos (1988) showed that the effects of grading on critical state parameters can also be dramatic. At a given confining stress, the critical state void ratio in e-ln p' space decreases with increasing uniformity coefficient. Thus, a very broadly graded sandy soil is comparatively more susceptible to collapse than a uniform soil for a given initial state (i.e. at a given initial stress level and density). De Matos (op cit) also suggested that liquefaction can take place in a well-graded material with an initial void ratio as low as 0.3 (presumably at a high confining stress level).

The above trends may also be influenced by the fines (viz. clay and silt) contents. Hird & Hassona (1990) demonstrated that the presence of small amounts (greater than 10%) of fine mica particles reduces the liquefaction potential of fine sands. This is possibly associated with fines filling voids in the sand skeleton, making it less likely to collapse. Also, the fines may be subjected to swelling on reduction of p' during wetting. Compressibility of the soil was suggested to have a major influence on undrained brittle behaviour in that as compressibility increases, brittleness appears to decrease (Dawson, 1994).

Dawson et al (1994) showed that the gradient of the collapse surface of a friable sandy gravelly soil in q-p' space decreases with increasing confining stress which suggests that crushing during consolidation may reduce the brittleness potential.

De Matos (1988) suggested that the collapse potential may be reflected by a simple parameter termed compactability (F_c) which reflects the nature of soil particles (e.g. shape, texture, size and crushing strength). F_c is defined as follows:

$$F_c = \frac{e_{max} - e_{min}}{e_{min}} \quad \text{..... (2)}$$

where e_{max} and e_{min} are the maximum and minimum void ratios respectively.

In practice, it is very difficult to determine e_{min} consistently for soils with a significant amount of silt-sized and finer particles, such as that in granitic or volcanic saprolites in Hong Kong.

Investigation into the influence of fines contents on the collapse potential of reconstituted loose sands has been carried out by Hird & Hassona (1990), Pitman et al (1994) and Skirrow & Robertson (1994). The fines were found to affect the interaction of the soil

grains and change the position of the critical state line hence affecting the static liquefaction potential of the soil at a given initial state. For Ottawa sand and Leighton Buzzard sand, a fines content in excess of 20% was found to reduce the brittleness significantly.

The critical state and collapse surface parameters reported in the literature are summarised in Table 2. Most of the soil specimens tested were either of sedimentary or glacial origin and the apparent ϕ' values mobilised at collapse for a given deviator stress, ϕ_{app}', range from 10° to 30° with an average value of 18°. The equivalent ϕ' values of the collapse surface (ϕ_{col}') were found to vary between 12° and 22° with a mean value of 17°. Figure 13 shows the relationship between ϕ_{col}' values and the corresponding state parameters as defined by Been & Jefferies (1985). There is no strong trend in Figure 13 which may be due to results from different sources and different materials being combined or that the state parameter is not a particularly good correlation parameter.

4.5 Behaviour of Soils with a Metastable Structure

Soils derived from insitu weathering of rocks can exhibit different engineering characteristics compared to transported soils of similar particle size distributions and plasticity characteristics (Massey et al, 1989). The soil may be in the form of aggregations of clay particles and its behaviour can be complex because of mechanical and chemical effects associated with hydrothermal alteration and weathering.

Residual and saprolitic soils are derived from weathering of the parent rocks under sub-tropical conditions. Crystallization associated with the formation of new minerals, precipitation of mineral salts and leaching due to solution of certain minerals can generate inter-particle bonding and a porous structure. Prior to breaking down of the soil structure, the behaviour of the natural soil will be controlled by the structure more than by its state (i.e. stress and density). Upon undrained shearing, the progressive breakage of the bonded soil structure will eventually lead to overall collapse which may be expected to result in rapid and significant strain softening. Leroueil & Vaughan (1990) postulated that a bonded material may exist in a state that is only possible due to presence of structure and/or bonding and where large plastic strains are unlikely. However, the structure may be metastable and large strains will develop when yielding occurs in the 'structure-permitted' stress space. Also, soils in the 'structure-permitted' state with a high degree of saturation may sustain severe loss of undrained strength and large sensitivity if it is sheared under undrained conditions. Burland (1990) also suggested that fabric and bonding can have a significant effect on the behaviour of natural clays.

For fill materials comprising decomposed granite or volcanics, grain angularity is expected to be high and the corresponding collapse surface in q-p' space, if it exists, can be expected to be relatively steep.

There is a dearth of good quality test data on local granitic and volcanic fill. Gray (1980) observed collapse behaviour of a loose granitic fill from King's Park (void ratios ranging from 0.75 to 0.78) in undrained triaxial compression tests. The test results indicate a ϕ_{app}' value of 29° to 31° and that the average gradient of the collapse surface in p'-q space is 1:1, corresponding to a ϕ_{col}' value of 25° (Figure 14). The corresponding results of isotropic compression tests prior to undrained shearing are shown in Figure 15. It can be seen that

some specimens were at a looser state than that of the normally consolidated state at a given pressure. This is evidence of soils with structure or bonding. As the consolidation pressure increased, the structure was progressively destroyed as shown in Figure 15.

5. NUMERICAL MODELLING OF STATIC LIQUEFACTION OF LOOSE FILL

5.1 General

Various constitutive soil models have been developed by different researchers to facilitate assessment of the collapse behaviour of loose soils through numerical modelling. In this Section, selected models that have been successfully implemented are reviewed. The numerical model that has been developed to study the failure trigger mechanics and nature of progressive failure in a loose material is then described. The model was applied to back analyse the 1976 Sau Mau Ping failure to assess the usefulness of the numerical model in understanding the mechanism of failure.

5.2 Numerical Models to Simulate Static Liquefaction

5.2.1 General

While simplified soil models may be used for modelling static liquefaction in situations involving no changes in void ratio or water flow during the course of collapse, more complex liquefaction models have also been developed to account for volumetric strains coupled with groundwater flow. So far, the application of more complex liquefaction soil models has been limited to simple problems or assessment of single-element behaviour.

5.2.2 Molenkamp's Model

Molenkamp (1981) developed a double-hardening plastic constitutive law. Figure 16 shows the failure surface and the two yield surfaces in q-p' space for dense and loose sands. Plastic volumetric strain is generated by the expansion or contraction of the isotropic (i.e. mean stress compression) and deviatoric (i.e. shear) yield surfaces. The failure surface for a dense sand is above the critical state line ($q = M\ p'$), and vice versa for a loose sand. Contractive strain is associated with the expansion of the deviatoric yield surface beneath the critical state line, while dilation will take place when it expands above the critical state line.

For a loose sand subjected to undrained loading, due to the constant volume condition, the expansion of the deviatoric yield surface is always enclosed by the failure surface, which is equal to the critical state line, and can result in stress paths being constrained to reach very low effective stress and shear strength, leading to liquefaction.

Using a general-purpose finite element computer program, Hicks & Wong (1988) carried out a series of analyses to investigate the use of the proposed soil model in comparison with the conventional Mohr-Coulomb model with regard to initiation of liquefaction of a submerged loose soil slope under different loading conditions. Marked differences were noted between the results from the two soil models. Contractive behaviour of the loose soil was shown by the double-hardening model. The conventional Mohr-Coulomb model predicted a much higher failure load than the Molenkamp model. This suggests that the

former model can be unsafe as the collapse behaviour of the soil is not accounted for in the assessment.

5.2.3 Gu's Model

A finite element model has been developed at the University of Alberta by Gu (1992) to simulate static liquefaction under a constant void ratio "undrained" condition, . The model incorporates the essential elements of critical state and collapse, loading and stress redistribution necessary for evaluating liquefaction. Liquefaction is assumed to take place in the constant volume plane and thus volumetric strains are taken to be negligible (i.e. pore pressure dissipation is very small) over the period involved. This is applicable where the abrupt collapse of the soil structure gives rise to a rate of build-up of pore water pressure that is much faster than the rate of dissipation. The model was used by Dawson et al (1992) to simulate the development of the collapse process for coal and mine waste stockpiles in several case histories. It was also used by Gu et al (1993) to analyse the post-earthquake progressive failure of a dam.

In the model, the stress-strain behaviour of liquefiable materials in the constant volume plane is divided into three zones defined by the critical state strength and the collapse surface, as shown in Figure 17 and described below.

Zone 1 is applicable for soil elements subjected to initial loading as well as elements taking up the unbalanced loads due to stress redistribution resulting from collapse of other soil elements. Linear elastic stress-strain behaviour is assumed. The stress paths of the soil elements in this zone are defined by incrementally changing the pore pressure parameter "A".

Zone 2 is applicable for soil elements which exhibit collapse and strain softening behaviour. Along the collapse surface, the reduction in shear strength is defined by an inverse hyperbolic stress-strain model (Figure 17). Excess pore water pressure will build up with increasing shear strain as the stress path is constrained to descend along the collapse surface towards critical state condition. Unbalanced loads which arise from soil elements in Zone 2 are transferred to adjacent elements leading to progressive failure.

For soil elements in Zone 3, a elasto-plastic stress-strain model is used. The stress path is constrained to travel down the critical state line. Excess pore water pressure increases upon collapse of the soil structure resulting in reduction of the mobilised undrained shear strength.

Following application of initial loading, unbalanced loads which arise in any of the soil elements are shed to elements capable of taking additional loading, and the system is brought to equilibrium by iteration. Non-convergence of the analysis during the iterative process means that equilibrium cannot be attained and failure is imminent. Further deformations are controlled by large-strain deformation processes.

Dawson et al (1992) made the following observations from their finite element studies:

(a) non-liquefiable material may yield and a collapse mechanism may form as a result of stress redistribution caused by liquefaction in other parts of the slope,

(b) where the non-liquefiable zone is large enough and has the capacity to withstand the loads shed onto it from the initial liquefaction zone, the subsequent yielding of this zone due to further stress transfer arising from continuing strain softening could release the accumulated strain energy and result in a sudden brittle failure of the slope with little prior warning and a potentially very mobile failure mass, and

(c) only a relatively small portion of the slope needs to be potentially liquefiable and saturated for a collapse mechanism to form and result in a flowslide.

5.2.4 Other Liquefaction Models

Other more complex liquefaction soil models have also been developed, see for example De Prisco et al (1993 & 1995) and Gu et al (1995). These models are characterised by mixed isotropic compression and shearing hardening laws and the continuous yield surface may widen, rotate and change shape with plastic straining. However, such models appear to be applicable to only single element behaviour at present and are yet to be implemented in a general continuum computer program for the analysis of loose fill slopes.

6. NUMERICAL MODELLING OF THE 1976 SAU MAU PING LANDSLIDE

6.1 The 1976 Sau Mau Ping Landslide

On the morning of 25 August 1976, following heavy rainfall associated with severe Tropical Storm Ellen, a very destructive landslide occurred at the Sau Mau Ping Resettlement Estate. In all, four landslides took place, all resulting from the collapse of the side-slopes of highway embankments formed of granitic fill. Three of these turned into flow slides. The most fatal one occurred on the face of an approximately 30 m high 33° embankment with a 2.5 m high toe wall. An occupied public housing block was situated less than 20 m from the toe of this slope.

The debris of the most fatal landslide moved downwards until it was arrested by building block no. 9, the ground floor rooms of which were inundated by fluid mud, trapping many occupants. Eighteen people were killed and 24 seriously injured. Subsequent investigation concluded that “These failures resulted from the development of a seepage condition within a wetted zone as water penetrated into the face of the slope. Consequent loss of strength in the fill resulted in downhill movement and an almost instantaneous conversion of the slope into a mud avalanche with considerable destructive energy” (Hong Kong Government, 1977). The investigation also identified that the collapse occurred because the fill forming the face of the slope was in a loose condition, having been placed by end-tipping without compaction.

According to eye witnesses, the main landslide “moved first as a whole: “Bare earth” above the moving sheet of soil as viewed from the bottom and as a “large sheet”, covered with bushes as viewed from the top of the slope - view restricted, however, by market stalls and long grass”, and the speed of the landslide “was like that of ‘a child on a playground

slide' and did not increase much".

The volume of the failure was about 4000 m^3 and the failure zone was generally confined to the top 3 m of the slope. A cross section through the landslide is shown in Figure 18.

6.2 Analysis of the 1976 Sau Mau Ping Landslide

6.2.1 General

A static liquefaction soil model (viz. the SP model) similar to that adopted by Gu (1992) has been developed as part of this project. The model was implemented in the finite difference computer program FLAC (version 3.3) for a preliminary analysis of the failure mechanism associated with liquefaction of the loose fill slope at Sau Mau Ping. The SP model considers undrained collapse brought about by water infiltration into an initially unsaturated slope. Details of the soil model are given in Appendix A.

Two sets of preliminary numerical calculations have been carried out to examine the application of this numerical modelling technique. The first set of analyses was designed to simulate the progressive development of the failure mechanism due to collapse caused by surface infiltration. The second set of analyses was to investigate the mobility of the landslide debris.

The models were set up under two-dimensional plane strain conditions to represent a 30.6 m high fill slope above a 2.5 m high toe wall. The inclination of the fill slope is taken as 33° to the horizontal. Liquefaction due to surface infiltration to 3 m depth was simulated.

6.2.2 Initiation of Liquefaction

In the first set of analyses, the top 5 m of the fill was represented by 5 layers of finite difference zones (Figure 19). In the second set of analyses, a comparatively coarser grid was adopted (Figure 20) and interface elements were used to allow the failed mass to detach completely from its original position. The resistance provided by the walls of the housing block was also accounted for approximately. In order to properly incorporate the effects of the momentum generated by the out-of-balance forces in the progressive failure mechanism, the dynamic modelling option available in FLAC was adopted for both sets of the analyses.

The various stages of modelling in the assessment of failure mechanism are summarised below. A more comprehensive description of the approach and parameters adopted is given in Appendix A.

Stage 1 (Construction of fill slope) - The fill slope was gradually built up in layers parallel to the slope surface. In the calculation of stress distribution, plastic yielding (corresponding to a strength envelope of $c' = 0$ kPa and $\phi' = 35°$) was permitted under the condition of zero pore water pressure.

Stage 2 (Surface infiltration) - The partially saturated state of the fill was modelled by assigning a suction of 80 kPa throughout the fill slope. The suction in the top 3 m of the fill

was reduced decrementally (Δu = 0.01 kPa per calculation step) so that stress paths with reducing p' at a constant q were followed. The reduction of suction was applied uniformly and once it was completely removed, positive pore water pressure was allowed to build up linearly with depth within the top 3 m of the slope. This in essence models the formation of a perched water table in the fill slope. The increase in pore water pressure was continued until the effective stress path in any one loose fill zone intercepted the collapse surface.

Stage 3 (Development of failure mechanism) - As soon as liquefaction or collapse started within any one zone, the modelling of infiltration was terminated. The development of the failure mechanism was modelled by continuing the time-stepping calculations for a prototype time of nine seconds. It should be noted that the rate of development of the failure mechanism is slightly different to that given by the analysis of mobility of the landslide debris because of the different formulations assumed. This aspect is discussed further in Section 6.2.3. The computed displacement vectors, distribution of shear strain, extent of liquefaction and the distribution of pore water pressure are shown in Figures 21 to 24 respectively.

Based on the results of the analyses, the following observations can be made:

(a) Liquefaction failure can be induced by water infiltration down to a certain depth. For the selected critical state parameters and void ratio (which have been interpreted from the results of tests for the Sau Mau Ping investigation) for the soil and assuming a homogeneous and isotropic material, liquefaction caused by infiltration was not predicted for the upper 2 m. For the parameters considered, collapse was induced when surface infiltration reached 3 m depth and hence the predicted depth of failure is between 2 m and 3 m.

(b) A failure mechanism involving the development of a shear band can be initiated by localized liquefaction due to surface infiltration. For the slope studied, liquefaction appears to initiate near the toe. An unstable failure mechanism is liable to develop rapidly by stress redistribution because of the inherent strain-softening characteristics of the soil.

(c) Some numerical problems were encountered with the distribution of excess pore water pressure within and outside the sliding mass. As the prototype time increases with further time stepping, the unbalanced force in the system increases progressively. At the same time, the pore pressure calculations became less realistic. This is because the algorithm of sharing of common pore pressure nodes between a zone undergoing liquefaction and an adjacent stable zone which is partially saturated led to an increase in pore pressure in the unsaturated zone inducing a deeper sliding zone beyond the depth of infiltration.

6.2.3 Mobility of Landslide Debris

The simulation stages for the modelling of debris mobility are summarised below. Appendix B presents the details of the approach and parameters adopted.

Stage 1 (Construction of fill slope) - The fill slope was built up in two stages by depositing layers parallel to the slope surface. After the bottom layer and the toe wall were built, the top 3 m of loose fill was modelled. In the calculation of stress distribution, plastic yielding (corresponding to a strength envelope of $c' = 0$ kPa and $\phi' = 35°$) was permitted under the condition of zero pore water pressure.

Stage 2 (Surface infiltration) - The partially saturated state of the fill was modelled by assigning a suction of 60 kPa throughout the fill slope (instead of 80 kPa used before in order to reduce computing time given the different objectives of this series of analyses). The suction in the top 3 m of the fill was reduced decrementally ($\Delta u = 0.01$ kPa per calculation step) in the same way as for the analysis for initiation of liquefaction failure described above.

Stage 3 (Development of failure mechanism) - As soon as liquefaction or collapse of soil structure started within any one zone, the modelling of infiltration was terminated. To allow for complete detachment of the sliding mass in the later stages of the calculation, a thin slice of the finite difference zones at 3 m depth was replaced by a series of interface elements, each of which represented the interface frictional behaviour of the sliding mass. For each interface, an undrained shear strength was assigned with account taken of the relative displacement between the sliding mass and the underlying stable material. The undrained shear strength of the interface was reduced in accordance with the same stress-strain relationship as for the collapse soil model (Appendix A). In the calculation of shear strain from relative displacements parallel to the direction of the interface, the shear band was taken to be 250 mm thick nominally. Compared with the 1 m thick finite difference zones in the analysis for modelling of initiation of liquefaction failure, the 250 mm thick shear band adopted in the analysis produced a faster stress redistribution and development of the overall sliding mechanism. Undrained steady state shear strength was expected to be attained fairly quickly after initiation of collapse, the thickness of the sliding surface would become less sensitive as far as debris movement is concerned. As the model was intended to give a preliminary assessment of debris runout, a single nominal thickness was considered adequate for the purpose.

Stage 4 (Debris runout) - Using the dynamic modelling option in FLAC, time stepping was carried out to simulate the runout of the landslide debris up to a prototype time of about 5 seconds. The debris sled over the toe wall and landed on the ground behind the housing block. With further time-stepping, it then travelled forward and hit the building. The resistance provided by the housing block to the movement of the debris was not known precisely. Based on energy considerations, the basal shear resistance of the debris within the width of the building was taken to be proportional to the square of the speed of the debris as a first approximation. The calculated profiles of the debris at different times are shown in Figure 25. The calculated time history of horizontal velocity is shown in Figure 26.

Based on the results of the analyses, the following observations can be made:

(a) Due to stress redistribution along an interface with strain-softening characteristics, a failure mechanism involving a

shear band can develop leading to sliding and rapid detachment of the failure mass.

(b) The maximum velocity of the landslide debris was estimated to be about 10 m/s from the analysis which appears to be of the right order according to eye-witnesses' accounts. The actual velocity of the debris is likely to be affected by the stress-strain behaviour of the material during motion, thickness of the shear band, pore water pressure generation and consolidation of the sliding plane. All these parameters are subject to considerable uncertainties and cannot be easily verified in practice.

(c) The time-stepping analysis was not completed because of some numerical problems. Due to 'locking up' of the finite difference grid modelling gross deformation of the landslide debris, the final stage of the analysis was terminated shortly after the debris entered the housing block.

6.3 Uncertainties in the Assessment of Liquefaction of Loose Fill

Although the framework for describing liquefaction of loose fill is reasonably advanced, there remain some uncertainties in extending it directly to predict the behaviour of local fill materials. The main uncertainties relate to the quantification of the triggering condition for liquefaction to initiate, as well as of degree of post-peak reduction in strength and the corresponding stress-strain characteristics.

The following are some of the factors that need to be investigated:

(a) Effects of particle size distribution, texture, shape, crushing strength and permeability of the soil. These could have a bearing on the soil's critical state strength and collapse behaviour. The fines content, in particular, may have a significant effect on the collapse potential. It should be noted that local loose fills are mostly derived from weathered rocks, which can have different engineering properties compared to those of sedimentary soils.

(b) Effects of partial saturation and the wetting-drying history of the soil. These may affect infiltration/wetting potential of the soil and the collapse behaviour.

(c) Possible effects of ageing and bonding of the soil. These may influence the field behaviour. It is expected that some disturbance is needed to cause a lightly cemented, high porosity material to collapse (which could be by way of sudden impact loading of the loose material from debris of upslope failure). Once disturbed, the degree of brittleness

of the soil may be more pronounced compared to that of an uncemented soil.

(d) Effects due to spatial variability of the fill material in the field. These may affect the development of the collapse mechanism and propagation of failure.

(e) Effects of wetting of loose fill at some depth below ground surface, instead of infiltration from the top.

(f) Effects of fill slope angle, post-collapse shear strength and downslope topography and obstacles on travel of debris downslope.

6.4 Discussion

Some numerical problems related to the evaluation of excess pore water pressures were encountered during the latter stages of the calculation of debris movement. This was partly related to the assumptions made in the algorithms regarding sharing of common pore water pressure nodes between a zone undergoing liquefaction and the adjacent unsaturated zone, and partly because of the very complex situation involving large strain flow processes that are being modelled. Notwithstanding this, the preliminary analyses are able to illustrate the triggering mechanism and stress redistribution involved in the progressive failure of a brittle material. The behaviour (both in terms of failure trigger and mode of movement of the failed mass) predicted by the liquefaction model was generally consistent with observations made of the 1976 Sau Mau Ping landslide. The preliminary model used to assess the mobility of failure debris was also able to approximately replicate the observed profile of the landslide debris.

The inherent uncertainties in the characterisation of fill materials at Sau Mau Ping and the simplifying assumptions necessary for numerical modelling prevent a precise back analysis of the operational shear strengths. Nevertheless, the reasonable matching of the analyses (based on best estimates of material properties interpreted from the available data) with observations suggests that the presence of collapsible materials was likely to have played an important role in the failure.

The analyses indicate that a complete evaluation of loose fill slope failure will require assessment of the following:

(a) the amount of potentially liquefiable material in the slope based on an evaluation of the insitu distribution of void ratio of the fill and the static stress field with respect to the critical state line and collapse surface,

(b) whether collapse can be initiated due to water ingress, taking into account soil permeability and any layering or voids observed, and

(c) the effects of stress redistribution causing overall instability

leading to collapse and flow slide.

7. INVESTIGATION OF FILL SLOPES

The methods adopted for routine investigation of fill slopes, which include trial pitting, drillholes, GCO probing, insitu density and standard compaction tests and determination of particle size distribution of the fill, are discussed by Yim & Siu (1997) and will not be repeated here. However, a number of pertinent issues which should be borne in mind in the investigation phase are highlighted below.

Aerial photographs, especially low altitude ones if available, could be very useful for assessing the site history, the likely lateral extent of filling, as well as for identifying the presence of any surface and buried water pathways that may affect the stability of the fill slope. Aerial photograph interpretation and a careful examination of old and recent topographical maps should be carried out prior to any field work to verify the findings of the desk study.

Apart from the conventional ground investigation techniques, geophysical methods may also be considered to determine the properties and extent of the fill. Recent trials involving the use of non-invasive technique (ground penetrating radar, resistivity imaging, frequency domain electromagnetic conductivity and spectral analysis of surface waves) during the Site Characterisation Study (Koor, 1997) reveal only limited success in assessing the thickness of loose fill in a slope. The interface between an upper layer of denser fill and the underlying layer of loose fill was reasonably interpreted but the techniques used were not able to delineate the depth of the loose fill zone. Further work is needed to identify more effective methods to establish the extent of loose fill and any layering and voids present in the fill body.

It is important that the field density should be determined with reasonable accuracy for the assessment of collapse potential. Sand replacement tests, which are commonly used in routine investigations, may be subject to errors where there are coarse fractions in the material. In such instances, consideration should be given to adopting better techniques such as water replacement tests to determine the insitu density of the fill mass and its soil matrix.

Given the potential that a local zone of instability may lead to stress redistribution and the failure may propagate and develop into a global failure of the slope, care should be taken in the appraisal of the field data, particularly where there are persistent layers or zones of very loose materials within the fill body.

Particular attention should be directed to examining the fabric and layering of the fill as these can provide preferential flow paths and profoundly affect the development of pore water pressure in the fill slope.

The existence of a collapse surface which may give rise to mobilised shear strength that is much lower than the critical state strength means that it is important to impose the correct stress path to the test specimen.

A programme of systematic laboratory testing of local fill materials is in progress to determine the generalised behaviour of loose soils under shear. The results may provide a

reasonable basis for designers to assess the likely range of properties of loose soils. Alternatively, designers may opt to conduct site-specific conventional constant rate of strain undrained triaxial compression tests (and dead load tests if desired) at the appropriate range of stress levels and field densities. In such cases, the variability of the fill should be examined in selecting representative samples for testing.

If laboratory shear strength testing of loose soils is to be carried out, care could be taken to ensure that the specimens are prepared to model the stress and void ratio states in the field. There is a potential error in the determination of the specimen void ratio which can be attributed to densification during the saturation stage. Therefore, care should be exercised in using the test results in the assessment of the soil's susceptibility to liquefaction. Sladen & Handford (1987) reported that the volume change during saturation is much higher for silty sands than for clean sands. The use of carbon dioxide gas may facilitate subsequent saturation at a smaller back pressure compared to use of water to flush through the specimen but in any case void ratio changes during saturation should be measured and allowed for in the interpretation of test results. An assessment should also be made of the likely presence of hydrated minerals in the soil (e.g. by moisture content tests at 45°C and 105°C), as these can affect the accuracy of the void ratio calculation.

In the investigation of existing fill slopes, it should be borne in mind that failure modes other than liquefaction, such as sliding failure and washout, should be considered. Particular attention should be paid to examining the effects of water-bearing services and overspill of surface water from paved areas such as roads or platforms. Reference should be made to the guidance given by Works Branch (1996) on the inspection and maintenance of water-carrying services. Where practicable, diversion or ducting of water-bearing services and preventive surface water/road drainage works should be implemented.

8. CONCLUSIONS

Apart from being subjected to sliding and washout failures, fill slopes also pose the hazard of liquefaction which can result in flowslides where the soils are sufficiently loose and saturated and collapse of the soil structure is triggered by, say, water ingress during intense rainstorms. Given that liquefaction failures of loose fill slopes would involve very mobile debris with the potential for severe consequences (e.g. multiple fatalities), special attention needs to be directed to tackling such hazards.

With the recent advances made in the understanding of fundamental behaviour of loose fill material, it is now possible to explain the cause, trigger and mechanism of static liquefaction in a rational framework involving the concept of collapse surface. This is important, for instance, in the consideration of methods other than surface recompaction to upgrade loose fill slopes. A systematic laboratory investigation of the local fill materials will assist in assessing their collapse behaviour.

A numerical model which integrates collapse surface and critical state concepts has been developed during the course of this study to investigate the development of failure mechanism of a slope that is comprised of loose fill in an initially unsaturated state. This has been used in a back analysis of the 1976 Sau Mau Ping failure. Field stress paths corresponding to surface infiltration of rainfall were imposed. Although work may be carried out to further refine the model, the results from the present preliminary model were

able to demonstrate the nature of progressive failure involving stress redistribution in a strain-softening material. The preliminary model used to assess the mobility of the failure debris was also able to approximately replicate the observed profile of the landslide debris.

Numerical modelling shows that the collapse of a local saturated (or near-saturated) zone can trigger significant yielding of non-liquefiable materials leading to progressive failure. Failure may be rapid and fast-moving, depending on the degree of brittleness of the material. It is important to note that given unfavourable hydraulic boundary conditions, only a portion of the slope needs to be potentially liquefiable and saturated for a flowslide to develop. This suggests that a loose layer at some depth that is liable to become saturated or wetted up via subsurface seepage from the upslope area or rising groundwater table may trigger a global failure even if the slope has a surface cover to eliminate direct infiltration.

Liquefaction of loose fill can be triggered with little prior warning. Conventional limit equilibrium calculations based on 'generalised' shear strength parameters for fill in Hong Kong (e.g. 33° to 35°) are not necessarily conservative if the material is prone to collapse with markedly strain-softening behaviour.

9. REFERENCES

Been, K. & Jefferies, M.G. (1985). A state parameter for sands. Géotechnique, vol. 35, pp 99-112.

Bishop, A.W. (1973). The stability of tips and spoil heaps. Quarterly Journal of Engineering Geology, vol. 6, pp 335-376.

Burland, J.B. (1990). On the compressibility and shear strength of natural clays. Géotechnique, vol. 40, pp 329-378.

Castro, G. & Poulos, S.J. (1977). Factors affecting liquefaction and cyclic mobility. Journal of the Geotechnical Engineering Division, American Society of Civil Engineers, vol. 103, pp 501-506.

Chu, J. & Lo, S.C.R. (1992). Discussion on "The critical state of sands" by Been et al. Géotechnique, vol. 42, pp 655-663.

Chung, W.K. (1997). Private Communication.

Dawson, R.F. (1994). Mine Waste Geotechnics. PhD Thesis, University of Alberta, 239 p.

Dawson, R.F., Morgenstern, N.R. & Gu, W.H. (1992). Instability Mechanisms Initiating Flow Failures in Mountainous Mine Waste Dumps, University of Alberta, 80 p.

De Matos, M.M. (1988). Mobility of Soil and Rock Avalanches. PhD Thesis, University of Alberta, 360 p.

Di Prisco, Nova, R. & Lanier, J. (1993). A mixed isotropic kinematic hardening constitutive law for sand. Modern Approaches to Plasticity, edited by Kolymbas, D., Balkema, pp 83-124.

Di Prisco, C., Matiotto, R. & Nova, R. (1995). Theoretical investigation of the undrained stability of shallow submerged slopes. Géotechnique, vol. 45, pp 479-496.

Eckersley, J.D. (1990). Instrumented laboratory flowslides. Géotechnique, vol. 40, pp 489-502.

Gray, M.N. (1980). The Behaviour of a Granitic Soil in Shear. Two volumes. GCO Report No. 5/80, Geotechnical Control Office, Hong Kong, 224 p.

Gu, W.H. (1992). Liquefaction and Post Earthquake Deformation Analysis. PhD Thesis, University of Alberta, 308 p.

Gu, W.H., Morgenstern, N.R. & Robertson, P.K. (1993). Progressive failure of Lower San Fernando Dam. Journal of Geotechnical Engineering, Americian Society of Civil Engineers, vol. 119, pp 333-349.

Gu, W.H., Cathro, D.C. & Horne, W.T. (1995). On the yielding of collapsible soils. Proceedings of the 48th Canadian Geotechnical Conference, Vancouver, vol. 2, pp 971-979.

Hicks, M.A. & Wong, S.W. (1988). Static liquefaction of loose slopes. Proceedings of the Conference on Numerical Methods in Geomechanics, Innsbuck, edited by Swoboda, pp 1361-1367.

Hird, C.C. & Hassona, F.A.K. (1990). Some factors affecting the liquefaction and flow of saturated sands in laboratory tests. Engineering Geology, vol. 28, pp 149-170.

Hong Kong Government (1977). Report on the Slope Failures at Sau Mau Ping, August 1976. Hong Kong Government Printer, 105 p. plus 8 drgs.

Hungr, O., Dawson, R., Kent, A., Campbell, D. & Morgenstern, N.R. (1997). Rapid flow slides of coal mine waste in British Columbia. GSA Reviews in Engineering Geology (in press).

Hutchinson, J.N. (1988). Morphological and geotechnical parameters of landslides in relation to geology and hydrogeology. Proceedings of the Fifth International Symposium on Landslides, Lausanne, vol. 1, pp 3-34.

Konrad, J.M. (1993). Undrained response of loosely compacted sands during monotonic and cyclic compression tests. Géotechnique, vol. 43, pp 69-89.

Koor, N.P. (1997). Site characterisation study - Phases 1 and 2. Special Project Report No. SPR 8/97, Geotechnical Engineering Office, Hong Kong, 188p.

Ishihara, K. (1993). Liquefaction and flow failure during earthquakes. Géotechnique, vol. 43, pp 351-415.

Itasca Consulting Group (1995). FLAC - Fast Lagrangian Analysis of Continua, Version 3.3. Volume 1: User's manual.

Law, K.T., Shen, J.M. & Lee, C.F. (1997). Strength of a loose remoulded granitic soil. Proceedings of the Seminar on Slope Engineering in Hong Kong, Geotechnical Division of the Hong Kong Institution of Engineers, Balkema (in press).

Leroueil, S. & Vaughan, P.R. (1990). The general and congruent effects of structure in natural soils and weak rocks. Géotechnique, vol. 40, pp 467-488.

Lumb, P. (1975). Slope failures in Hong Kong. Quarterly Journal of Engineering Geology, vol. 8, pp 31-65.

Malone, A.W. & Pun, W.K. (1997). New engineering tools for landslip risk control. Proceedings of the Second International Symposium on Structures and Foundations, Hong Kong, pp 1-27.

Massey, J.B., Irfan, T.Y. & Cipullo, A. (1989). The characterization of granitic saprolitic soils. Proceedings of the Twelfth International Conference on Soil Mechanics and Foundation Engineering, Rio de Janeiro, vol. 6, pp 535-542.

Molenkamp, F. (1981). Elasto-plastic double hardening model MONOT. Delft Soil Mechanics Laboratory, Report No CO-218595.

Morgenstern, N.R. (1978). Mobile soil and rock flows. Geotechnical Engineering, vol. 9, pp 123-141.

Phillips, R. & Byrne, P.M. (1994). Modelling slope liquefaction due to static loading. Proceedings of 47th Canadian Geotechnical Conference, Halifax, pp 317-328.

Pitman, T.D., Robertson, P.K. & Sego, D.C. (1994). Influence of fines on the collapse of loose sands. Canadian Geotechnical Journal, vol. 31, pp 728-739.

Poulos, S.J. (1971). The steady state of deformation. Journal of the Geotechnical Engineering Division, Americian Society of Civil Engineers, vol. 100, pp 553-562.

Poulos, S.J., Castro, G. & France, J.W. (1985). Liquefaction evaluation procedure. Journal of Geotechnical Engineering Division, Americian Society of Civil Engineers, vol. 111, pp 772-792.

Sasitharan, S., Robertson, P.K., Sego, D.C. & Morgenstern, N.R. (1993). Collapse behaviour of sand. Canadian Geotechnical Journal, vol. 30, pp 569-577. (Discussion, vol. 31, pp 1022-1023).

Sasitharan, S., Robertson, P.K., Sego, D.C. & Morgenstern, N.R. (1994). State-boundary surface for very loose sand and its practical implications. Canadian Geotechnical Journal, vol. 31, pp 321-334.

Sassa, K. (1985). The mechanism of debris flow. Proceedings of the Eleventh International Conference in Soil Mechanics and Foundation Engineering, San Francisco, vol 3, pp 1173- 1178.

Schofield, A.N. (1980). Cambridge Geotechnical Centrifuge operations. Géotechnique, vol. 30, pp 227-268.

Shen, J.M. (1985). GCO Research into Unsaturated Shear Strength 1978-1982. Research Report No. RR 1/85, Geotechnical Control Office, Hong Kong, 183 p.

Siddle, H.J., Wright, M.D. & Hutchinson, J.N. (1996). Rapid failures of colliery spoil heaps in the South Wales Coalfield. Quarterly Journal of Engineering Geology, vol. 29, pp 103-132.

Skirrow, R.K. & Robertson, P.K. (1994). Effect of kaolin content on steady state parameters and shear wave velocity measurements for Ottawa sand. Proceedings of the 47th Canadian Geotechnical Conference, Halifax, pp 703-710.

Skopek, P., Morgenstern, N.R., Robertson, P.K. & Sego, D.C. (1994). Collapse of dry sand. Canadian Geotechnical Journal, vol. 31, pp 1008-1014.

Sladen, J.A. & Handford, G. (1987). A potential systematic error in laboratory testing of very loose sands. Canadian Geotechnical Journal, vol. 24, pp 462-466.

Sladen, J.A., D'Hollander, R.D.D. & Krahn, J. (1985). The liquefaction of sands, a collapse surface approach. Canadian Geotechnical Journal, vol. 22, pp 564-578.

Vaid, Y.P. & Thomas, J. (1995). Liquefaction and post-liquefaction behaviour of sand. Journal of Geotechnical Engineering Division, Americian Society of Civil Engineers, vol. 121, pp 163-173.

Wong, H.N. & Ho, K.K.S. (1996). Travel distance of landslide debris. Proceedings of the Seventh International Symposium on Landslides, Trondheim, vol. 1, pp 417-422.

Wong, H.N., Ho, K.K.S. & Chan, Y.C. (1997a). Assessment of consequence of landslides. Proceedings of the Workshop on Landslide Risk, IUGS Working Group on Landslides, Honolulu, pp 111-149.

Wong, H.N., Ho, K.K.S., Pun, W.K. & Pang, P.L.R. (1997b). Observations from some landslide studies in Hong Kong. Proceedings of the Seminar on Slope Engineering in Hong Kong, Geotechnical Division of the Hong Kong Institution of Engineers, Balkema (in press).

Works Branch (1996). Code of Practice on Inspection & Maintenance of Water Carrying Services Affecting Slopes. Works Branch, Hong Kong Government, 59 p.

Yim, K.P. & Siu, C.K. (1997). Stability investigation and preventive works design for old fill slopes in Hong Kong. Proceedings of the Seminar on Slope Engineering in Hong Kong, Geotechnical Division of the Hong Kong Institution of Engineers, Balkema (in press).

LIST OF TABLES

Table 1 - Critical State Parameters for Three Granitic Saprolites in Hong Kong

Critical State Parameter		Γ	λ	M
Sau Mau Ping	average	2.225	0.1228	1.50
	upper bound	2.375	0.1526	
	lower bound	2.075	0.0929	
King's Park (Gray, 1980)		1.956	0.0790	1.50
Shouson Hill (Chung, 1997)		1.990	0.0784	1.58

Note: The upper and lower bound Γ and λ values for fill specimens from Sau Mau Ping are determined from the 75% confidence upper and lower bound values of 15 oedometer tests.

Table 2 - Critical State and Collapse Surface Parameters Reported in the Literature (Sheet 1 of 7)

Test	e	Stress conditions at start of collapse		ϕ_{col}' (degrees)	ϕ_{cv}' (degrees)	Critical state parameters		Description of Material	Remarks	References
		p' (kPa)	q (kPa)			λ	Γ			
CIU	0.84	583	471		34			Sydney sand		Chu & Lo (1992)
CIU	0.85	483	416		34			as above		as above
CIU	0.88	207	140		34			as above		as above
CIU	0.92	115	83	17	33	0.031	2.002	Hostun LF sand		Konrad (1993)
CIU	0.92	493	330	15	33	0.031	2.049	as above		as above
CIU	0.92	113	69	13	33	0.031	2.002	as above		as above
CIU	0.93	31	24	12	33	0.031	2.002	as above		as above
CIU	0.91	222	173	19	33	0.031	2.002	as above		as above
CIU	0.93	271	205	16	33	0.031	2.049	as above		as above
CIU	0.96	218	165	18	33	0.031	2.049	as above		as above
CIU	0.98	190	129	17	33	0.031	2.049	as above		as above
CIU	0.83	1341	1073	17	33	0.031	2.002	as above		as above
CIU	0.56	144	139	20	35	0.062	1.789	till sand		Konrad (1993)
CIU	0.54	150	147	19	35	0.062	1.789	as above		as above
CIU	0.48	211	221	23	35	0.062	1.738	as above		as above
CIU	0.53	170	201	26	35	0.062	1.789	as above		as above
CIU	0.60	134	116	20	35	0.062	1.789	as above		as above

Legend:

CIU	Isotropically consolidated, undrained test	CACq	Anisotropically consolidated, constant q test
CAU	Anisotropically consolidated, undrained test	CA-cyclic	Anisotropically consolidated, cyclic test

Table 2 - Critical State and Collapse Surface Parameters Reported in the Literature (Sheet 2 of 7)

Test	e	Stress conditions at start of collapse		ϕ_{col}' (degrees)	ϕ_{cv}' (degrees)	Critical state parameters		Description of Material	Remarks	References
		p' (kPa)	q (kPa)			λ	Γ			
CIU	0.62	157	134	21	35	0.062	1.789	as above		as above
CA-cyclic	0.55	148	146	20	34	0.062	1.789	till sand	consolidation q/p' = 1.61	Konrad (1993)
CA-cyclic	0.55	160	147	18	35	0.062	1.789	as above	consolidation q/p' = 1.54	as above
CA-cyclic	0.55	145	129	16	35	0.062	1.789	as above	consolidation q/p' = 1.54	as above
CA-cyclic	0.55	141	119	19	35	0.062	1.738	till sand	consolidation q/p' = 1.38	Konrad (1993)
CA-cyclic	0.61	256	225	22	34	0.062	1.789	as above	consolidation q/p' = 1.34	as above
CA-cyclic	0.59	211	185	21	34	0.062	1.789	as above	consolidation q/p' = 1.37	as above
CA-cyclic	0.62	257	219	21	32	0.062	1.789	as above	consolidation q/p' = 1.28	as above
CA-cyclic	0.60	216	194	22	33	0.062	1.789	as above	consolidation q/p' = 1.33	as above
CA-cyclic	0.65	405	349	22	32	0.062	1.789	as above	consolidation q/p' = 1.21	as above
CIU	0.83	183	100	14	30	0.019	1.874	Ottawa sand C-109		Pitman et al (1994)
CIU	0.42	198	132		30			+10% kaolin fines		as above
CIU	0.16	198	132		30			+20% kaolin fines		as above
CIU	0.22	198	132		30			+30% kaolin fines		as above

Legend:

CIU	Isotropically consolidated, undrained test	CACq	Anisotropically consolidated, constant q test
CAU	Anisotropically consolidated, undrained test	CA-cyclic	Anisotropically consolidated, cyclic test

Table 2 - Critical State and Collapse Surface Parameters Reported in the Literature (Sheet 3 of 7)

Test	e	Stress conditions at start of collapse		ϕ_{col}' (degrees)	ϕ_{cv}' (degrees)	Critical state parameters		Description of Material	Remarks	References
		p' (kPa)	q (kPa)			λ	Γ			
CIU	0.56							+40% kaoline fines		as above
CIU	0.78	218	116		30			+10% crushed silica fines		as above
CIU	0.67	203	105		30			+20% crushed silica fines		as above
CIU	0.74	203	105		30			+30% crushed silica fines		as above
CIU	0.77							+40% crushed silica fines		as above
CIU	0.83	206	96		30			+10% 70-140 silica sand		as above
CIU	0.83	206	96		30			+20% 70-140 silica fines		as above
CIU	0.83	206	96		30			Ottawa Sand C109 +30% 70-140 silica fines		Pitman et al (1994)
CIU	0.83	207	88		30			+40% 70-140 silica fines		as above
CIU	1.00	734	-436		32			Fraser river sand	triaxial extension test	Vaid & Thomas (1995)
CIU	1.00	518	-266		32			as above	as above	as above

Legend:

CIU	Isotropically consolidated, undrained test	CACq	Anisotropically consolidated, constant q test
CAU	Anisotropically consolidated, undrained test	CA-cyclic	Anisotropically consolidated, cyclic test

Table 2 - Critical State and Collapse Surface Parameters Reported in the Literature (Sheet 4 of 7)

Test	e	Stress conditions at start of collapse		ϕ_{col}' (degrees)	ϕ_{cv}' (degrees)	Critical state parameters		Description of Material	Remarks			References
		p' (kPa)	q (kPa)			λ	Γ					
CIU	1.00	264	-91		32			as above	as above			as above
CIU	1.00	111	-73		32			as above	as above			as above
CIU	0.79	300	210	15	30	0.017	1.864	Ottawa sand C-109				Sasitharan et al (1994)
CIU	0.79	295	208	14	30	0.017	1.864	as above				as above
CIU	0.79	253	190	16	30	0.017	1.864	as above				as above
CIU	0.80	210	140	15	30	0.017	1.864	as above				as above
CIU	0.81	348	214	15	30	0.017	1.864	as above				as above
CIU	0.81	210	124	13	30	0.017	1.864	as above				as above
CIU	0.76	1000	850	12	30	0.017	1.864	as above				as above
									e_{max}	e_{min}	G_s	
				14	30	0.017	1.864	Ottawa sand C-109	0.82	0.50	2.66	Sasitharan et al (1994)
				18	31	0.013	1.820	Erksak	0.75	0.53	2.66	as above
				15	31	0.004	1.938	Toyoura	0.97	0.64	2.64	as above
				21	35	0.022	2.100	Lornex	1.08	0.68	2.68	as above
				19	36	0.042	2.112	Brenda	1.06	0.69	2.70	as above
				13	30	0.017	1.847	Syncrude	0.93	0.55		Sasitharan et al (1994)

Legend:

CIU	Isotropically consolidated, undrained test	CACq	Anisotropically consolidated, constant q test
CAU	Anisotropically consolidated, undrained test	CA-cyclic	Anisotropically consolidated, cyclic test

Table 2 - Critical State and Collapse Surface Parameters Reported in the Literature (Sheet 5 of 7)

Test	e	Stress conditions at start of collapse		ϕ_{col}' (degrees)	ϕ_{cv}' (degrees)	Critical state parameters		Description of Material	Remarks		References
		p' (kPa)	q (kPa)			λ	Γ				
									e_{max}	e_{min}	
				16	30	0.015	1.885	Nerlerk	0.89	0.66	as above
				14	30	0.035	2.000	LBS	0.75	0.58	as above
CIU				16	30			Erklerk			Sladen et al (1985)
CIU				16	30	0.017	1.880	Erklerk with 2% fines			as above
CIU				16	31	0.030	1.800	Erklerk with 12% fines			as above
CIU				14	30	0.035	2.000	Leighton Buzzard (LBS)			as above
				18	35	0.026	1.930	as above	simple shear test		as above
				19	32	0.009	1.850	Banding sand			as above
				17	30	0.020	1.920	as above			as above
					29	0.017	1.850	as above			as above
					27	0.013	1.850	as above			as above
CIU	0.74	33	15		36			USU torrent deposit	saturation 99.5%		Sassa (1985)
CIU	0.84	35	24		36			as above	saturation 84.9%		as above

Legend:

CIU Isotropically consolidated, undrained test
CAU Anisotropically consolidated, undrained test
CACq Anisotropically consolidated, constant q test
CA-cyclic Anisotropically consolidated, cyclic test

Table 2 - Critical State and Collapse Surface Parameters Reported in the Literature (Sheet 6 of 7)

Test	e	Stress conditions at start of collapse		ϕ_{col}' (degrees)	ϕ_{cv}' (degrees)	Critical state parameters		Description of Material	Remarks	References
		p' (kPa)	q (kPa)			λ	Γ			
CIU	0.83	34	29		36			as above	saturation 90.2%	as above
CIU	0.65	416	277	17	30	0.018	1.702	LBS		Hird & Hassona (1990)
CIU	0.70	188	162	22	30	0.018	1.702	as above		as above
CIU	0.65	483	245	13	30	0.018	1.702	as above	sedimented specimen	as above
CAU	0.65	458	273	15	30	0.018	1.702	as above		as above
CAU	0.65	500	283	14	30	0.018	1.702	LBS		Hird & Hassona (1990)
CIU	0.73	83	43	14	30	0.018	1.702	as above		as above
CIU	0.87	62	39	14	22	0.078	2.100	LBS + 17% mica fines		as above
						0.019	1.800	Banding sand		Hird & Hassona (1990)
						0.018	1.702	LBS		Hird & Hassona (1990)
						0.055	1.966	LBS + 10% mica fines		as above
						0.078	2.100	LBS + 17% mica fines		as above

Legend:

CIU	Isotropically consolidated, undrained test	CACq	Anisotropically consolidated, constant q test
CAU	Anisotropically consolidated, undrained test	CA-cyclic	Anisotropically consolidated, cyclic test

Table 2 - Critical State and Collapse Surface Parameters Reported in the Literature (Sheet 7 of 7)

Test	e	Stress conditions at start of collapse		ϕ_{col}' (degrees)	ϕ_{cv}' (degrees)	Critical state parameters		Description of Material	Remarks	References
		p' (kPa)	q (kPa)			λ	Γ			
						0.163	2.575	LBS + 30% mica fines		as above
						0.018	1.669	Glass beads		as above
						0.017	1.741	Carborundum granules		as above
CIU	0.92	76	84	15	31	0.004	1.938	Toyoura sand	Ishihara (1993)	
CIU	0.83	1835	1286	15	31	0.004	1.938	as above		as above
CACq	0.83	123	81	17	30	0.017	1.864	Ottawa sand C-109 (dry)		Skopek et al (1994)
CACq	0.83	182	108	15	30	0.017	1.864	as above		as above
CACq	0.81	191	131	16	30	0.017	1.864	as above		as above
CIU		65	39	13	33			Hostun Sand RF, Dr 20%	relative density = 20%	Di Prisco et al (1995)
CAU		81	44	10	41			as above	as above	as above

Legend:

CIU	Isotropically consolidated, undrained test	CACq	Anisotropically consolidated, constant q test
CAU	Anisotropically consolidated, undrained test	CA-cyclic	Anisotropically consolidated, cyclic test

LIST OF FIGURES

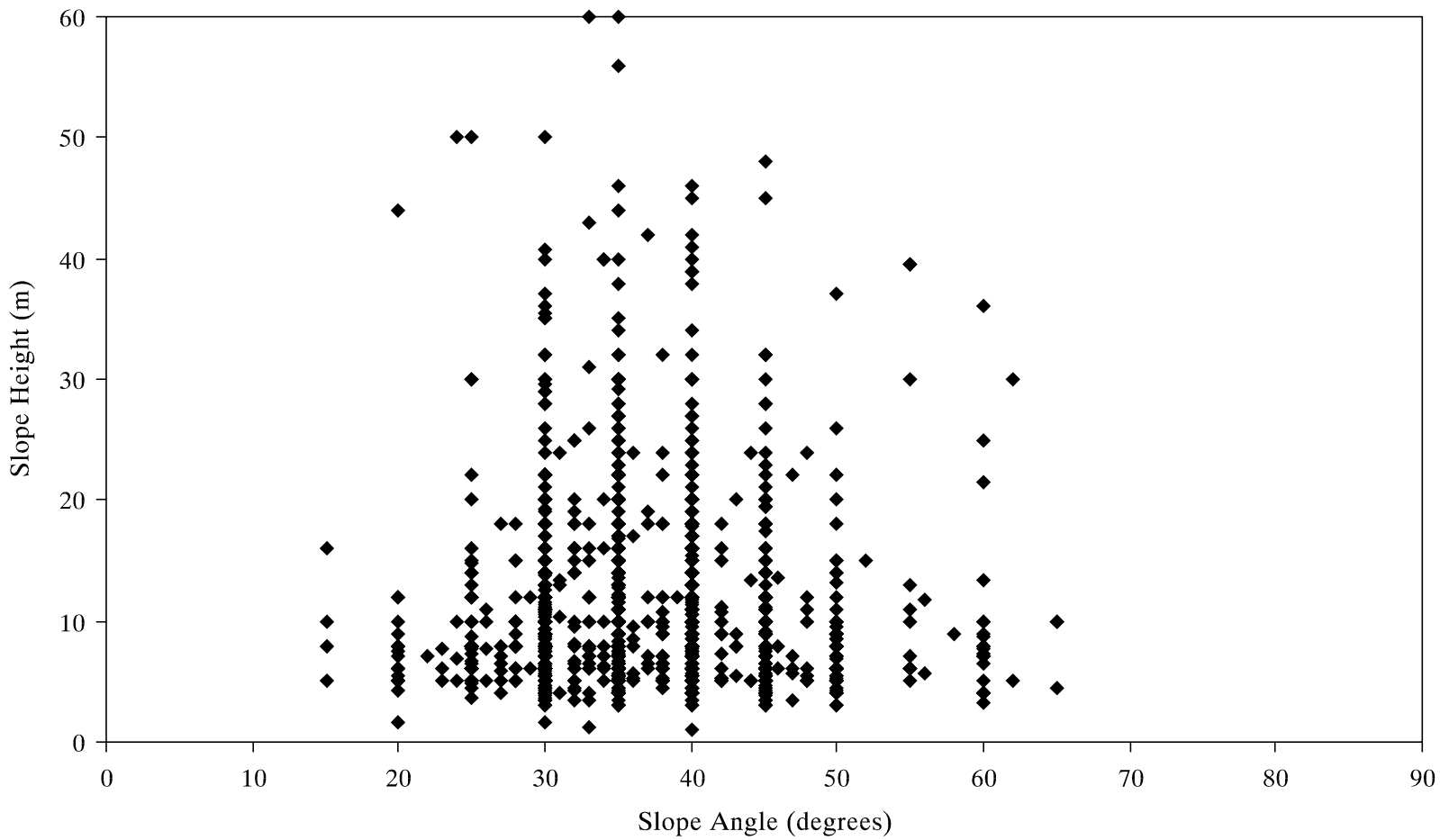

Notes: (1) Data extracted from the New Slope Catalogue which is being compiled (covering 2000 fill slopes in the Catalogue up to February 1998).
(2) Data based on site observation only.

Figure 1 - Distribution of Slope Height and Slope Angle for Pre-GCO Fill Slopes

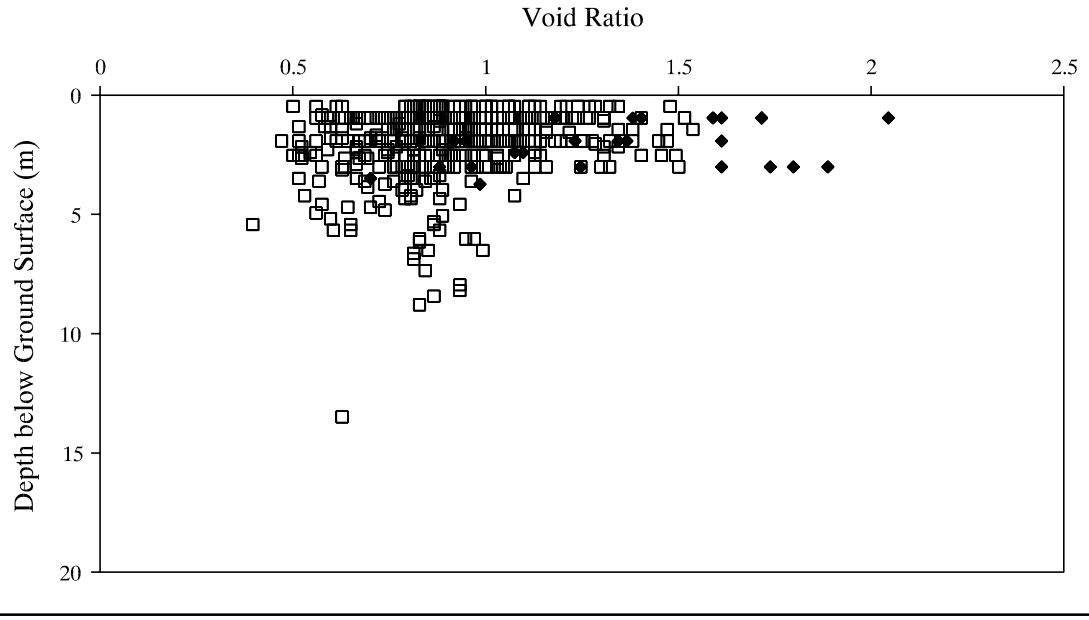

Legend:

◆ Fill with siginificant coarse fraction (i.e. cobbles and brick fragments)

Note: Total number of samples equals 509, from 68 fill slopes.

Figure 2 - Profile of Void Ratio for Selected Pre-GCO Fill Slopes in Hong Kong

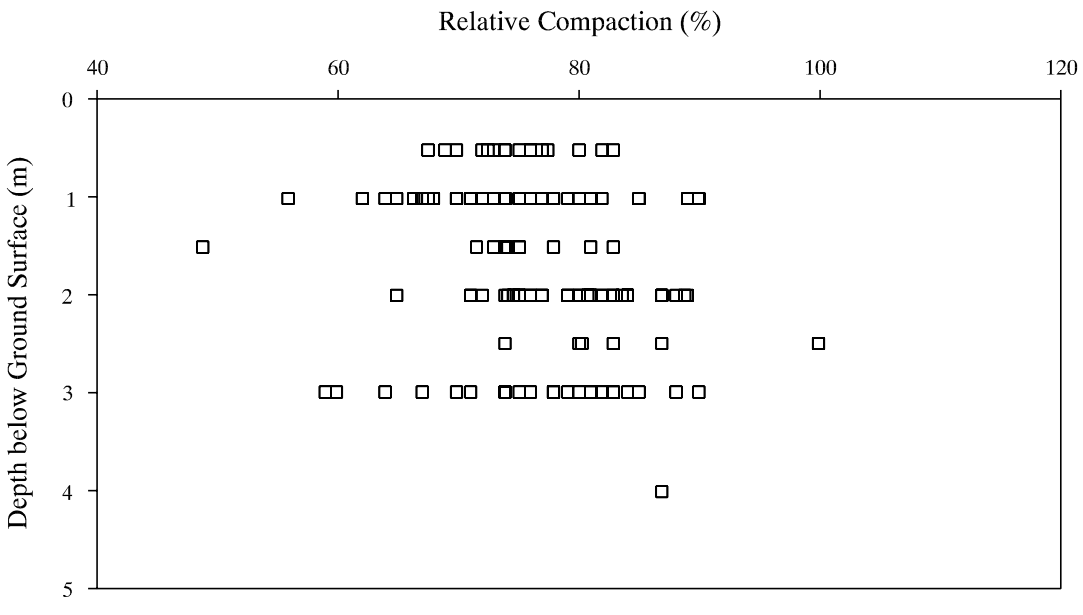

Notes: (1) Relative compaction is defined as the ratio of insitu dry density to the maximum dry density.

(2) Total number of samples equals 150, from 68 fill slopes.

Figure 3 - Profile of Relative Compaction for Selected Pre-GCO Fill Slopes in Hong Kong

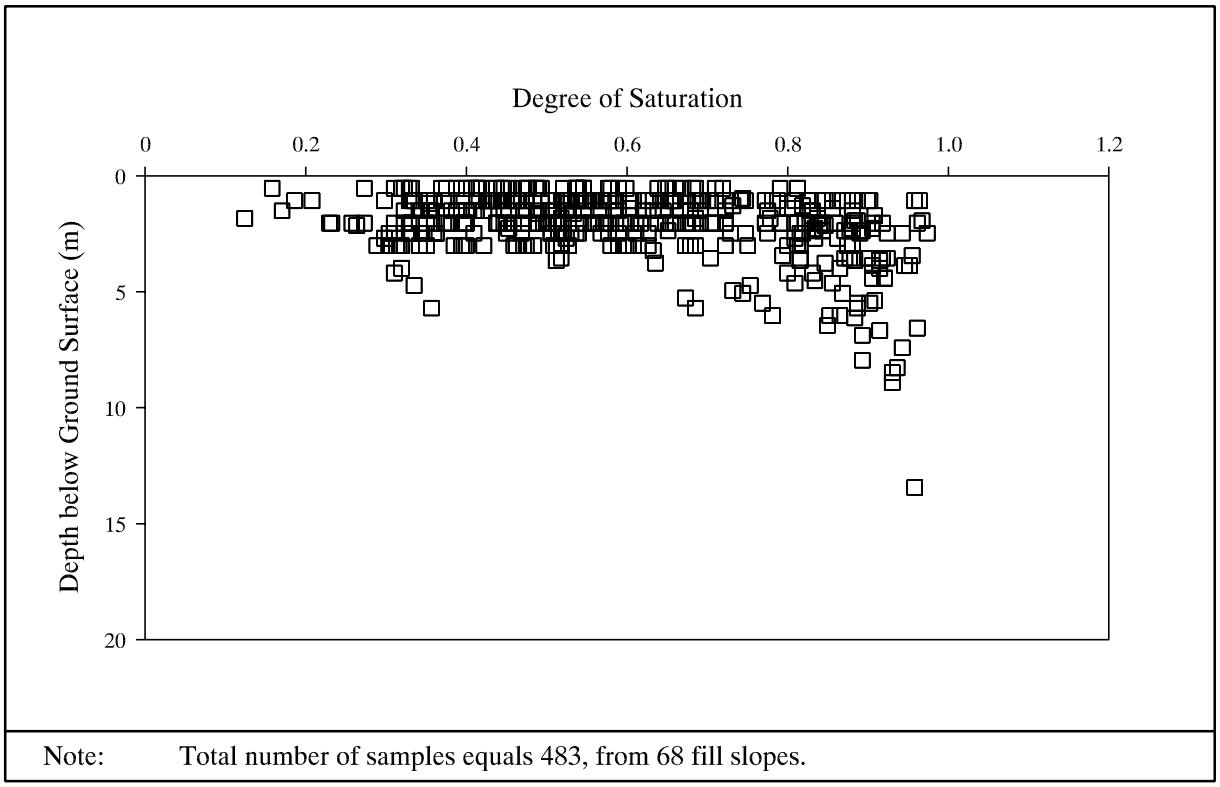

Note: Total number of samples equals 483, from 68 fill slopes.

Figure 4 - Profile of Degree of Saturation for Selected Pre-GCO Fill Slopes in Hong Kong

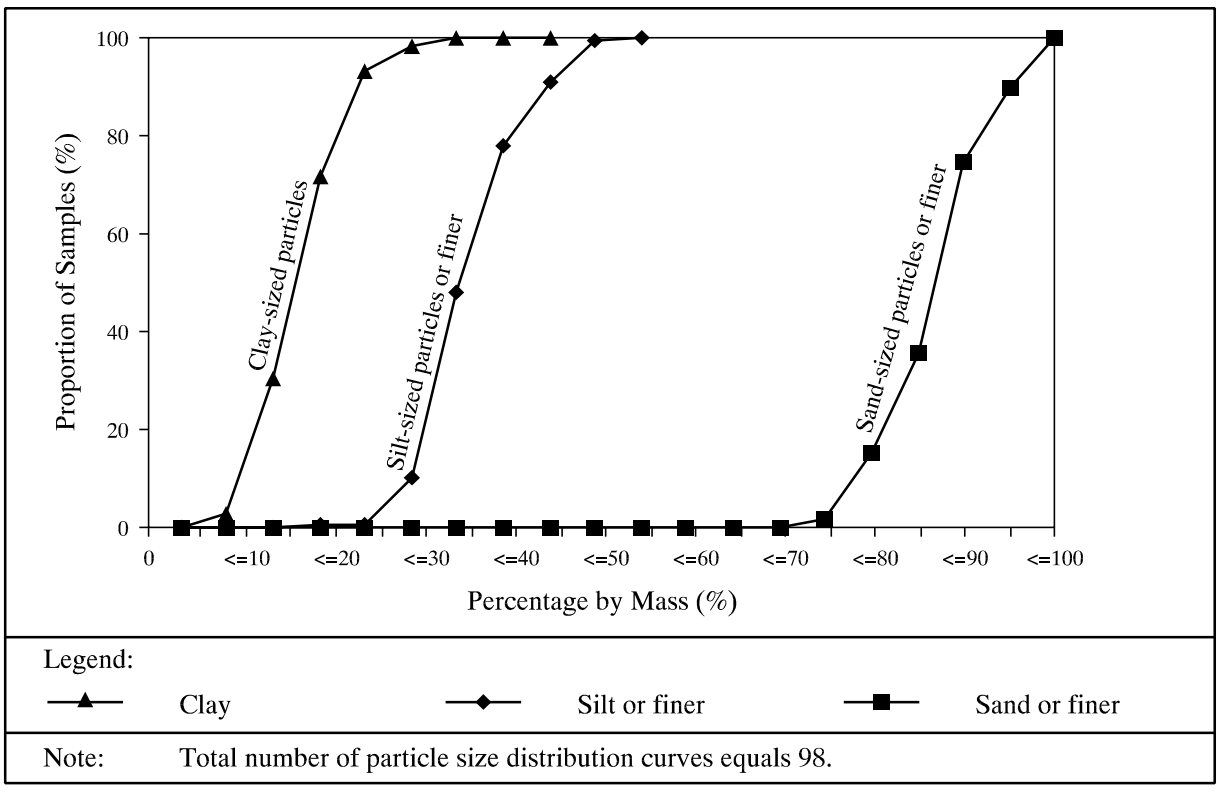

Note: Total number of particle size distribution curves equals 98.

Figure 5 - Summary of Results of Particle Size Distribution for the 1976 Sau Mau Ping Failure

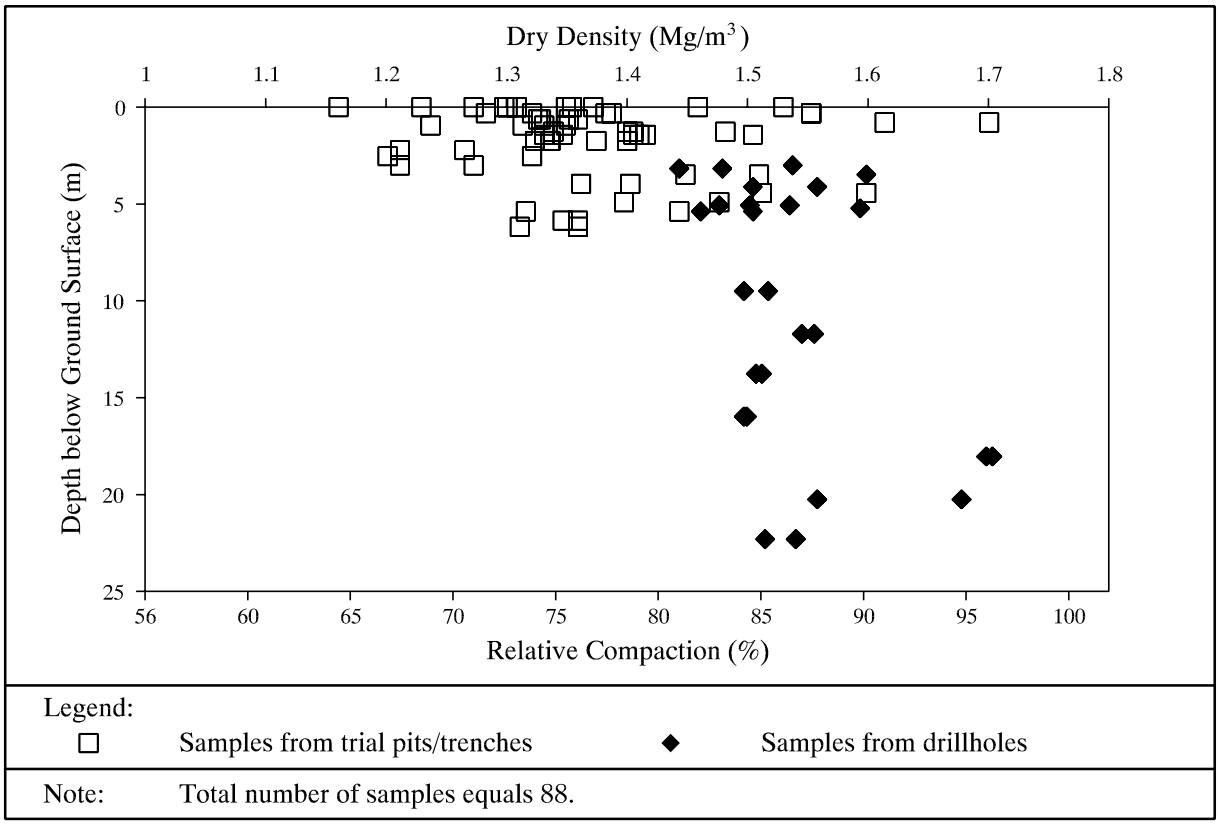

Figure 6 - Profiles of Dry Density and Relative Compaction for Fill Samples from the 1976 Sau Mau Ping Failure

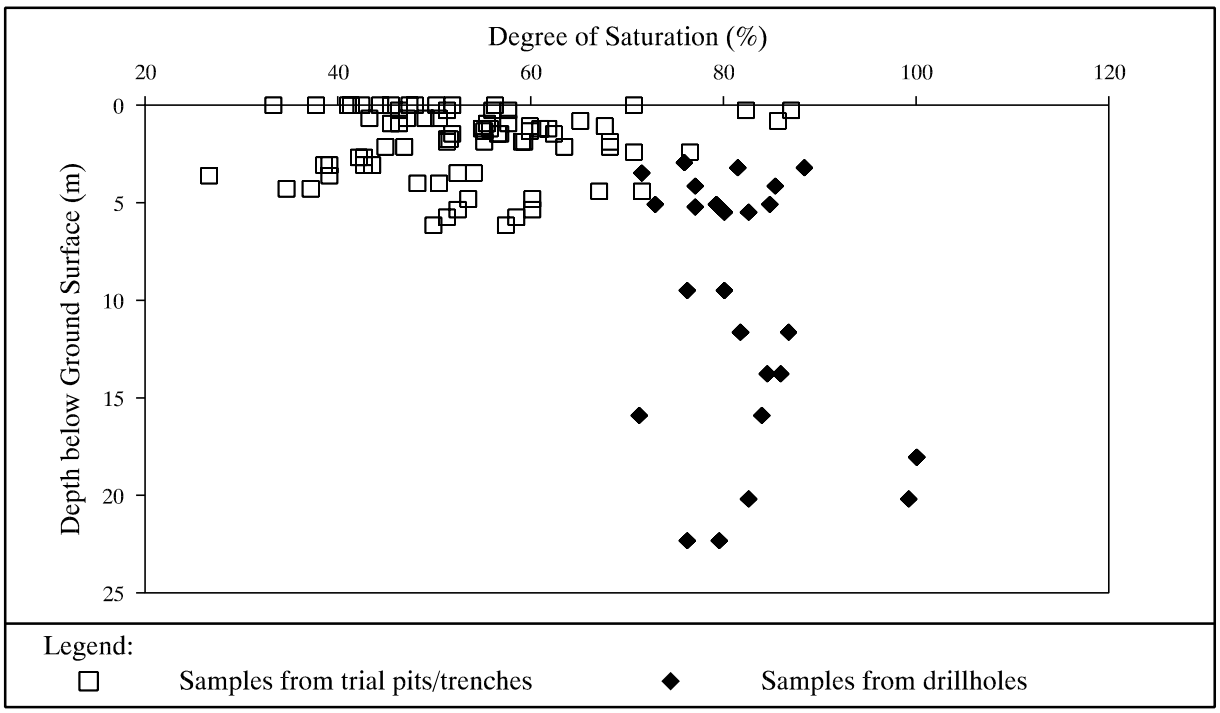

Figure 7 - Profile of Degree of Saturation for Fill Samples from the 1976 Sau Mau Ping Failure

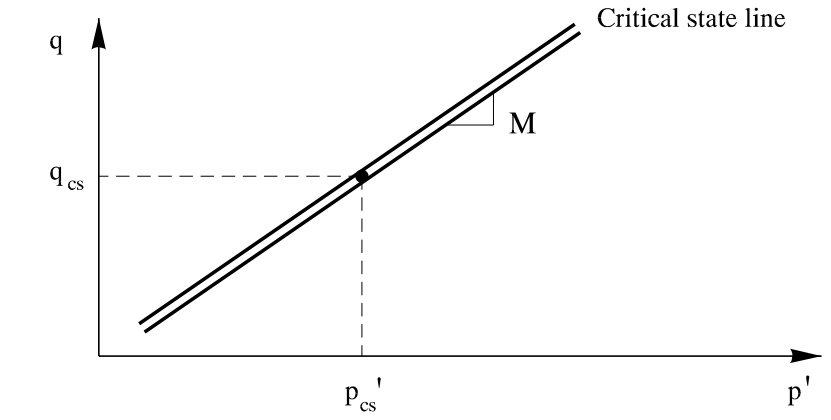

(a)

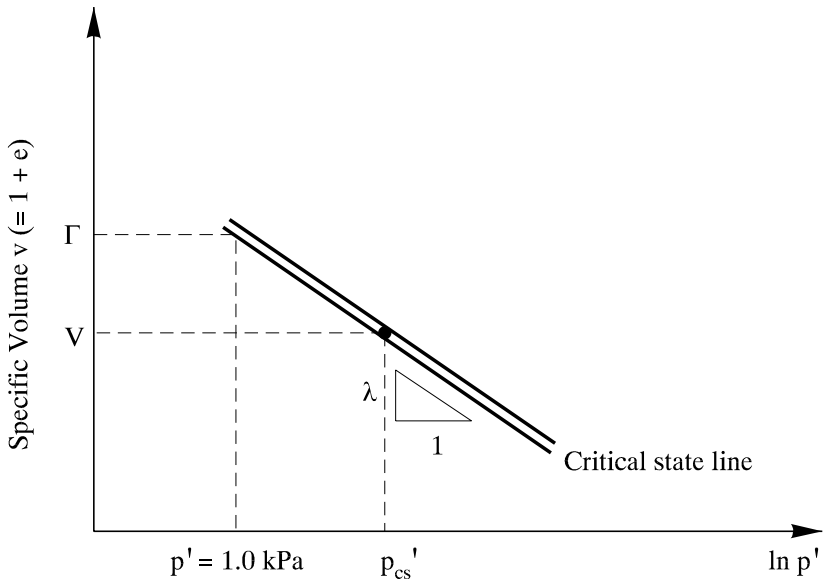

(b)

Legend:

p_{cs}'	Critical state p' for a given void ratio
q_{cs}	Critical state q for a given void ratio

Note: For definition of p' and q, refer to Figure 12.

Figure 8 - Definition of Critical State Parameters

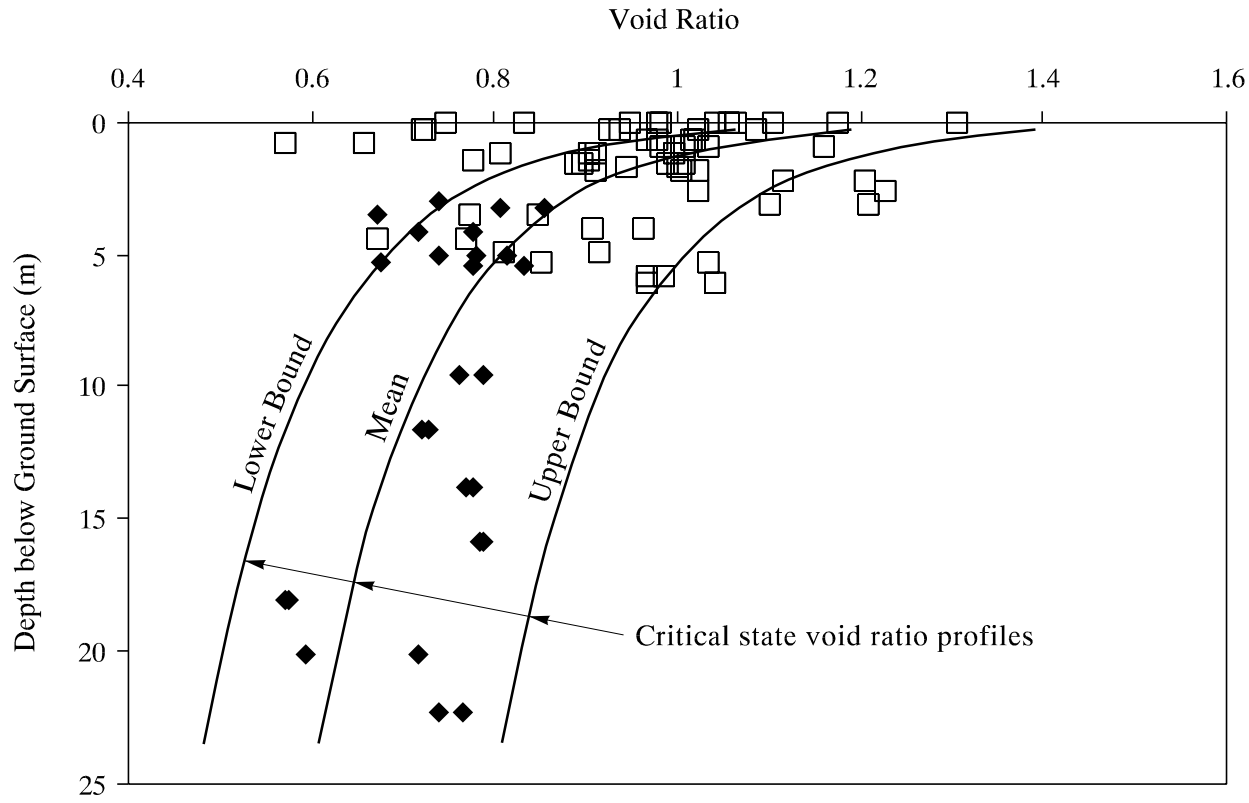

Legend:

□ Samples from trial pits/trenches

◆ Samples from drillholes

Notes:
(1) Assume p' equals vertical stress.
(2) Total number of samples equals 88.
(3) Upper and lower bounds critical state void ratio profiles are determined from 75% confidence upper and lower bound λ values from results of oedometer tests.

Figure 9 - Profile of Insitu Void Ratio and Critical State Void Ratio for Fill Samples from the 1976 Sau Mau Ping Failure

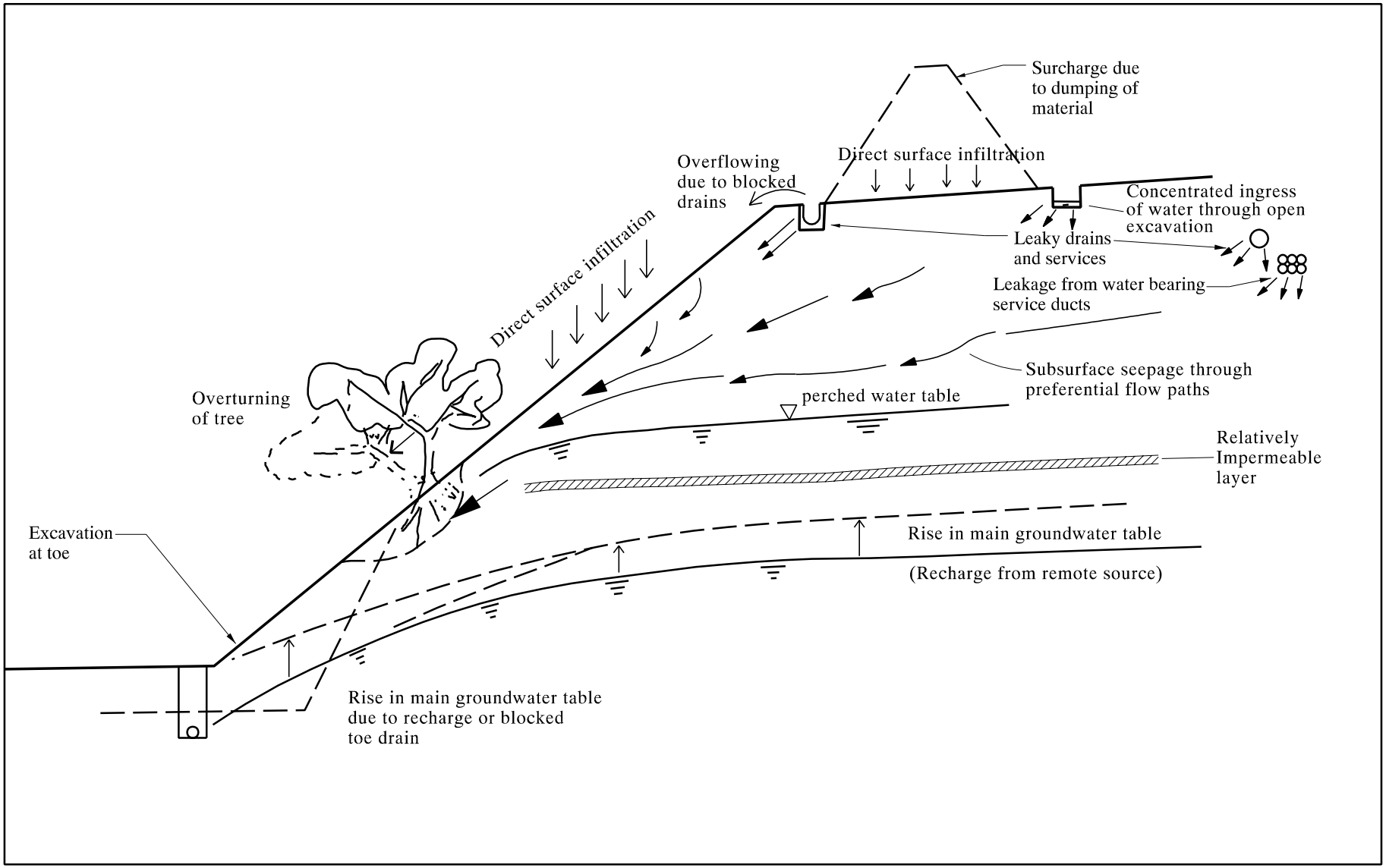

Figure 10 - Triggers and Contributory Factors for Fill Slope Failure

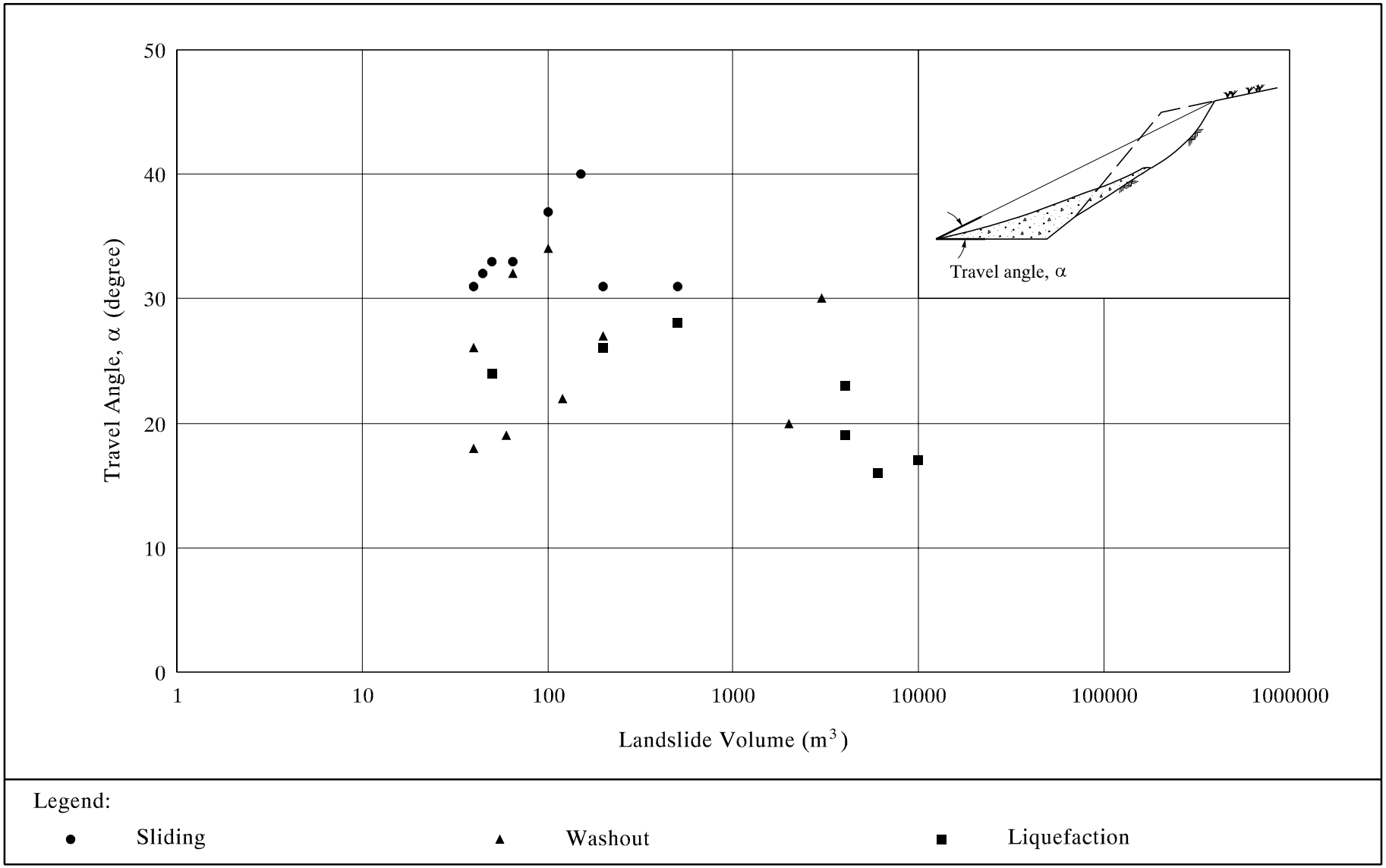

Figure 11 - Debris Mobility for Fill Slope Failures in Hong Kong

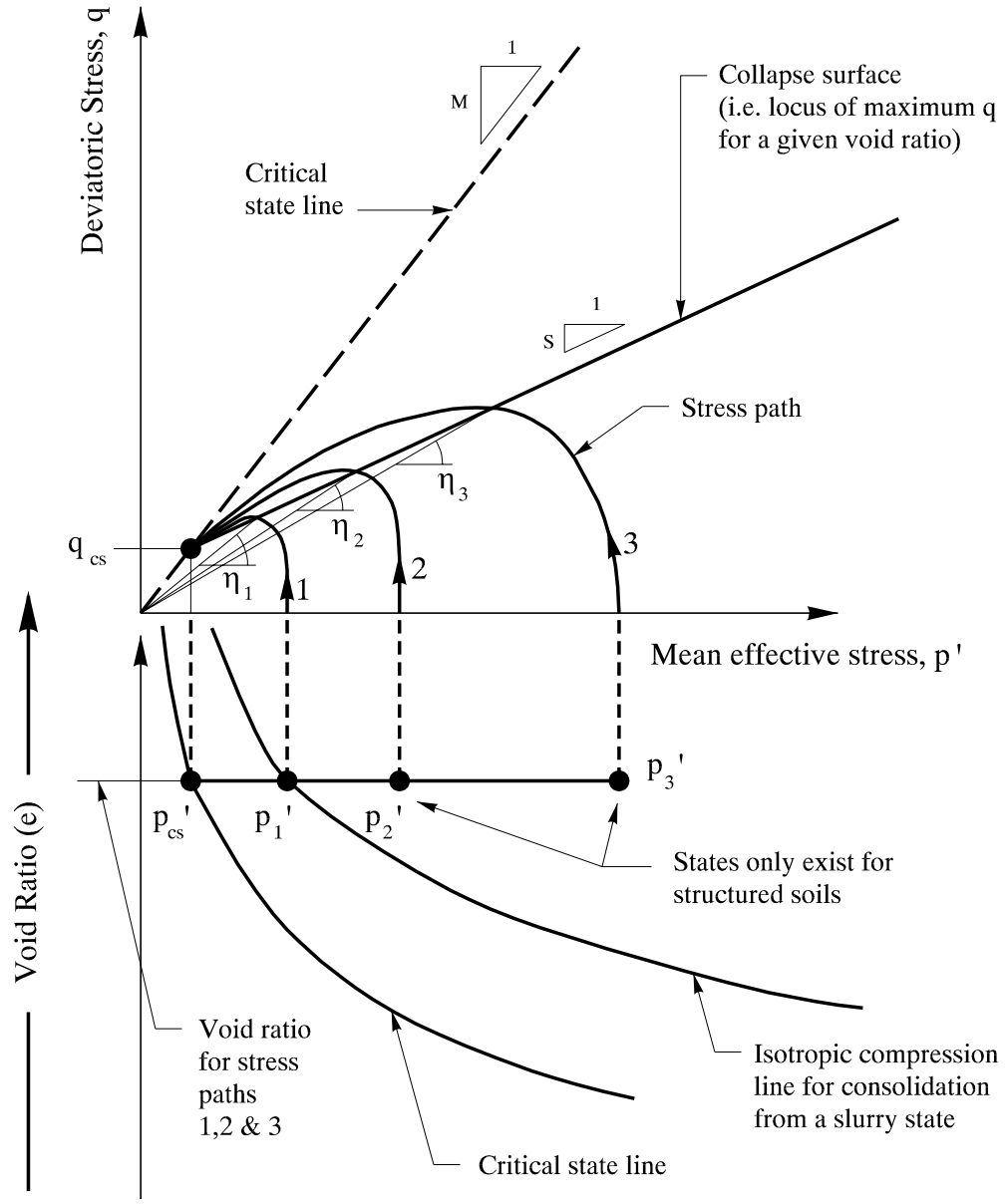

Legend:

$p' = (\sigma_1 + 2\sigma_3)/3 - u$
$q = \sigma_1 - \sigma_3$
u = Pore water pressure
σ_1 = Major principal stress
σ_3 = Minor principal stress

$$\sin \phi_{cv}' = \frac{3M}{6 + M}$$

$$\sin \phi_{col}' = \frac{3S}{6 + S}$$

$$\sin \phi_{app}' = \frac{3\eta}{6 + \eta}$$

Notes: (1) p' and q defined above are applicable for triaxial stress condition.

(2) For definition of p_{cs}' and q_{cs}, refer to Figure 8.

Figure 12 - Collapse Surface of a Loose Sand

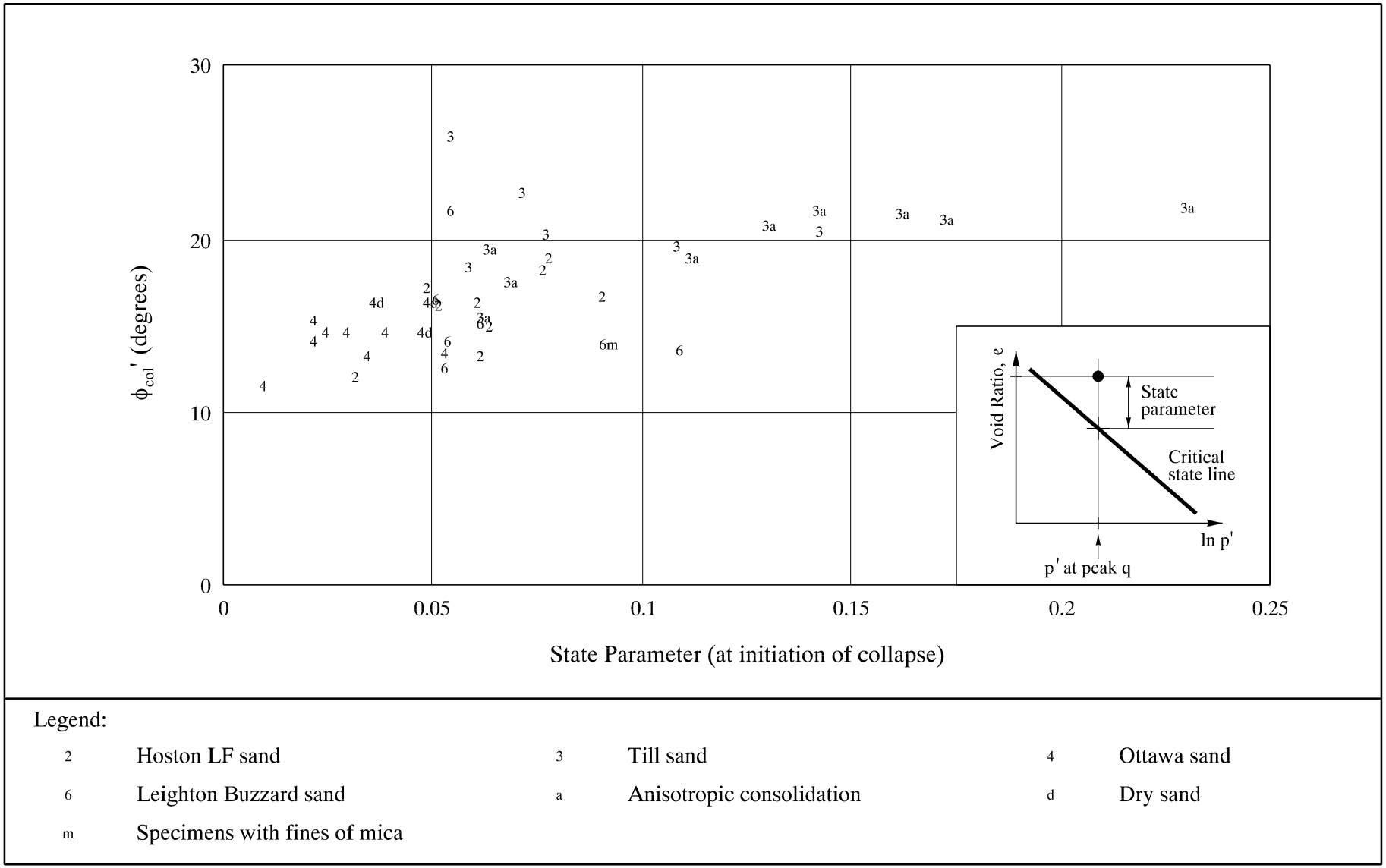

Legend:

2	Hoston LF sand	3	Till sand	4	Ottawa sand
6	Leighton Buzzard sand	a	Anisotropic consolidation	d	Dry sand
m	Specimens with fines of mica				

Figure 13 - Correlation of ϕ_{col}' Values with State Parameter

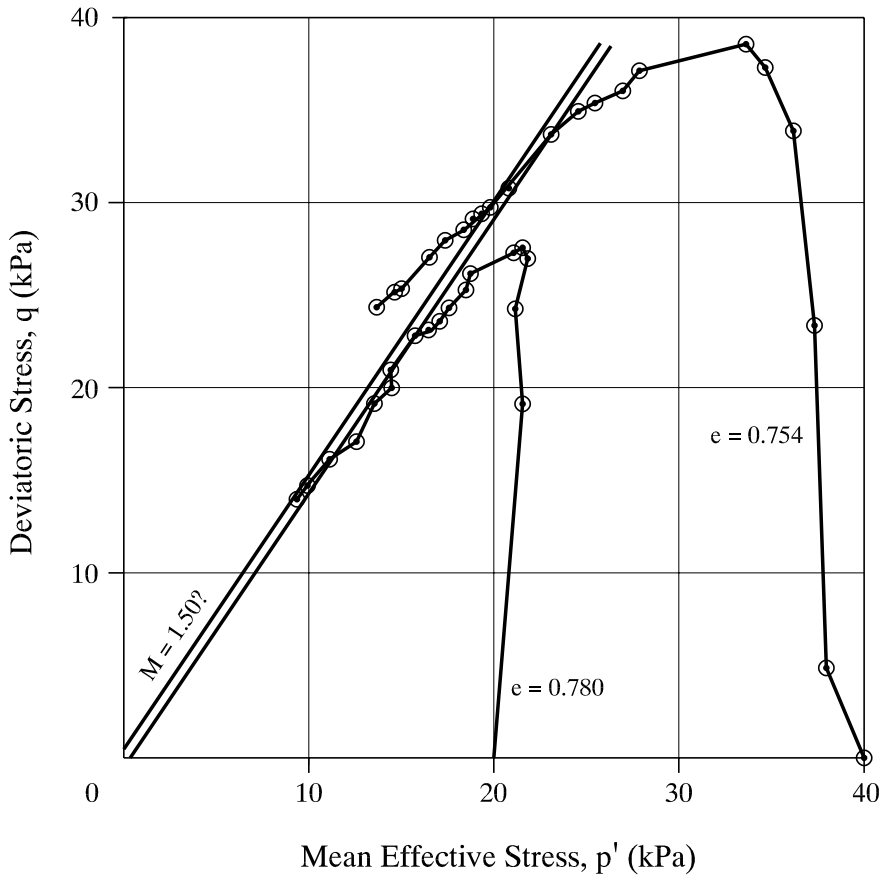

Note: Figure extracted from Gray (1980); e values refer to those after consolidation and before shearing.

Figure 14 - Results of Isotropically Consolidated Undrained Triaxial Compression Tests on a Loose Completely Decomposed Granite

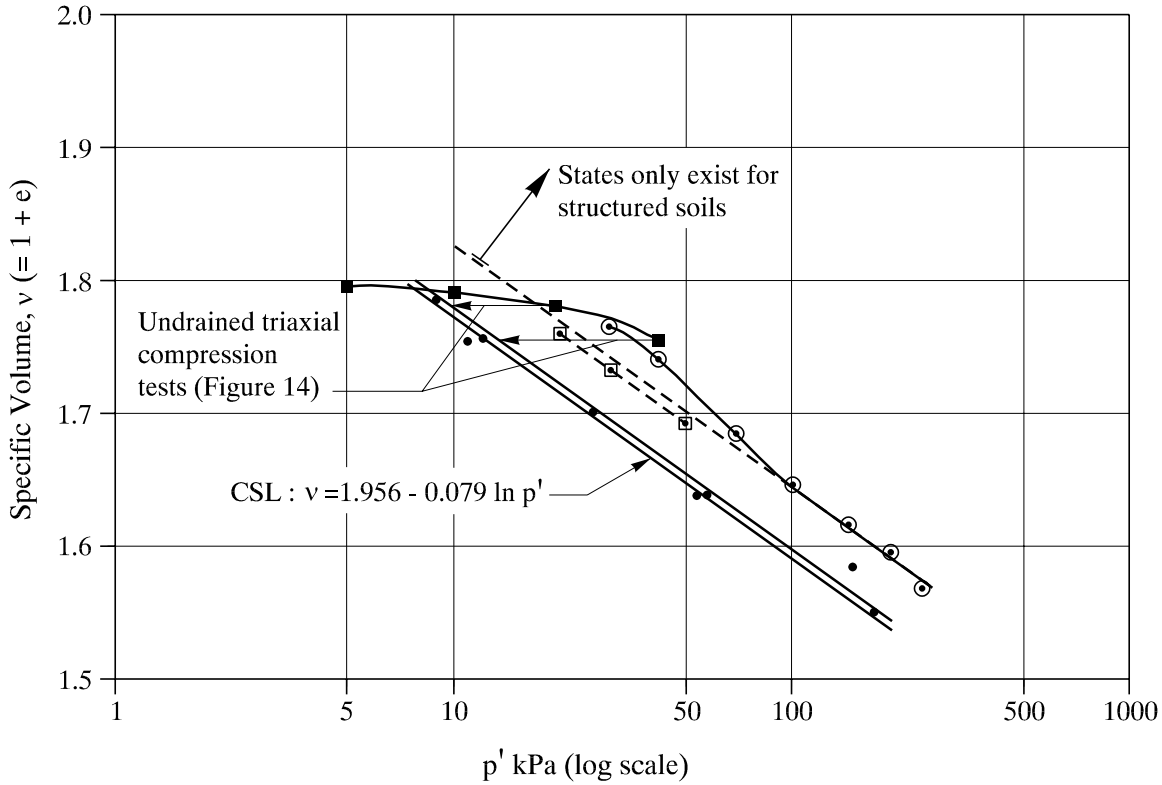

Legend:

- Isotropic compression of specimens prepared to 85% maximum dry density at optimum moisture content and saturated by back pressure
- Isotropic compression of specimen prepared to 75% maximum dry density at optimum moisture content and saturated by back pressure
- Isotropic compression material placed under water
- Points of minimum p' observed during shear

Note: Figure extracted from Gray (1980); ν values indicated are those after back pressure saturation.

Figure 15 - Results of Isotropic Compression Tests on a Loose Completely Decomposed Granite

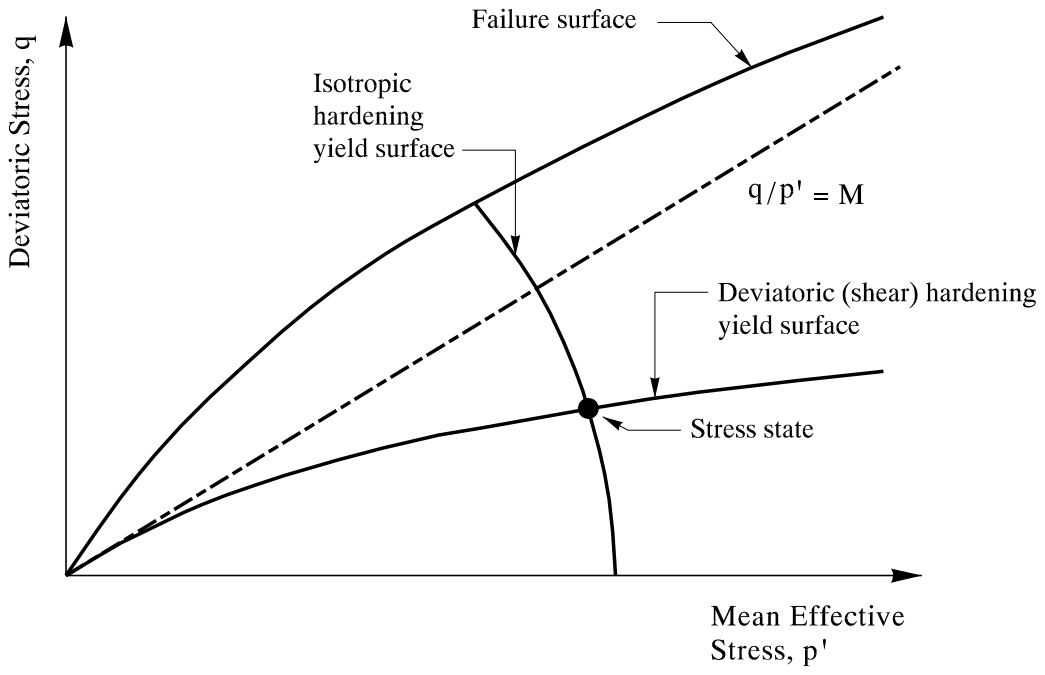

(a) Dense Sand

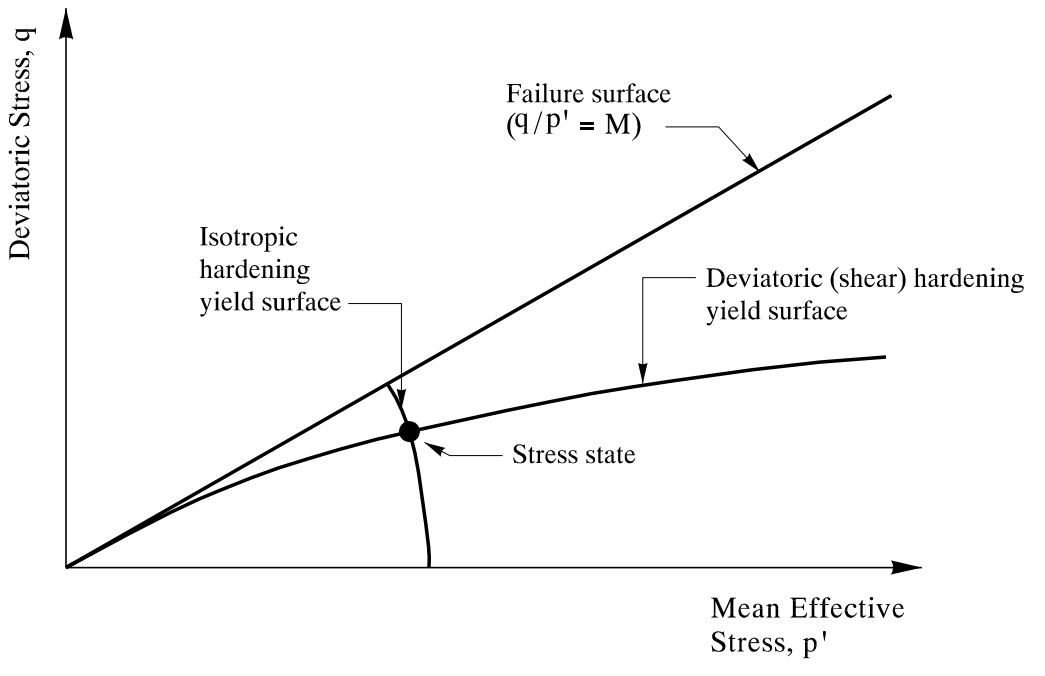

(b) Loose Sand

Note: Figure extracted from Hicks & Wong (1988).

Figure 16 - Collapse Model Proposed by Molenkamp

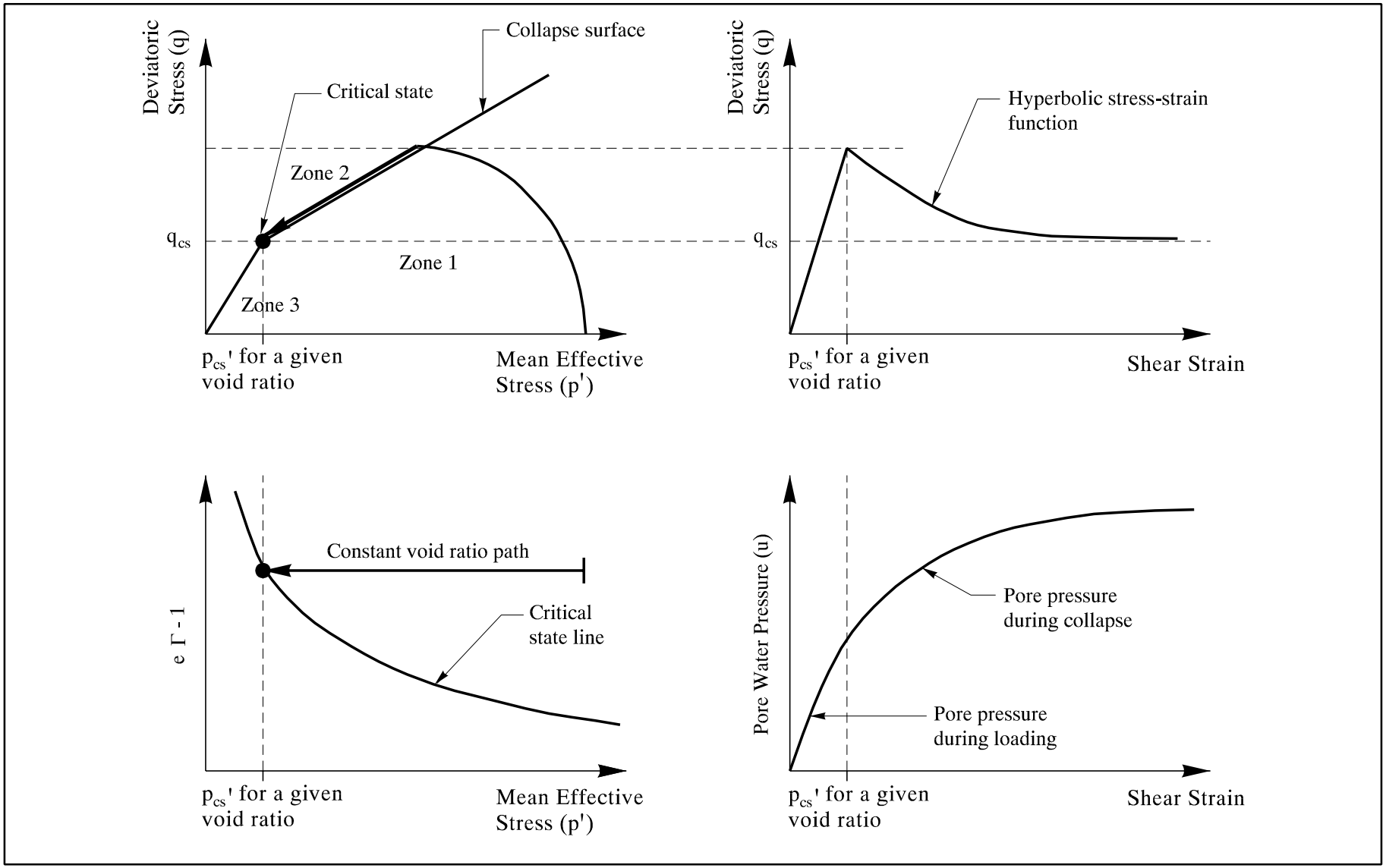

Figure 17 - Liquefaction Model Proposed by Gu et al (1993)

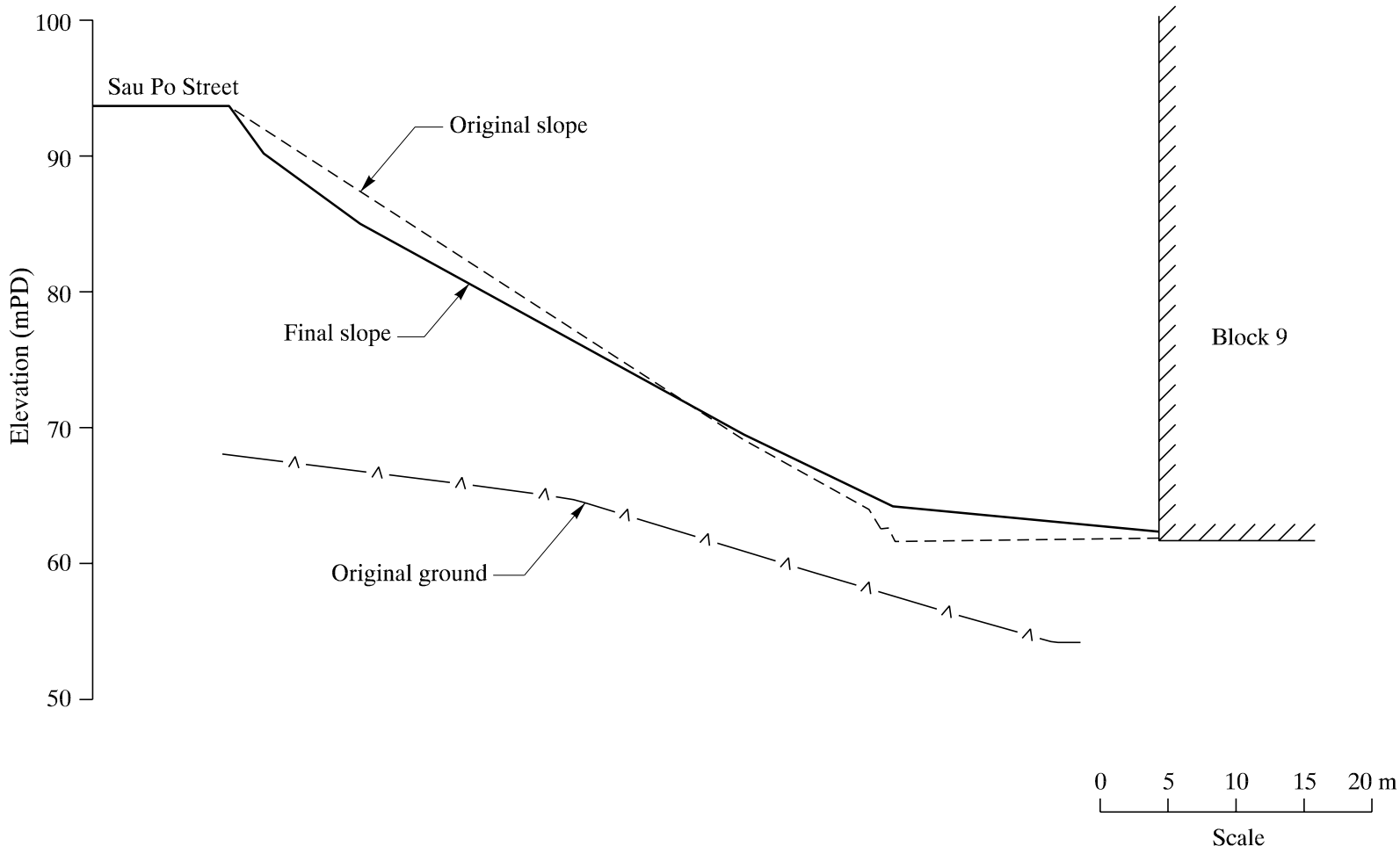

Note: Figure extracted from Hong Kong Government (1977).

Figure 18 - Section Through the 1976 Sau Mau Ping Landslide

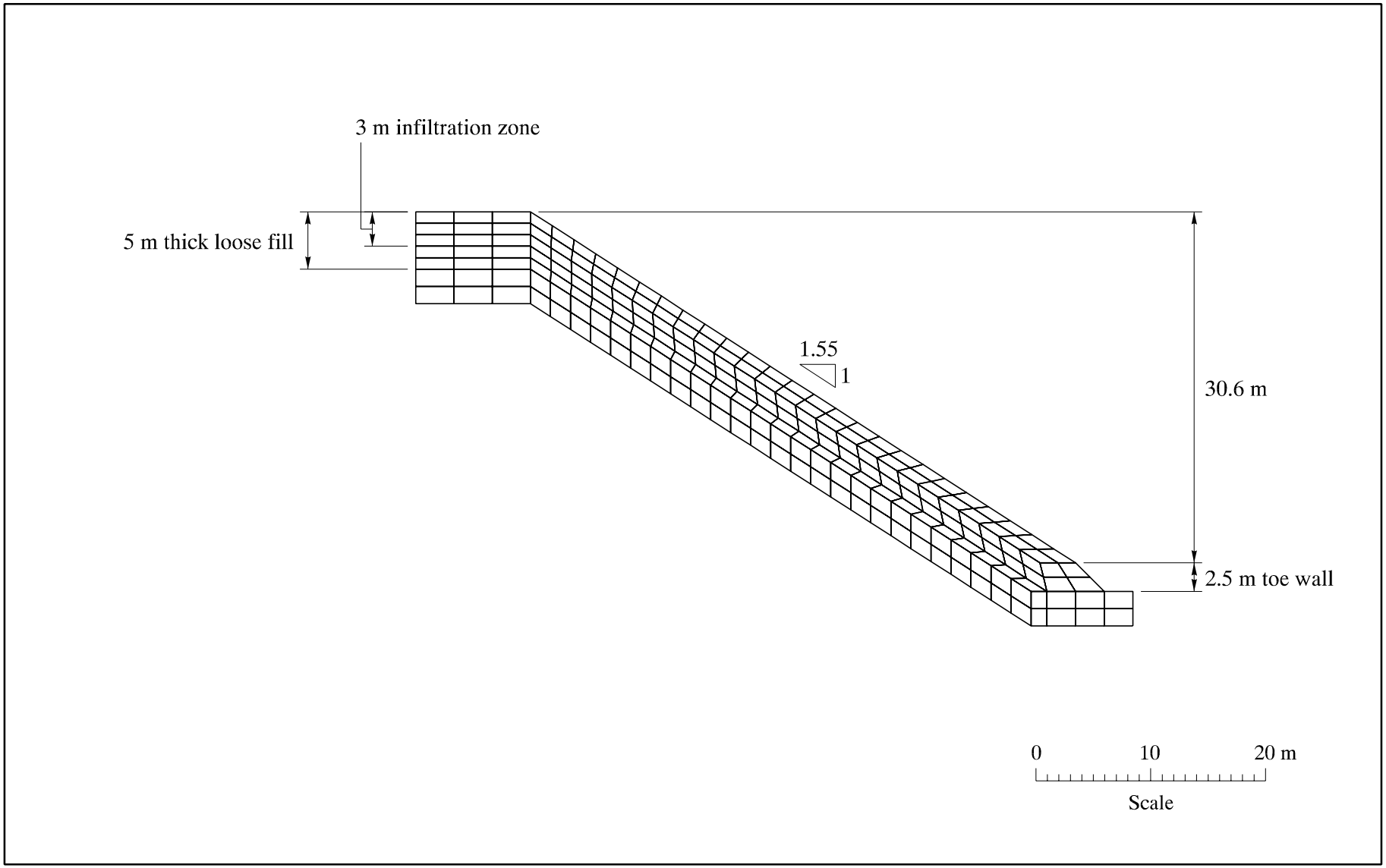

Figure 19 - Finite Difference Grid for the Analysis of Initiation of the 1976 Sau Mau Ping Failure

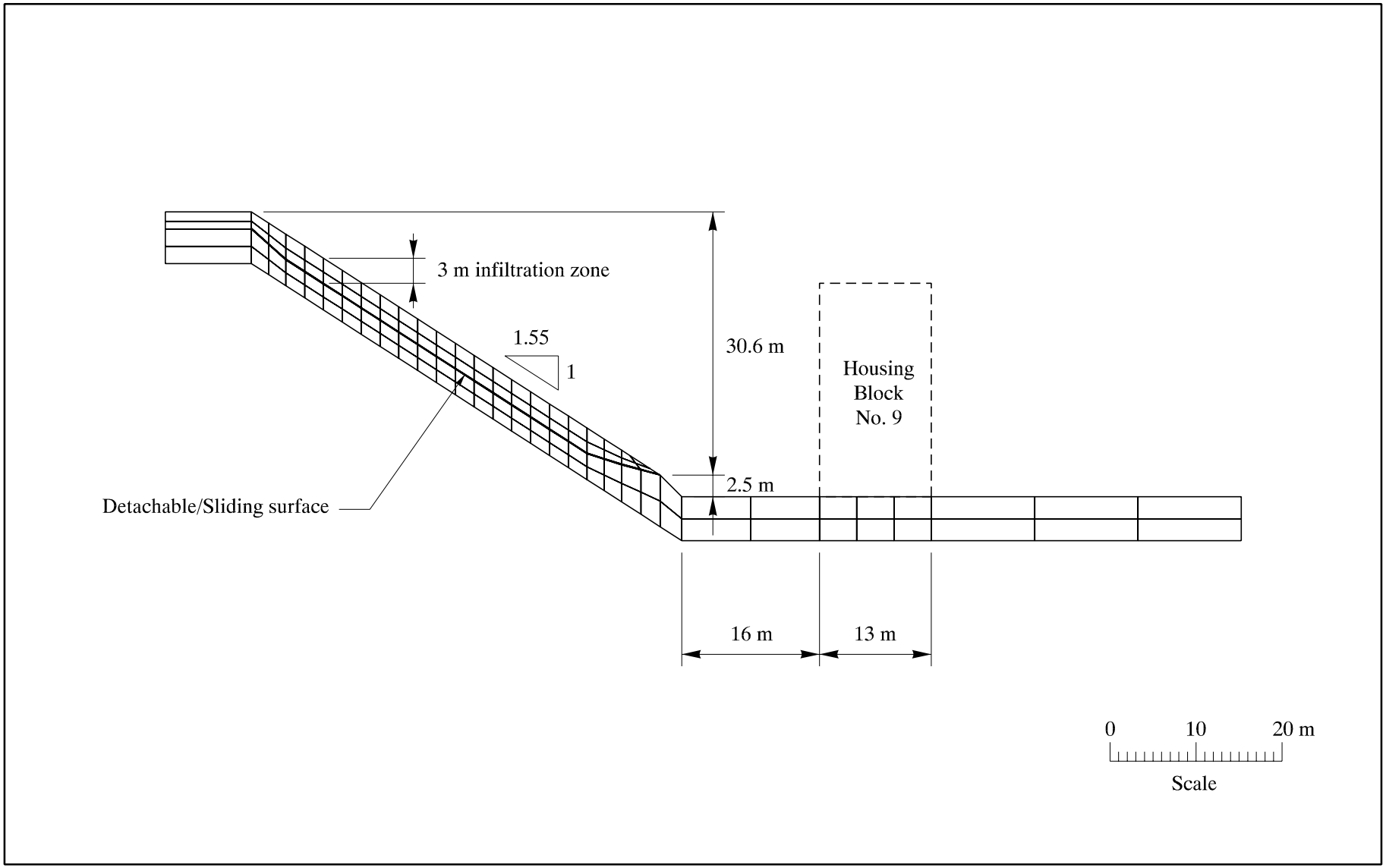

Figure 20 - Finite Difference Grid for the Analysis of Mobility of the 1976 Sau Mau Ping Failure

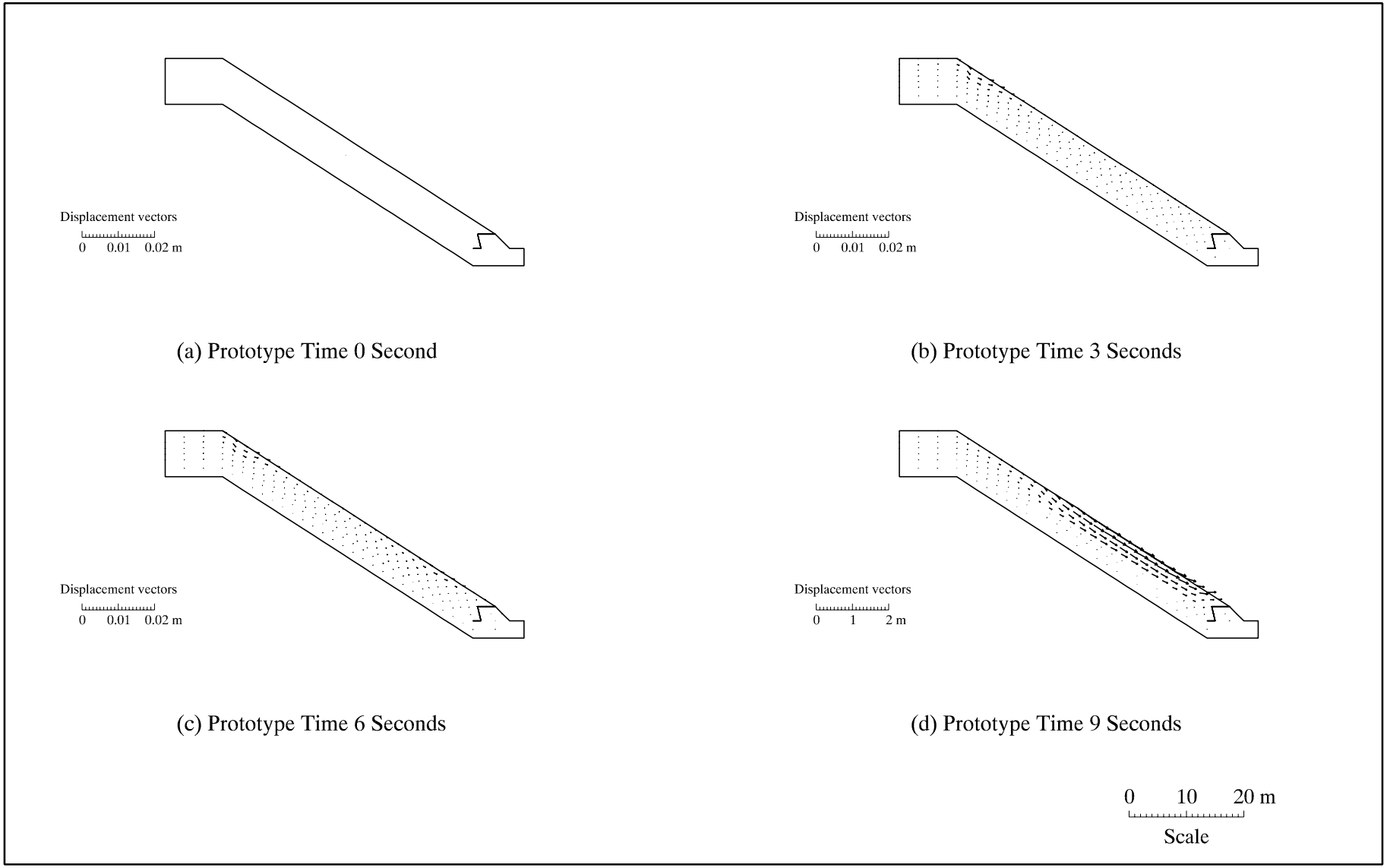

Figure 21 - Analysis of the Initiation of the 1976 Sau Mau Ping Failure - Displacement Vectors

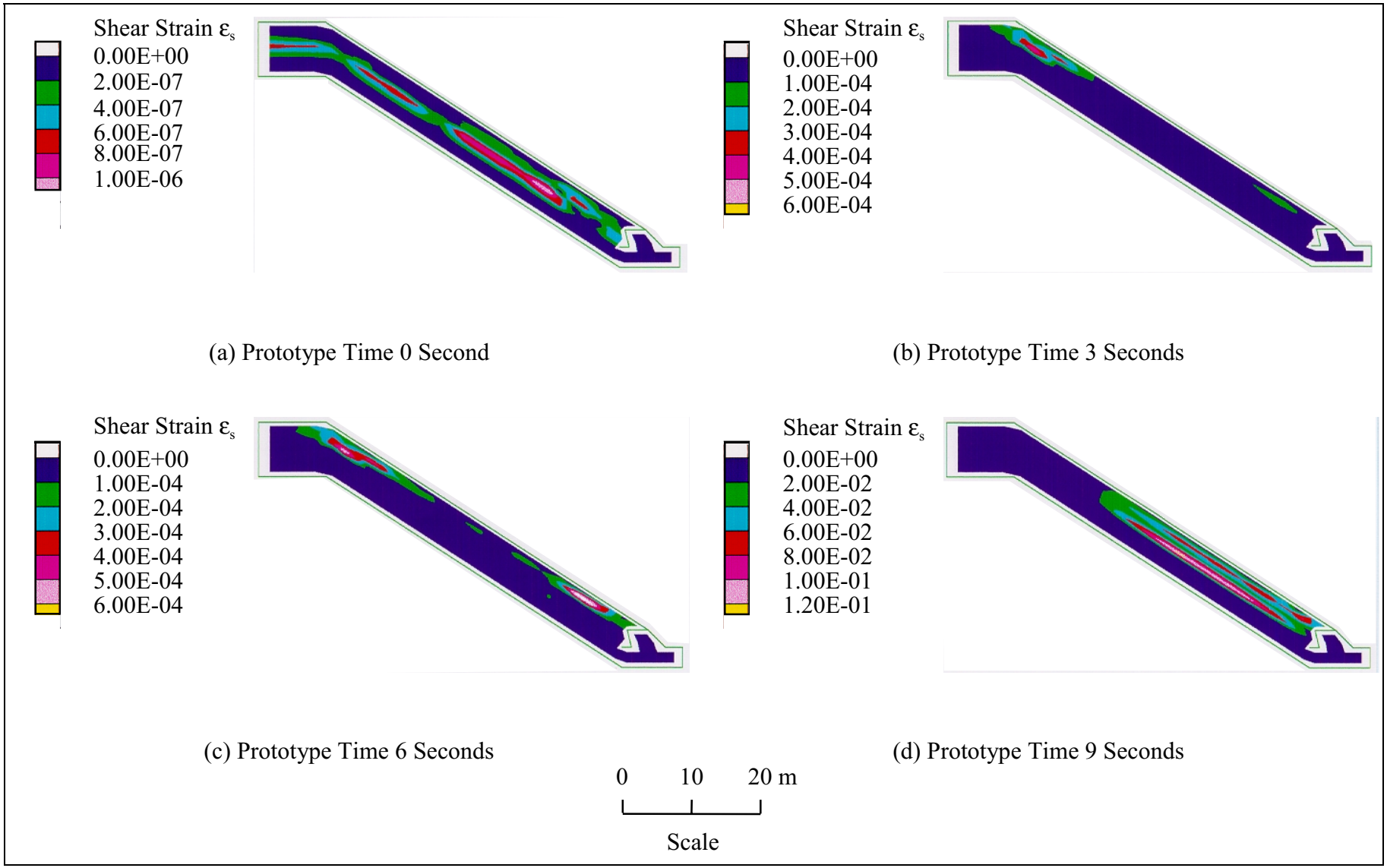

Figure 22 - Analysis of the Initiation of the 1976 Sau Mau Ping Failure - Distribution of Shear Strains

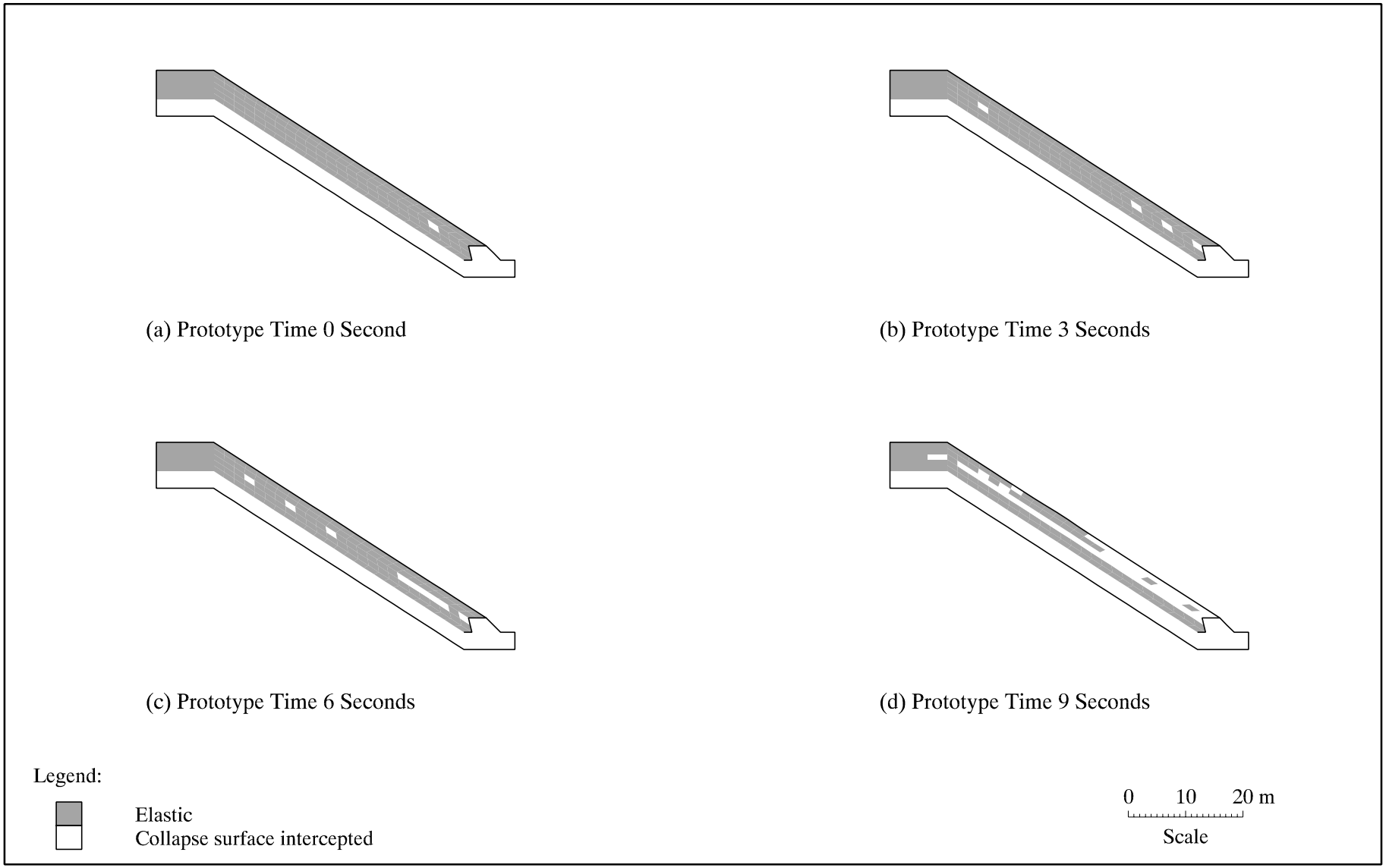

Figure 23 - Analysis of the Initiation of the 1976 Sau Mau Ping Failure - Extent of Liquefaction

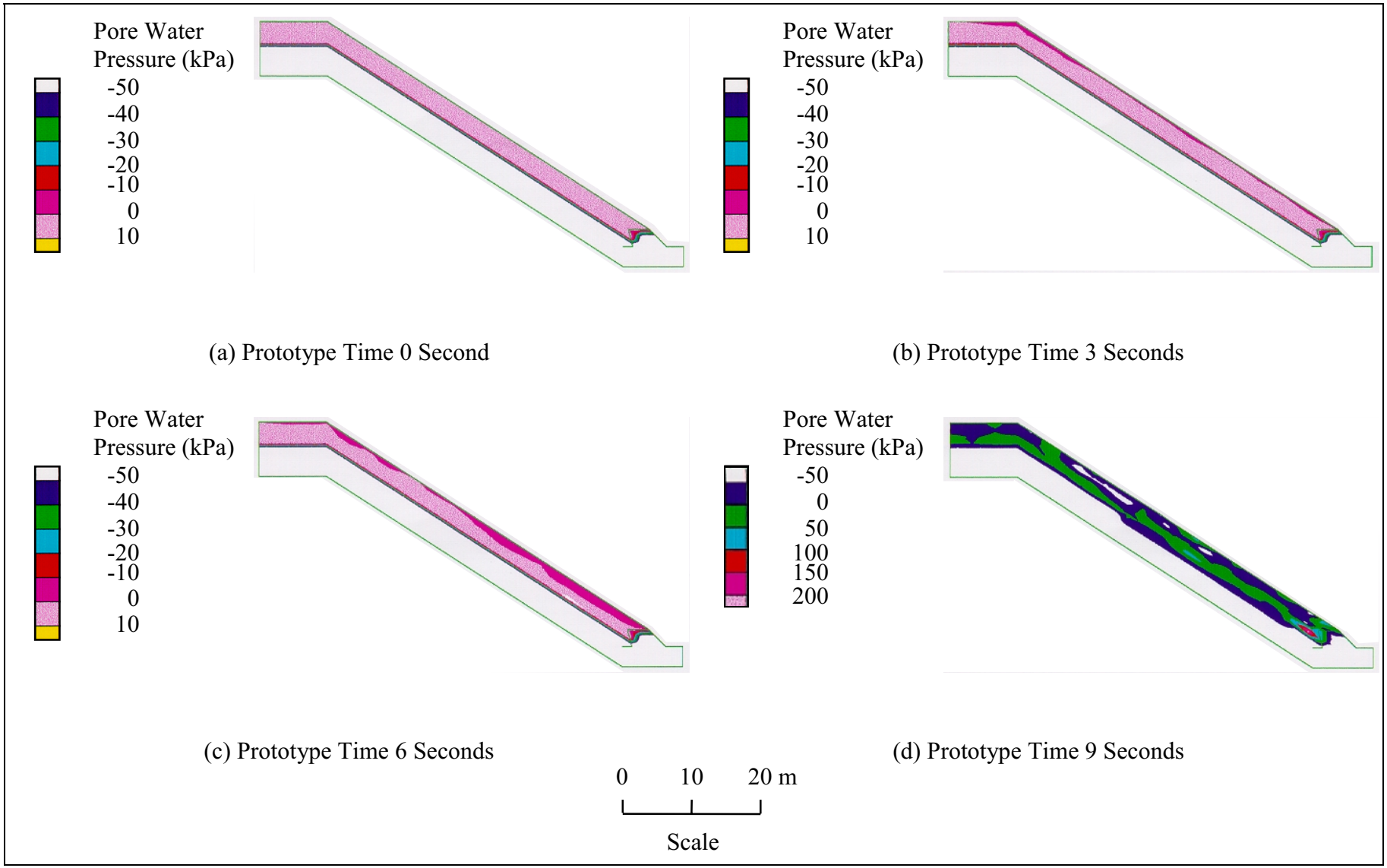

Figure 24 - Analysis of the Initiation of the 1976 Sau Mau Ping Failure - Distribution of Pore Water Pressures

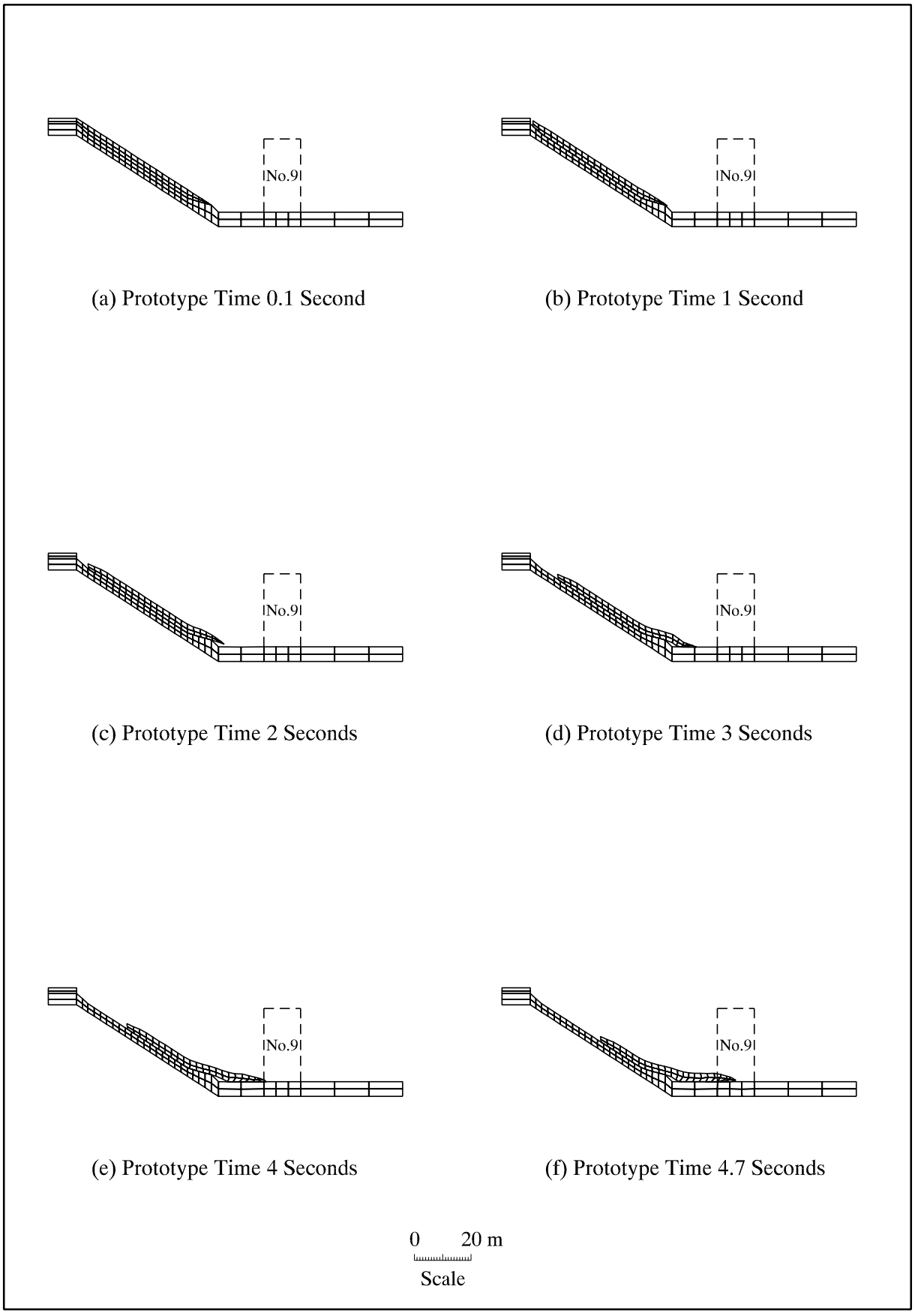

Figure 25 - Results of Analysis of the Mobility of the 1976 Sau Mau Ping Failure

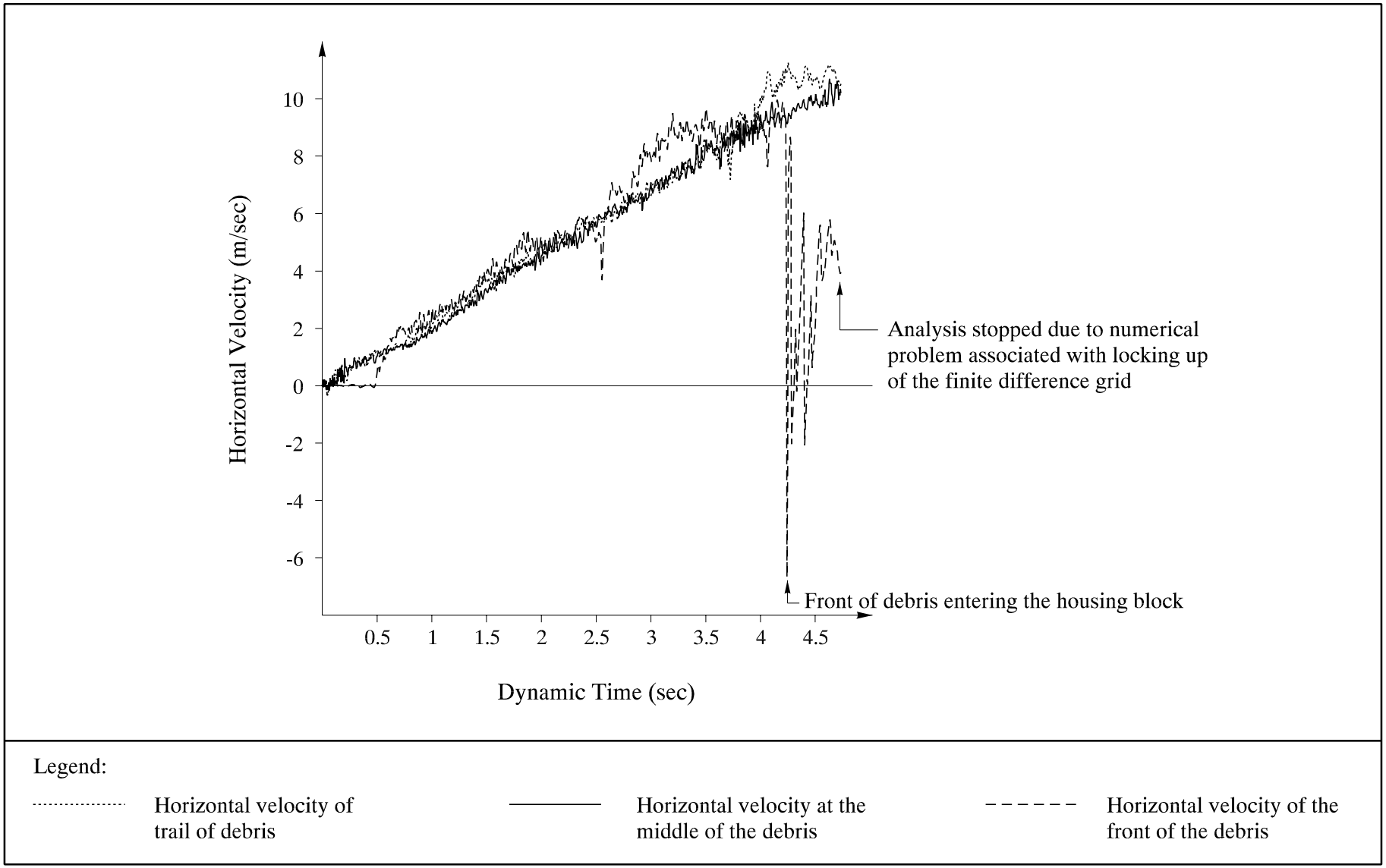

Figure 26 - Analysis of the Mobility of the 1976 Sau Mau Ping Failure - Time-History of Horizontal Velocity

APPENDIX A

FINITE DIFFERENCE ANALYSIS OF INITIATION OF THE 1976 SAU MAU PING LANDSLIDE

CONTENTS

A.1 GEOMETRY AND BOUNDARY CONDITIONS

The model was set up to represent a 30.6 m high fill slope above a 2.5 m high toe wall (Figure A1). The gradient of the fill slope is 1:1.55 (i.e. about 33° to the horizontal). The two-dimensional plane strain model was implemented in the finite difference computer program FLAC (version 3.3 with the dynamic modelling option).

The top 5 m of the fill was represented by 5 layers of finite difference zones using the SP collapse model (see Section 6.2) to simulate the potential for liquefaction due to surface infiltration to 3 m depth.

The bottom boundary of the model was fixed in horizontal and vertical directions whilst the vertical boundaries along the two ends of the model were fixed in the horizontal direction.

A.2 STAGES OF MODELLING

A.2.1 Construction of Fill Slope

The construction of the fill slope was modelled using 6 stages as follows (Figure A2):

Stage 1 - A linear elastic model was used for the toe wall and its foundation. A linear elastic-plastic model with a Mohr-Coulomb yield surface using high c'-ϕ' values (viz. c' = 22 kPa and ϕ' = 36.8°) was assumed for material below 5 m depth (it should be noted that the average depth of the Sau Mau Ping failure was about 3 m). Dynamic and groundwater flow calculations were not permitted at the initiation stage. Pore water pressure was set to be zero. The bulk modulus of water was also set to zero and so no excess pore pressure was generated during this stage.

Stage 2 - The first 1 m thick loose fill layer was built up using an elastic-plastic soil model assuming a Mohr-Coulomb yield surface with low c'-ϕ' values (viz. c' = 0 kPa and ϕ' = 35°) to allow for plastic straining that would be induced during construction by end-tipping. Dynamic and groundwater flow calculations were not permitted. Pore water pressure was set to be zero. The bulk modulus of water was also set to zero and so no excess pore pressure was generated during this stage.

Stages 3 to 6 - The successive fill layers were built up in 1 m thick layers as described in Stage 2 for the first layer.

A.2.2 Simulation of Surface Infiltration

Partially saturated fill was modelled by assigning a suction of 80 kPa throughout the fill slope. FLAC automatically discounts any suction in its calculation of effective stresses for stress-strain modelling. Modifications were therefore made in the successive stages of stress-strain calculations to allow for the consideration of suction in effective stress calculations.

For the top 5 m of fill, the Mohr-Coulomb model was replaced by the SP collapse

model. Due to the presence of suction, the stress states of all zones were below the collapse surface and the Mohr-Coulomb yield surface and in equilibrium.

In order to simulate surface infiltration, the suction in the top 3 m of the fill slope was reduced gradually (Δu = 0.01 kPa per calculation step) so that a constant q, reducing p' stress path was followed. The reduction of suction was applied uniformly. Once suction was completely removed, positive pore water pressure was allowed to build up linearly with depth below ground surface within the top 3 m. The reduction in p' was continued until the effective stress path in any one loose fill zone tried to traverse the collapse surface.

To capture the failure mechanism involving strain softening of the loose fill, the dynamic mode of FLAC was adopted at the beginning of this calculation stage. A relatively small dynamic time step of 2.5 x 10^{-6} second was used. No groundwater flow calculations were carried out, and the geometry of the finite difference grid was updated automatically as grid displacements were calculated from the strains resulting from the stress changes.

A.2.3 Development of Failure Mechanism

As soon as the effective stress path in any one zone intercepted the collapse surface, infiltration in a drained manner (modelled by the imposed Δu) was stopped. Dynamic time stepping was continued assuming an undrained (i.e. no void ratio change) condition. The development of the failure mechanism was modelled by carrying out the dynamic analysis for nine prototype seconds, with a dynamic time step of 2.5 x 10^{-6} second. No groundwater flow calculations were carried out and the geometry of the finite difference grid was updated automatically as grid displacements were calculated.

A.3 CONSTITUTIVE MODELS AND PARAMETERS ASSUMED

For the saturated loose fill, the dry density was taken to be 14 Mg/m^3, with a porosity of 0.44, saturated bulk density of 18.4 Mg/m^3 and a unit weight of about 18 kN/m^3. As the degree of saturation was fixed in the model, the unit weight of the material remained constant throughout.

The Young's modulus (E) of the fill was taken to be 15000 kPa based on correlations between E and SPT-N values and a typical SPT-N value of 10. The Poisson's ratio (υ) was assumed to be 0.3 and hence the shear modulus (G) was 5769 kPa and the bulk modulus (K) was 12500 kPa.

To simulate shear stress mobilization during end-tipping of loose fill, the material was represented by a linear elasto-plastic soil model with a Mohr-Coulomb yield surface corresponding to c' = 0, ϕ' = 35° and an angle of dilation (ψ) = 0°.

The Mohr-Coulomb yield surface (i.e. that on the dry side of the critical state line) for the loose fill is based on parameters deduced from the 1976 Sau Mau Ping investigation (Figure A3) and corresponds to c' = 0, ϕ' = 36.8° and ψ = 15°.

The critical state parameters for the SP collapse model for the loose fill interpreted

from the 1976 Sau Mau Ping investigation are as follows:

$M = 1.5$ (i.e. a ϕ' value of 36.8° as above)

$\lambda = 0.108$ (based on oedometer test results, Figure A4).

$\Gamma = 2.2$ (for saturated materials as interpreted from triaxial and shear box tests, Figure A5).

From a back analysis of triaxial compression tests on saturated and partially saturated completely decomposed granite (Law et al, 1997), the critical state strengths of unsaturated materials were found to be greater than that for saturated materials. The parameter Γ as defined in Figure 8 increased approximately by 0.15 where the degree of saturation (S_r) reduced from unity to about 0.65. During the infiltration stage, the ratio ($\Delta\Gamma/-\Delta S_r$) was taken to be about 0.43 for the analyses.

For a typical void ratio of 0.8 and assuming the best-estimate values of λ and Γ, the critical state stress conditions correspond to p' = 25.1 kPa and q = 37.6 kPa.

Collapse of loose fill was modelled on the basis of constant void ratio condition. The collapse surface was modelled assuming the Drucker-Prager criterion in a three-dimensional stress space whilst the Mohr-Coulomb yield criterion was taken as the state boundary for stresses below the critical state line (Figure A6). The inclination of the collapse surface in q-p' space was taken to be 1.2, which is equivalent to a ϕ_{col}' value of 30°.

The simulation of liquefaction of the loose fill began once the collapse surface was intercepted by the effective stress path. During the first calculation step after the collapse surface was intercepted, the mobilized q value was corrected and taken to be that given by the collapse surface corresponding to the p' value prevailing at that juncture (Figure A7). In the subsequent calculation steps, the effective stress path corresponding to increase in pore water pressure was constrained to descend along the collapse surface towards critical state condition. When the critical state condition was reached, the effective stress state will not vary further by definition.

During the generation of excess positive pore water pressure in the process of structural collapse, the mobilized q value reduced. This gave rise to an unbalanced stress state which was related to the incremental shear strain (ε_s) experienced during collapse, where ε_s is defined as the radius of the Mohr strain circle and is equal to : ε_a in undrained triaxial compression condition (with ε_a being the axial strain).

The post-peak stress-strain curve was defined by the following equation:

$$q_{mob} = q_{max} - (q_{max} - q_{cs}) \sqrt{1 - \left[\frac{(\varepsilon_{s\,max} - \varepsilon_s - s)}{\varepsilon_{s\,max}} \right]^2} \quad \text{.....(A1)}$$

$$\text{where} \quad s = \varepsilon_{s\,max}\left[1 - \sqrt{1 - \left(\frac{q_{max} - q_1}{q_{max} - q_{cs}}\right)^2}\right]$$

The terms in the above equations are defined in Figure A6. It should be noted that ε_s is the incremental shear strain after the collapse surface was intercepted by the effective stress path (i.e. the post-peak shear strain). The parameter s relates ε_s to the user-defined post-peak stress-strain curve as shown in Figure A6. Nominal values of q_{max} = 150 kPa and ε_{smax} = 3% are adopted for the present assessment. This curve corresponds to a circular arc as opposed to a hyperbolic function adopted by Gu (1992). As yet, there is a lack of good quality experimental data on the post-peak stress-strain characteristics of local loose materials.

For unsaturated fill approaching saturation, the determination of bulk modulus of pore water was updated in accordance with the varying S_r value as follows:

(a) S_r was determined from the suction (u_s) value during the infiltration stage. Figure A8 shows the relationship between S_r and matric suction for a range of Hong Kong soils. For the present analysis, S_r was related to u_s by the following expression:

$$S_r = 1 - 0.25 \log(u_s) \quad \text{.....(A2)}$$

For a u_s of less than 1 kPa, the material was taken to be fully saturated.

(b) With reference to Black & Lee (1973) and data on a Hong Kong granitic saprolite by Chung (1997), the relationship between S_r and the pore pressure parameter 'B' may be defined as follows:

$$B = 0.4375\ S_r \qquad \text{for } S_r < 0.80$$

$$B = 0.35 + 3.0\ (S_r - 0.8) \qquad \text{for } 0.80 \le S_r < 0.95$$

$$B = 0.80 + 4.0\ (S_r - 0.95) \qquad \text{for } 0.95 \le S_r < 1.0$$

Considering the relatively low positive pore water pressure involved in shallow slope failures as compared with the range of back pressures typically used in triaxial tests, the maximum 'B' value was limited to 0.85.

(c) The overall bulk stiffness ($K_{overall}$) of the soil matrix and its pore fluid is given by the following:

$$K_{overall} = K_s + K_w/n \quad \text{.....(A3)}$$

where K_s is the stiffness of the soil matrix, K_w is the effective bulk stiffness of the pore fluid and n is the porosity.

For a soil subjected to an all round pressure, the pore water pressure response is governed by the relative stiffnesses between K_w/n and K_s. Therefore, K_w can be related to pore pressure parameter B by the following:

$$K_w = \frac{B}{1-B} n \quad K_s \qquad \text{.....(A4)}$$

A.4 REFERENCES

Black, D.K. & Lee, K.L. (1973). Saturating laboratory samples by back pressure. Journal of Soil Mechanics and Foundations Division, Americian Society of Civil Engineers, vol. 99, pp 75-93.

LIST OF FIGURES

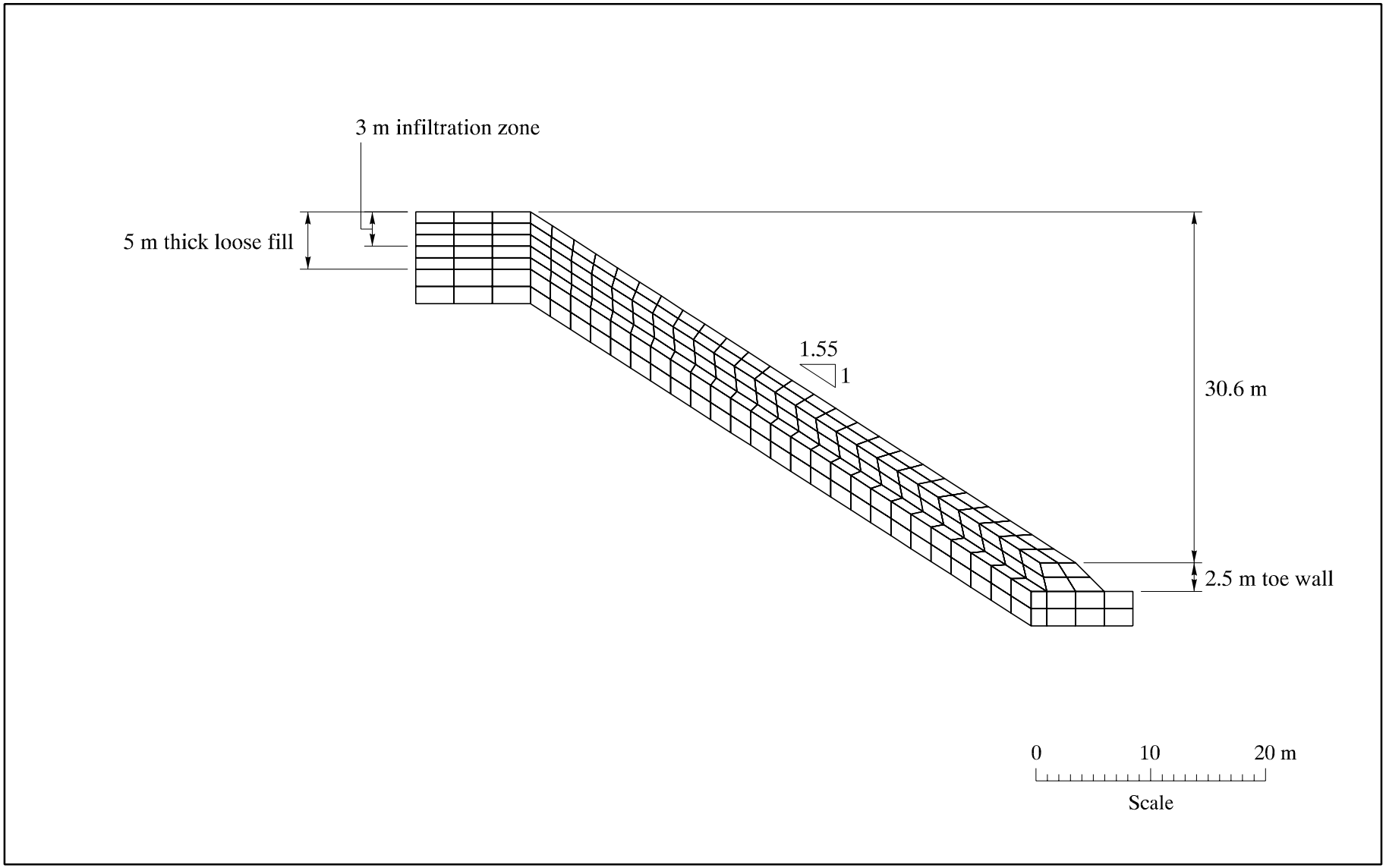

Figure A1 - Finite Difference Grid for the Analysis of Initiation of the 1976 Sau Mau Ping Failure

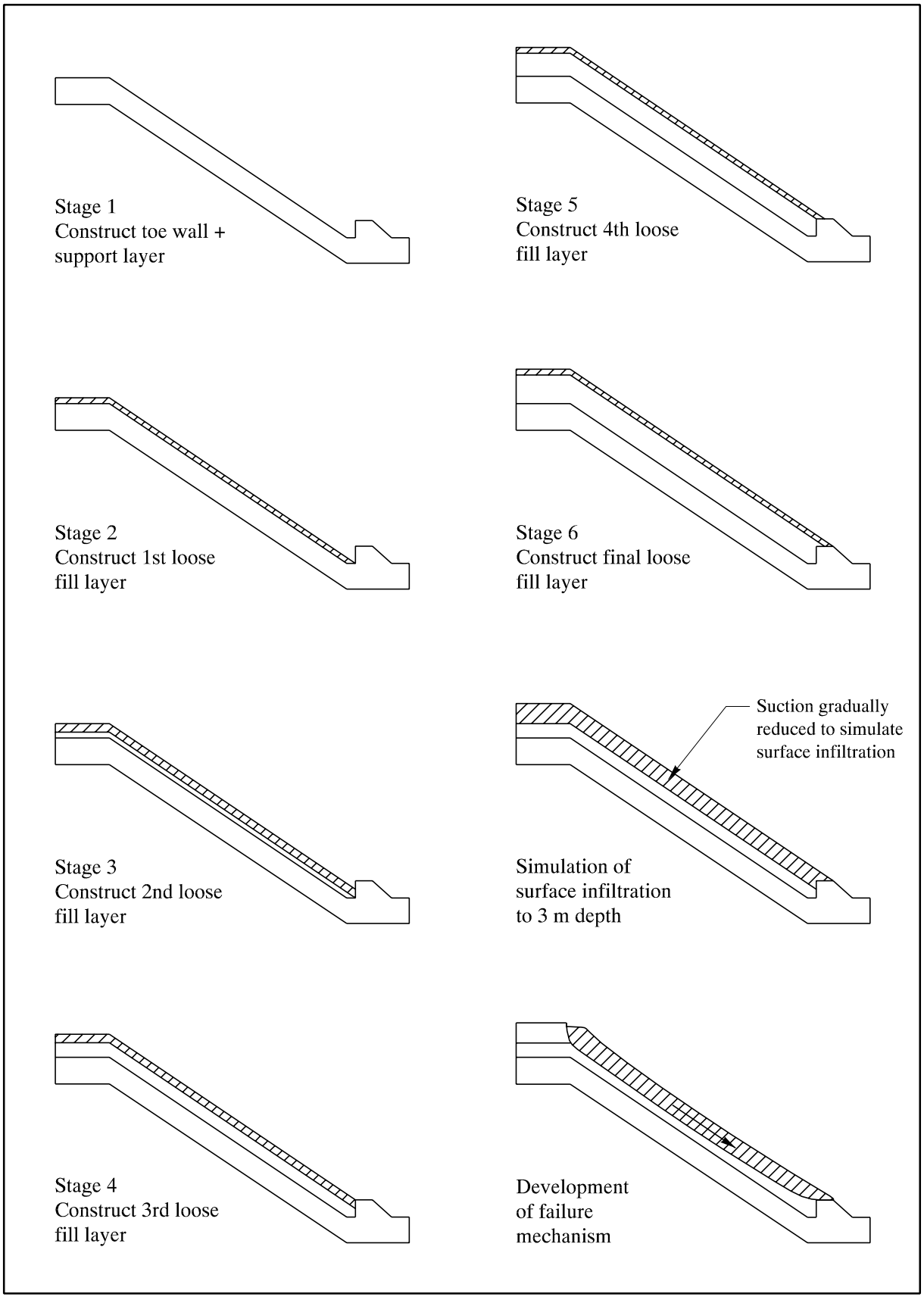

Figure A2 - Finite Difference Model for the Staged Construction of the Loose Fill Slope

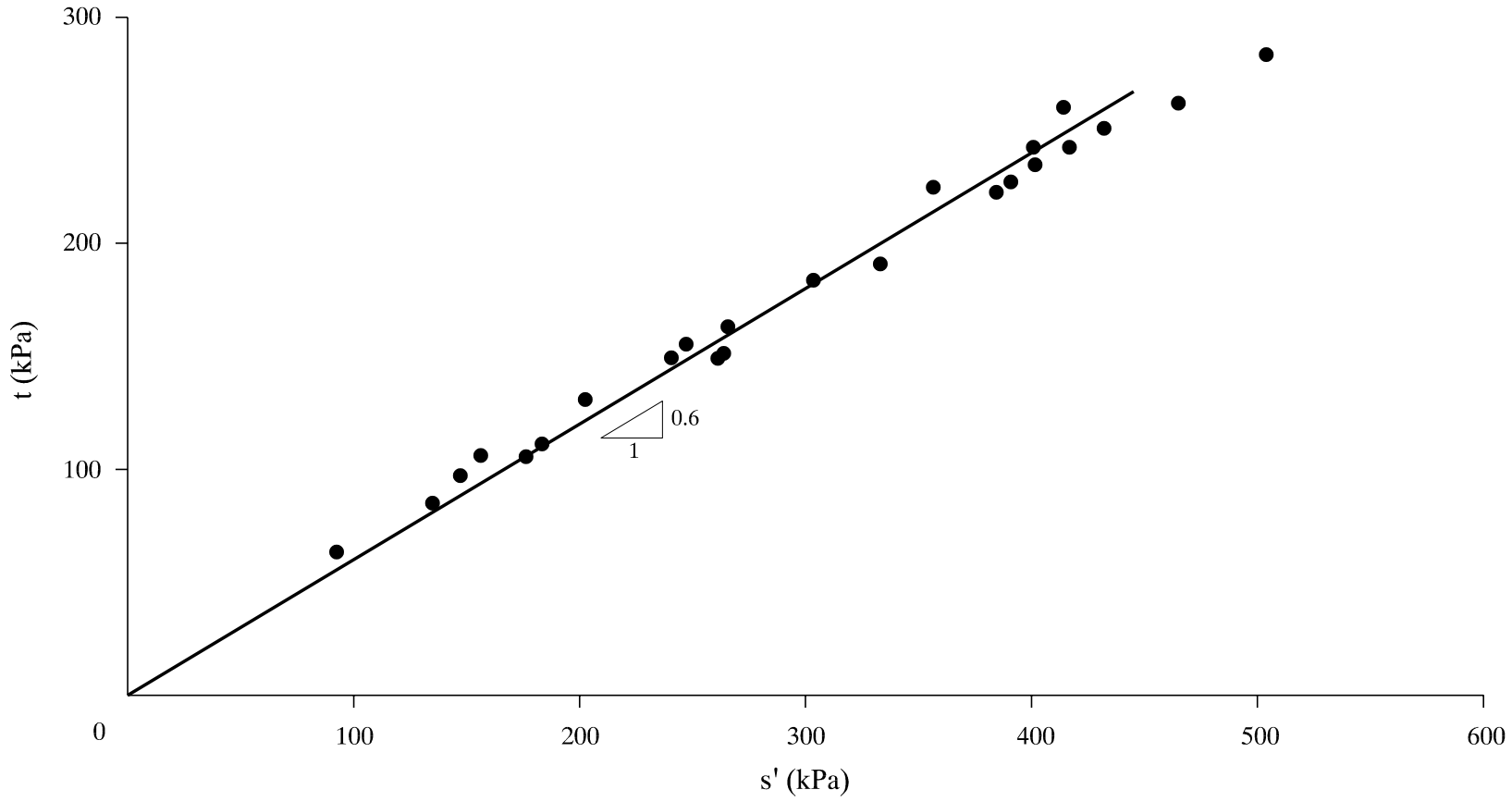

Legend:

σ_1'	Major principal effective stress	$s' = (\sigma_1' + \sigma_3')/2$
σ_3'	Minor principal effective stress	$t = (\sigma_1' - \sigma_3')/2$

Note: The slope of the regression line in t - s' space give correspond to a ϕ_{cv}' of 36.8°.

Figure A3 - Effective Stress Shear Strength Parameters of the Fill Material from the 1976 Sau Mau Ping Investigation

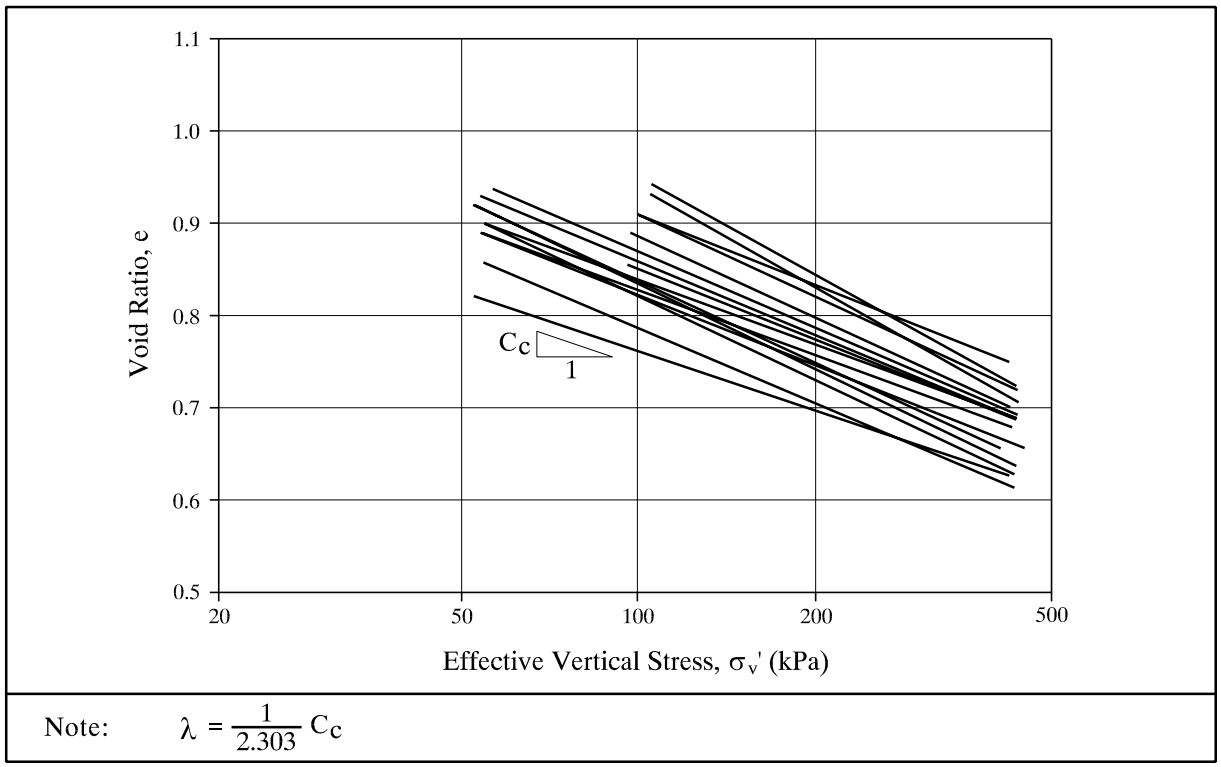

Figure A4 - Interpretation of Critical State Parameter λ from Results of Oedometer Tests in the 1976 Sau Mau Ping Investigation

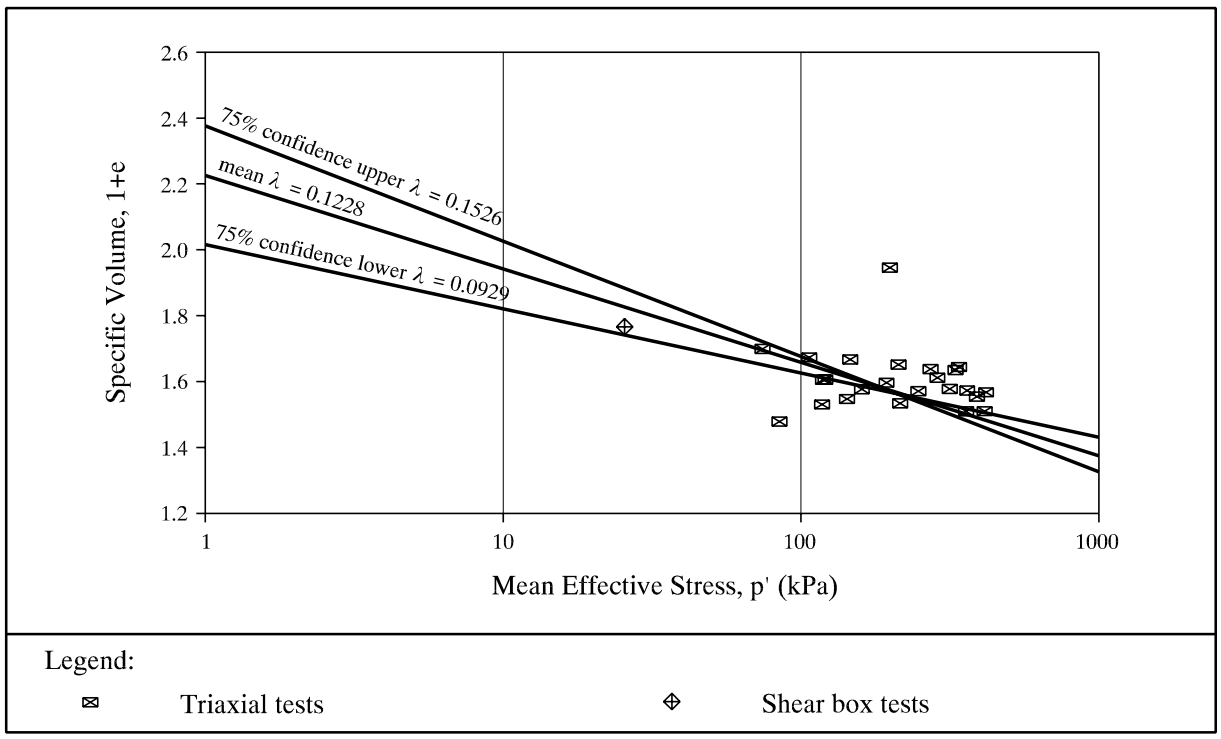

Figure A5 - Interpretation of Critical State Parameter Γ from Results of Triaxial Tests and Shear Box Tests in the 1976 Sau Mau Ping Investigation

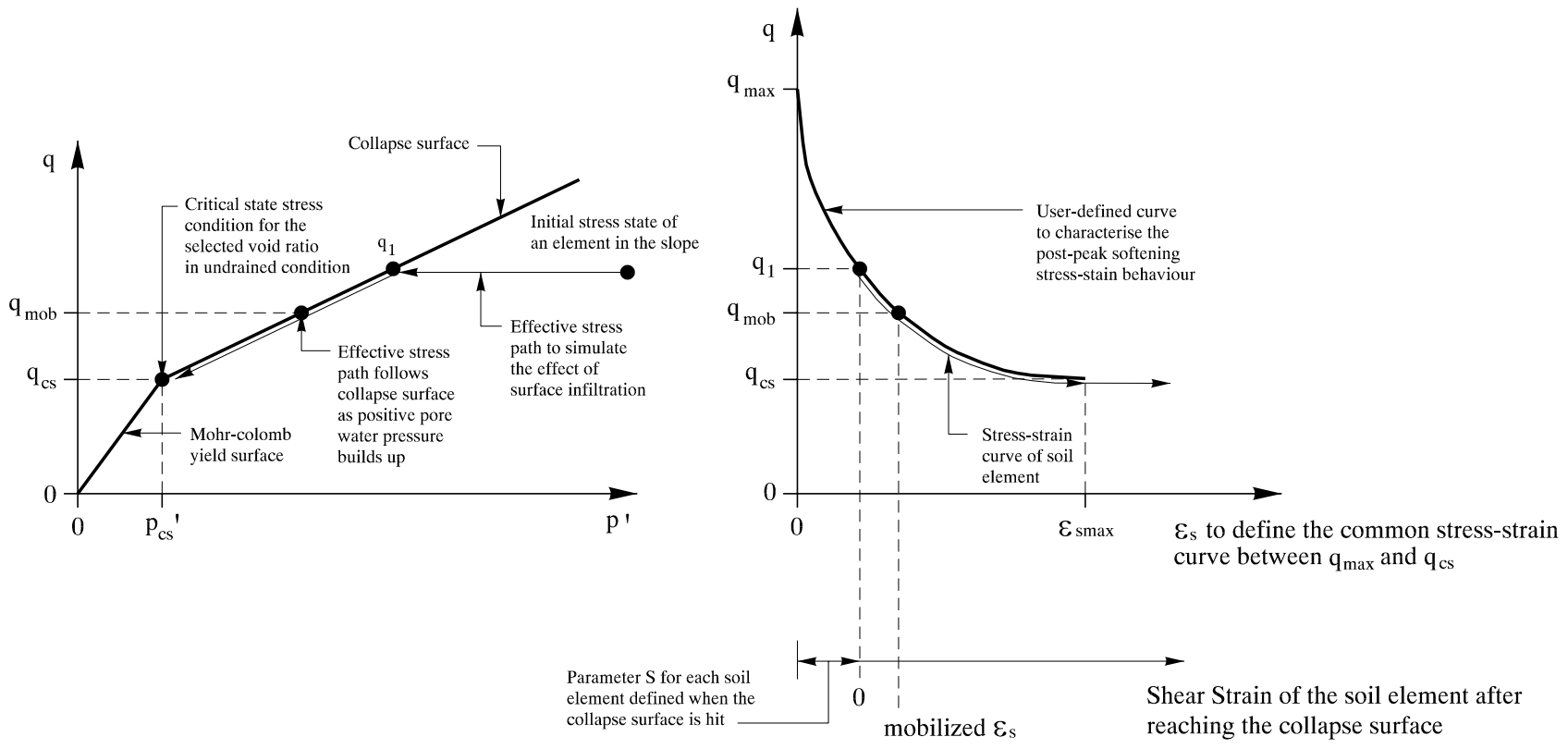

Legend:

p'	p - u	ε_s	$\frac{1}{2}(\varepsilon_1 - \varepsilon_3)$, ε_1 & ε_3 are major and minor principal strain
u	Positive pore water pressure	q_{max}, ε_{smax}	Parameters to define the strain-softening characteristics for effective stress paths along the collapse surface

Note: Refer to Figures 1 & 12 for definition of other terms.

Figure A6 - The SP Model for Static Liquefaction of Loose Fill

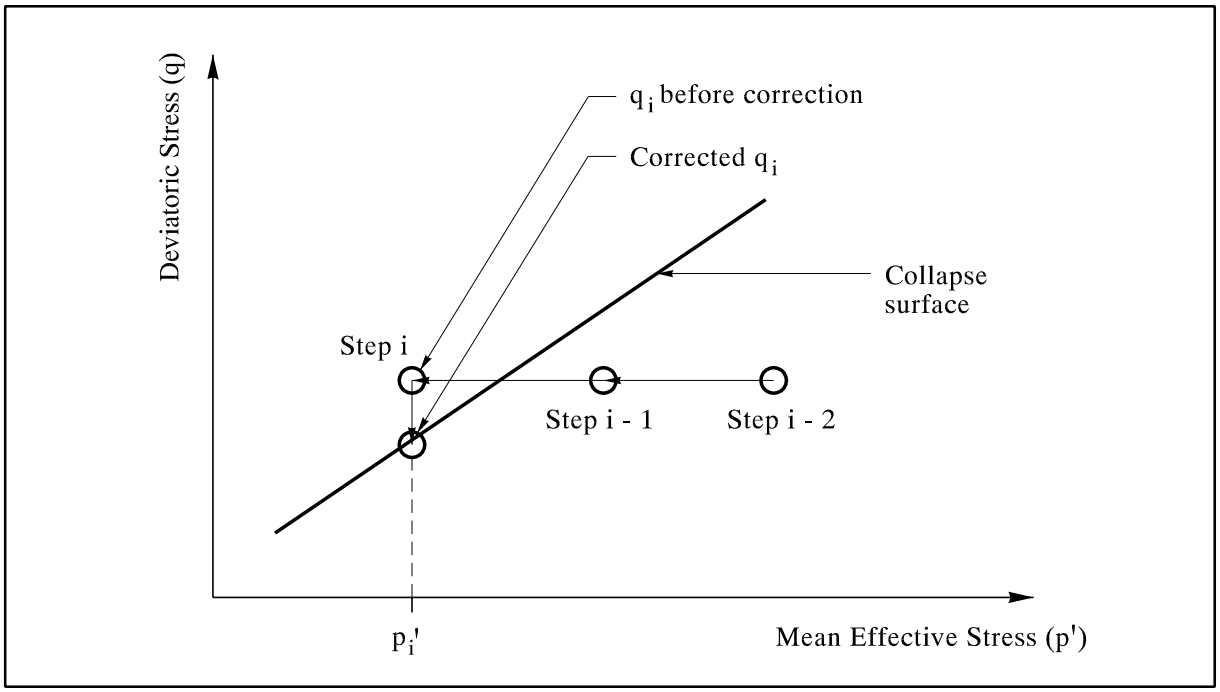

Figure A7 - Correction of Stress Condition in the SP Model When the Collapse Surface is Intercepted

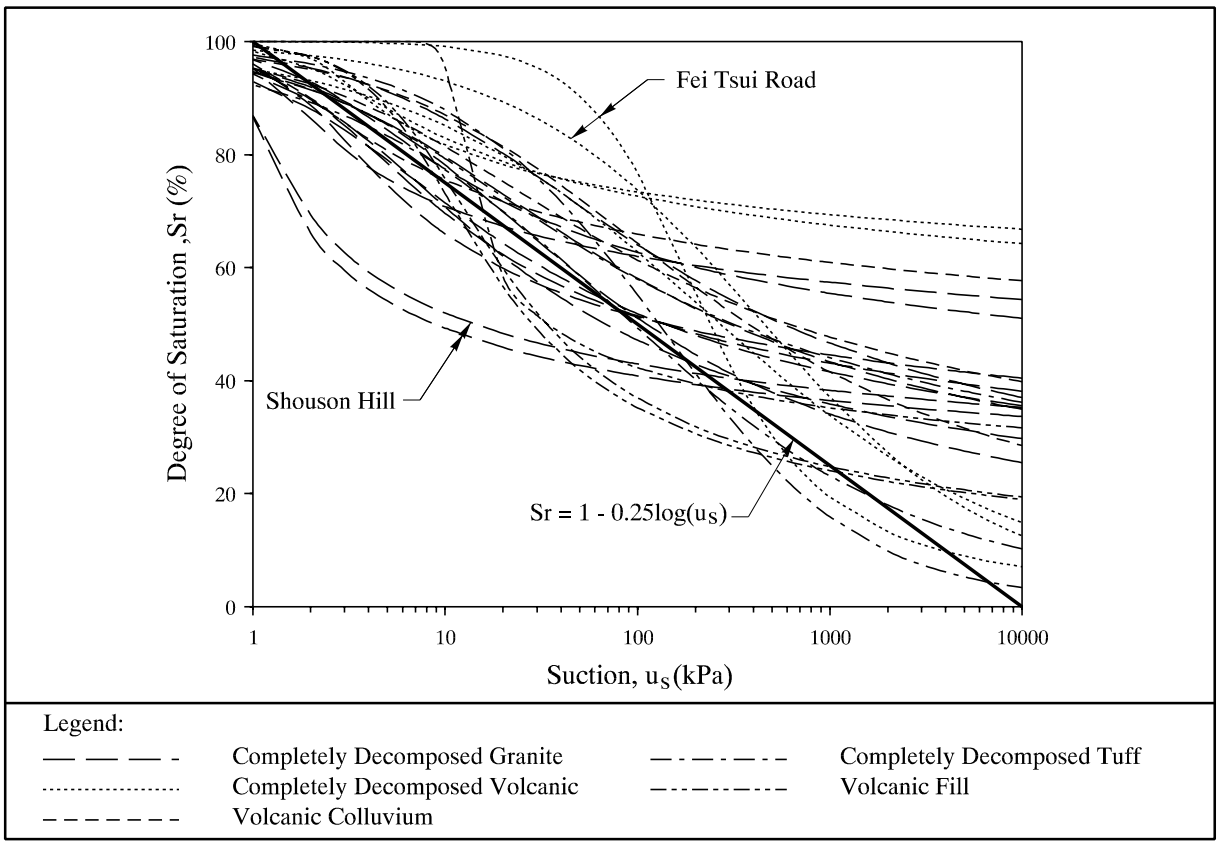

Figure A8 - Soil-water Characteristic Curves for a Range of Soils in Hong Kong

APPENDIX B

FINITE DIFFERENCE ANALYSIS OF MOBILITY OF THE 1976 SAU MAU PING LANDSLIDE

CONTENTS

B.1 GEOMETRY AND BOUNDARY CONDITIONS

The geometry and boundary conditions of the model are the same as that described in Section A1, except that the top 3 m of the fill was represented by two 1.45 m thick layers and a 0.1 m thick bottom layer of finite difference zones using the SP collapse model to simulate the potential for liquefaction due to surface infiltration to 3 m depth. The bottom layer of finite difference zones representing the sliding mass was set to represent the sliding surface between the landslide debris and the ground beneath it. This layer was replaced by a series of interface elements in the latter stages of the analysis to allow for complete detachment of the unstable sliding mass from its original position (Figure B1).

B.2 STAGES OF MODELLING

B.2.1 Construction of Fill Slope

The construction of the fill slope was modelled using 6 stages in the same manner as that described in Section A2.1.

B.2.2 Simulation of Surface Infiltration

The simulation of surface infiltration was the same as that described in Section A2.2, except that an initial suction of 60 kPa was imposed. As the focus of this series of analyses is on the runout of the debris, a somewhat smaller initial suction compared to the previous set of analyses was adopted for efficiency. This simplification would not have significantly affected the results.

B.2.3 Development of Failure Mechanism and Debris Runout

As soon as the effective stress path in any one zone intercepted the collapse surface, infiltration in a drained manner (as modelled by the imposed Δu) was terminated. The bottom layer of the infiltration zone was replaced by a series of strain-softening interface elements. Dynamic time stepping was continued assuming an undrained (i.e. no volume change) condition. The development of the failure mechanism and debris runout was modelled using the dynamic modelling option in FLAC, with a dynamic time step of 1×10^{-5} second, extending to five seconds of prototype time. No groundwater flow calculations were carried out during this stage of the modelling and the geometry of the finite difference grid was updated automatically as grid displacements were calculated.

The debris sled over the toe wall and landed on the ground behind the housing block. With further stepping, it travelled forward and hit the building. The resistance provided by the housing block to the movement of the debris was not known precisely. As a first approximation, the basal shear resistance of the debris within the width of the building was taken to be proportional to the square of the speed of the debris.

B.3 CONSTITUTIVE MODELS AND PARAMETERS ASSUMED

The constitutive models and parameters assumed were as described in Section A3. To avoid the breaking up of the debris above the sliding surface, the two layers of finite difference zones were assigned a critical state undrained shear strength that was 2 kPa higher than that for the sliding surface.

For the interface elements, the undrained shear strength assigned was a function of relative displacement between the sliding mass and the underlying stable material. The reduction in undrained shear strength of the interface with incremental shear strain was in accordance with the same stress-strain relationship as that described in Section A3. In the calculation of incremental shear strain from relative displacements parallel to the direction of the interface, the shear band was taken to be 250 mm thick nominally, which is broadly consistent with site observations.

LIST OF FIGURES

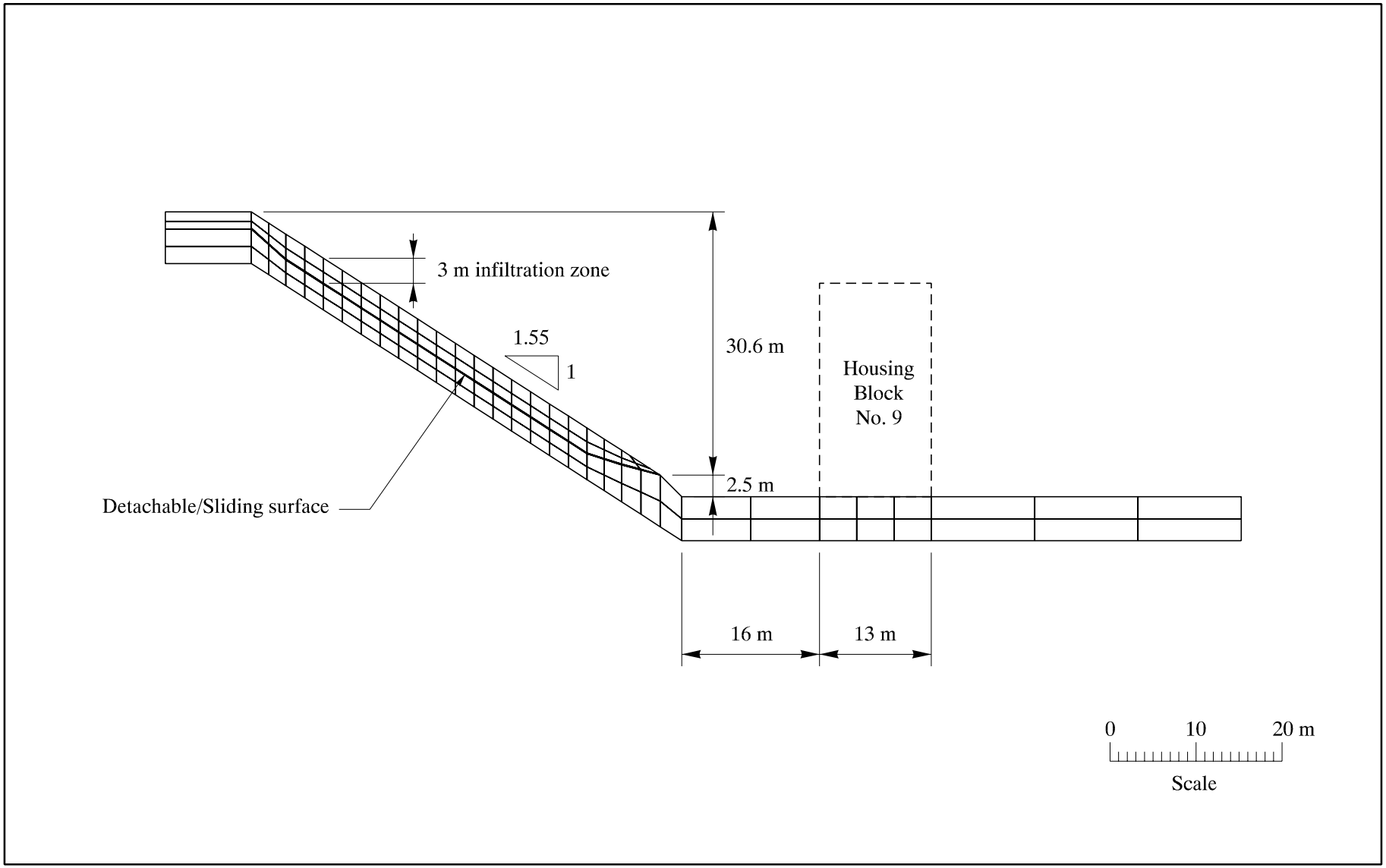

Figure B1 - Finite Difference Grid for the Analysis of Mobility of the 1976 Sau Mau Ping Failure